TWO-PHASE FLOW STABILITY IN
HORIZONTAL CHANNELS

By

HAMID NESHAN

Bachelor of Science
Tehran Polytechnic Institute
Tehran, Iran
1967

Master of Science
Oklahoma State University
Stillwater, Oklahoma
1971

Submitted to the Faculty of the Graduate College
of the Oklahoma State University
in partial fulfillment of the requirements
for the Degree of
DOCTOR OF PHILOSOPHY
December, 1973

TWO-PHASE FLOW STABILITY IN

HORIZONTAL CHANNELS

Thesis Approved:

Jerald D. Parker
Thesis Adviser

Bela M. Ulrich

W. G. Tiederman

Kenneth J. Bell

D. D. Durham
Dean of the Graduate College

879985

ACKNOWLEDGMENTS

I wish to express my sincere appreciation to my major adviser, Professor Jerald D. Parker, who provided support and assistance far beyond the call of duty throughout this study. His perceptive advice, guidance, and encouragement are in large part responsible for surmounting of obstacles encountered in this study.

I also wish to express my appreciation to the other members of my committee, Dr. K. J. Bell, Dr. W. G. Tiederman, and Dr. P. M. Moretti for their technical advice and their invaluable assistance in the preparation of the final manuscript.

An additional thanks is given to Dr. K. J. Bell for his kindness in allowing the use of equipment from his laboratory.

A special thanks is due to Dr. M. M. Mamoun for his support and encouragement throughout this work.

The assistance of Mr. R. R. Lowrie and Mr. H. Bina in the experimental phase of this study is gratefully acknowledged. I would like to thank Dr. M. N. Farukhi, now with Babcock & Wilcox Company, for his helpful suggestions throughout this work.

I wish to take this opportunity to thank Mr. George Cooper of the Mechanical Engineering Laboratory for his advice and assistance during the construction of the test apparatus.

The financial assistance which has made this study possible was received from the Oklahoma State University and is gratefully acknowledged.

I wish to note my gratitude to the Oklahoma State University and the State of Oklahoma for making their educational facilities available to students from other countries.

I would like to add my special thanks to my wife, Roya, who endured the day-to-day frustration of being married to a graduate student.

I sincerely thank my parents for their sacrifice, encouragement, and support throughout my undergraduate and graduate years.

Finally, I would like to express my gratitude to all concerned.

TABLE OF CONTENTS

Chapter | Page

I. INTRODUCTION 1

II. BACKGROUND OF THE PROBLEM AND LITERATURE REVIEW 3

2.1 Two-Phase Flow Instability 3
2.2 Excursive Instability 3
2.3 Flow Pattern Transition Instability 6
2.4 Density Wave Instability 8
2.5 Pressure Drop Oscillations 9
2.6 Instabilities in a Forced-Convection System 12
2.7 Single Heated Channels 12
2.8 Parallel Heated Channels 16
2.9 Closure 19

III. EXPERIMENTAL APPARATUS 20

3.1 Hydraulic System 20
3.2 Power Supply 28
3.3 Instrumentation 30

IV. EXPERIMENTAL PROCEDURE 34

4.1 Range of Experimental Parameters 34
4.2 Operation Procedure and Data Taking 35
4.3 Test Section Heat Balance 38

V. EXPERIMENTAL RESULTS AND DISCUSSION 39

5.1 Pressure Drop Flow Rate Curve 39
5.2 Effect of Various Parameters 71
5.3 Inlet Subcooling 71
5.4 Pressure 71
5.5 Heat Flux 72
5.6 Length to Diameter Ratio 72
5.7 Inlet Orificing 74

VI. CORRELATION OF THE RESULTS 77

VII. CONCLUSIONS AND RECOMMENDATIONS 88

Chapter Page

A SELECTED BIBLIOGRAPHY. 91

APPENDIX A - DERIVATION OF CRITERIA FOR EXCURSIVE INSTABILITY 95

APPENDIX B - EXPERIMENTAL DATA 98

APPENDIX C - CALIBRATION CURVES FOR MEASURING DEVICES. 167

LIST OF TABLES

Table — Page

I. Dimensions of the Test Sections. 28

II. Range of Experimental Parameters 34

LIST OF FIGURES

Figure		Page
1.	Pressure Drop Characteristics Versus Flow Rate	5
2.	Flow Patterns in Horizontal Two-Phase Flow	7
3.	Density Wave and Pressure Drop Oscillations	10
4.	Schematic Diagram of the Loop	21
5.	Schematic Diagram of Test Section	23
6.	General Arrangement of Apparatus, Front View	24
7.	General Arrangement of Apparatus, Back View	24
8.	Inlet Header and Inlet Orifice Arrangement	25
9.	General Arrangement of Apparatus, Side View	26
10.	Test Section Pressure Drop Versus Mass Flow Rate; L/D = 204, T_i = 85° F, P_{ex} = 25 psia	40
11.	Test Section Pressure Drop Versus Mass Flow Rate; L/D = 204, T_i = 85° F, P_{ex} = 35 psia	41
12.	Test Section Pressure Drop Versus Mass Flow Rate; L/D = 204, T_i = 85° F, P_{ex} = 45 psia	42
13.	Test Section Pressure Drop Versus Mass Flow Rate; L/D = 204, T_i = 85° F, P_{ex} = 55 psia	43
14.	Test Section Pressure Drop Versus Mass Flow Rate; L/D = 204, T_i = 85° F, P_{ex} = 70 psia	44
15.	Test Section Pressure Drop Versus Mass Flow Rate; L/D = 204, T_i = 95° F, P_{ex} = 25 psia	45
16.	Test Section Pressure Drop Versus Mass Flow Rate; L/D = 204, T_i = 95° F, P_{ex} = 35 psia	46
17.	Test Section Pressure Drop Versus Mass Flow Rate; L/D = 204, T_i = 95° F, P_{ex} = 45 psia	47

Figure | Page

18. Test Section Pressure Drop Versus Mass Flow Rate; L/D = 204, T_i = 95° F, P_{ex} = 55 psia 48

19. Test Section Pressure Drop Versus Mass Flow Rate; L/D = 204, T_i = 95° F, P_{ex} = 70 psia 49

20. Test Section Pressure Drop Versus Mass Flow Rate; L/D = 204, T_i = 110° F, P_{ex} = 35 psia. 50

21. Test Section Pressure Drop Versus Mass Flow Rate; L/D = 204, T_i = 110° F, P_{ex} = 45 psia. 51

22. Test Section Pressure Drop Versus Mass Flow Rate; L/D = 204, T_i = 110° F, P_{ex} = 55 psia. 52

23. Test Section Pressure Drop Versus Mass Flow Rate; L/D = 204, T_i = 110° F, P_{ex} = 70 psia. 53

24. Test Section Pressure Drop Versus Mass Flow Rate; L/D = 204, T_i = 120° F, P_{ex} = 45 psia. 54

25. Test Section Pressure Drop Versus Mass Flow Rate; L/D = 204, T_i = 120° F, P_{ex} = 55 psia. 55

26. Test Section Pressure Drop Versus Mass Flow Rate; L/D = 204, T_i = 120° F, P_{ex} = 70 psia. 56

27. Test Section Pressure Drop Versus Mass Flow Rate; L/D = 153, T_i = 95° F, P_{ex} = 35 psia 57

28. Test Section Pressure Drop Versus Mass Flow Rate; L/D = 153, T_i = 95° F, P_{ex} = 45 psia 58

29. Test Section Pressure Drop Versus Mass Flow Rate; L/D = 153, T_i = 110° F, P_{ex} = 35 psia. 59

30. Test Section Pressure Drop Versus Mass Flow Rate; L/D = 153, T_i = 110° F, P_{ex} = 45 psia. 60

31. Test Section Pressure Drop Versus Mass Flow Rate; L/D = 102, T_i = 95° F, P_{ex} = 35 psia 61

32. Test Section Pressure Drop Versus Mass Flow Rate; L/D = 102, T_i = 95° F, P_{ex} = 45 psia 62

33. Test Section Pressure Drop Versus Mass Flow Rate; L/D = 102, T_i = 110° F, P_{ex} = 35 psia. 63

34. Test Section Pressure Drop Versus Mass Flow Rate; L/D = 102, T_i = 110° F, P_{ex} = 45 psia. 64

Figure		Page

35. Test Section Pressure Drop Versus Mass Flow Rate; L/D = 51, T_i = 95° F, P_{ex} = 35 psia. 65

36. Test Section Pressure Drop Versus Mass Flow Rate; L/D = 51, T_i = 95° F, P_{ex} = 45 psia. 66

37. Test Section Pressure Drop Versus Mass Flow Rate; L/D = 51, T_i = 110° F, P_{ex} = 35 psia 67

38. Test Section Pressure Drop Versus Mass Flow Rate; L/D = 51, T_i = 110° F, P_{ex} = 45 psia 68

39. Regions of Pressure Drop in Forced Convection Boiling With Inlet Subcooling. 70

40. Effect of Inlet Orificing on the Pressure Drop-Flow Rate Curve 76

41. Correlation of Data, $\Delta P_o/\Delta P_{adb}$ = 0.0 80

42. Correlation of Data, $\Delta P_o/\Delta P_{adb}$ = 0.5 81

43. Correlation of Data, $\Delta P_o/\Delta P_{adb}$ = 1.0 82

44. Correlation of Data, $\Delta P_o/\Delta P_{adb}$ = 2.0 83

45. Correlation of Data, $\dot{q}/\dot{q}_{se}$ With L/D; $\Delta P_o/\Delta P_{adb}$ = 0.0 86

46. Correlation of Data, $\dot{q}/\dot{q}_{se}$ With L/D; $\Delta P_o/\Delta P_{adb}$ = 0.0, $\Delta P_o/\Delta P_{adb}$ = 0.5, $\Delta P_o/\Delta P_{adb}$ = 1.0, $\Delta P_o/\Delta P_{adb}$ = 2.0. 87

47. Schematic Diagram of Heated Section. 96

48. Calibration Curve for Water Flow Meter 168

49. Calibration Curve for Freon Flow Meter (Cox Rotameter) 169

50. Calibration Curve for Freon Flow Meter (Fischer & Porter Rotameter) 170

51. Calibration Curve for Freon Flow Meter (Brooks Rotameter). . . 171

52. Calibration Curve for Gage Pressure. 172

NOMENCLATURE

A	surface area of heated section, ft^2
A_c	cross sectional area of heated section, ft^2
C_p	specific heat of liquid, $BTU.\ lb_m^{-1}, °F^{-1}$
D	tube inside diameter, ft
F_x	force in the X-direction, lb_f
g_c	conversion factor, 32.2 $lb_m.\ lb_f^{-1}.\ ft.\ sec^{-2}$
G	mass velocity, $lb_m.\ hr^{-1}.\ ft^{-2}$
h_{fg}	latent heat of vaporization, $BTU.\ lb_m^{-1}$
L	test section length, ft
m	mass, lb_m
$\dot{m}$	mass flow rate, $lb_m\ min^{-1}$
P	pressure, $lb_f.\ in^{-2}$
P_{ex}	pressure at the channel exit, $lb_f.\ in^{-2}$
$\dot{q}$	heat flow rate, $BTU.\ hr^{-1}$
$\dot{q}_{se}$	heat flow rate required to obtain a saturation condition at the channel exit, $BTU.\ hr^{-1}$
t	time, sec.
T_e	fluid temperature at the channel exit, °F
T_i	fluid temperature at the channel inlet, °F
T_s	saturation temperature at the channel exit, °F
v	fluid velocity, $ft.\ sec^{-1}$
ΔP_{adb}	adiabatic pressure drop, $lb_f.\ in^{-2}$
ΔP_{ext}	external system pressure drop, $lb_f.\ in^{-2}$

ΔP_{int}	internal system pressure drop, $lb_f \cdot in^{-2}$
ΔP_o	orifice pressure drop, $lb_f \cdot in^{-2}$
ρ	density, $lb_m \cdot ft^{-3}$
ρ_ℓ	liquid density, $lb_m \cdot ft^{-3}$
ρ_ν	vapor density, $lb_m \cdot ft^{-3}$
τ	shear stress, $lb_f \cdot in^{-2}$

CHAPTER I

INTRODUCTION

There are many practical applications in which liquid from a central header is distributed to a number of separate parallel channels where each channel receives heat and the mixture of liquid and vapor, saturated vapor or superheated vapor will discharge into a common outlet. Heat exchangers, evaporators, boilers and boiling water nuclear reactors are common examples.

When a large number of parallel heated flow channels are operating between common inlet and outlet headers, each channel is subject to the same pressure difference and each channel receives a share of the flow, the amount of which depends upon the channel geometry, and pressure drop flow characteristic of each channel. Formation of vapor in one channel will cause less fluid to flow, thereby causing more vapor to form.

The additional resistance to flow, caused by generation of more and more vapor, may even cause the flow of liquid to stop entirely, and burnout of the channel may occur. Moreover, with a given pressure drop, heat flux, channel flow rate, inlet enthalpy, etc. a resonance condition may occur in which the flow rates in the channels may start to oscillate.

A knowledge of conditions under which these oscillations occur and knowledge of the factors affecting flow distribution is of particular importance in the design of heat exchange equipment.

It is well known that flow oscillations may be prevented by providing sufficient inlet throttling on the individual channels. Determination of the minimum adequate inlet throttling which is an important economic factor is one of the objectives of this study.

Flow instability in a forced-convection system with boiling is often associated with the shape of the pressure drop versus flow rate curve. Inlet subcooling, system pressure, heat flux, mass flow rate, and inlet throttling have a strong effect on the shape of this curve and thus on flow stability. An additional purpose of this study is to find the effect of these parameters on flow stability.

Moreover, the main objective of this work is to find the conditions which assure steady operation in a horizontal, parallel-channel, forced-convection boiling flow system so as to be able to predict whether such systems are stable or not.

CHAPTER II

BACKGROUND OF THE PROBLEM AND LITERATURE REVIEW

2.1 Two-Phase Flow Instability

Because of its technological importance the problem of two-phase flow instability has received a great deal of attention in the past several years. The results, however, have not given a clear picture of the problem and in some areas contradictory conclusions have been obtained. This is mainly because of the fact that there are a great number of mechanisms which cause unstable behavior and also because understanding and analysis of the flow instability problem requires a knowledge of many related technical specialties.

In the following sections the different types of hydrodynamic instability will be reviewed, and an attempt will be made to categorize these instabilities. A more general review of this subject is given by Boure, et al. (1).

2.2 Excursive Instability

Excursive or Ledinegg instability is the one in which the operating point of the system shifts from one flow rate to another (usually to a lower flow) in a non-recurring manner.

The details of analysis for excursive instability are given in Appendix A. The final result is given by the following equation which gives the criterion for instability to happen.

$$\frac{\partial}{\partial \dot{m}} (\Delta P_{ext.}) - \frac{\partial}{\partial \dot{m}} (\Delta P_{int.}) > 0 \tag{2.1}$$

Equation (2.1) means that if at a certain point the slope of the pressure drop characteristic of the external system is more positive than that of the channel, an excursive instability will take place.

Figure 1 is a typical curve of over all channel pressure drop versus flow rate for a given heat flux, inlet subcooling, and system pressure.

Consider line ABC which characterizes a constant pressure drop system. Practically, this happens when we are dealing with parallel channels between two large common headers. If a significant change in flow rate occurs in one channel, the total flow rate will be distributed in other channels, and the system pressure drop will remain essentially constant. At points A and C,

$$\frac{\partial}{\partial \dot{m}} (\Delta P_{ext.}) - \frac{\partial}{\partial \dot{m}} (\Delta P_{int.}) < 0$$

and the flow is stable. At point B,

$$\frac{\partial}{\partial \dot{m}} (\Delta P_{ext.}) - \frac{\partial}{\partial \dot{m}} (\Delta P_{int.}) > 0$$

an unstable operation is predicted. If the flow rate at point B is decreased slightly, the flow will jump to point A since point A is the only stable point for slightly lower flow rate. Similarly a small increase in flow rate will cause the operating point of the system to shift to point C.

Curve EFG shows a typical pump characteristic. In this case, with the above arguments, the operation at point F is unstable and the flow will shift either to point E or G.

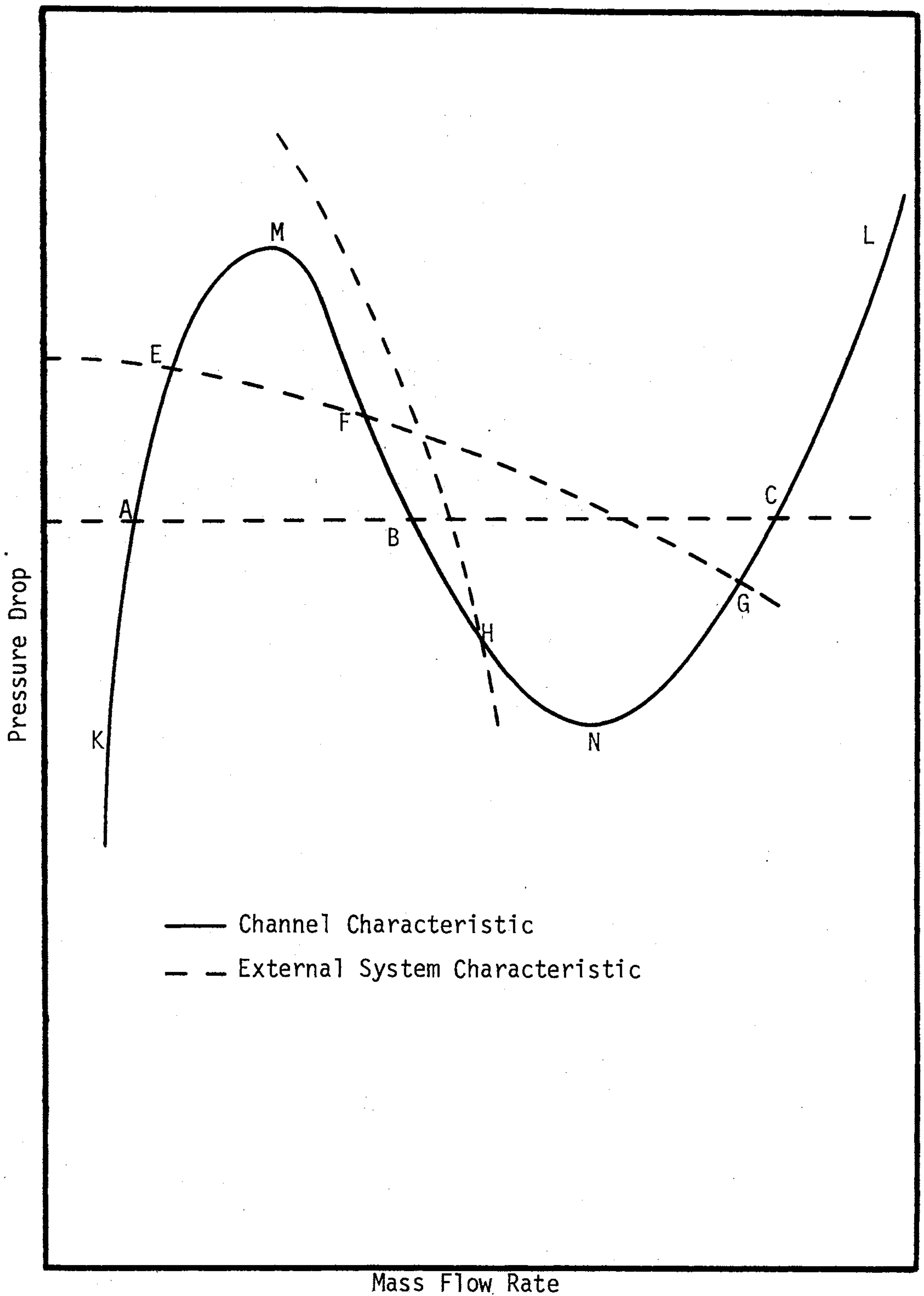

Figure 1. Pressure Drop Characteristics Versus Flow Rate

Another external system is shown in Figure 1 which intersects channel characteristic curve at point H. Although point H is in the negative slope region of the channel characteristic curve, the operation at this point is stable because

$$\frac{\partial}{\partial \dot{m}} (\Delta P_{ext}) - \frac{\partial}{\partial \dot{m}} (\Delta P_{int.}) < 0.$$

In a system with many parallel channels, flows between points M and N are never experienced and a small decrease in flow rate at point N will shift the operation point to K, and a small increase in flow rate at point M will shift the flow rate to point L.

It is to be noted that in a large bank of parallel tubes between common headers where any individual tube sees an essentially constant pressure drop, excursive instability is the dominant mechanism. Stable operation beyond the minimum point can be obtained only by orificing individual channels at their inlet.

2.3 Flow Pattern Transition Instability

This type of instability is due to the fact that when gas and liquid flow together in a channel, there are many possible configurations in which the two phases can arrange themselves. Some of these arrangements known as flow regimes are given in Figure 2.

The most important regime as far as instability is concerned is "slug" flow which is characterized by alternating flow of liquid slugs separated by large vapor bubbles. At any point the oscillations in pressure, flow rate, and heat transfer coeficient can be observed as the liquid slugs pass over this point. The reason is that at the point in question, the channel is filled alternately by liquid and gas. The time

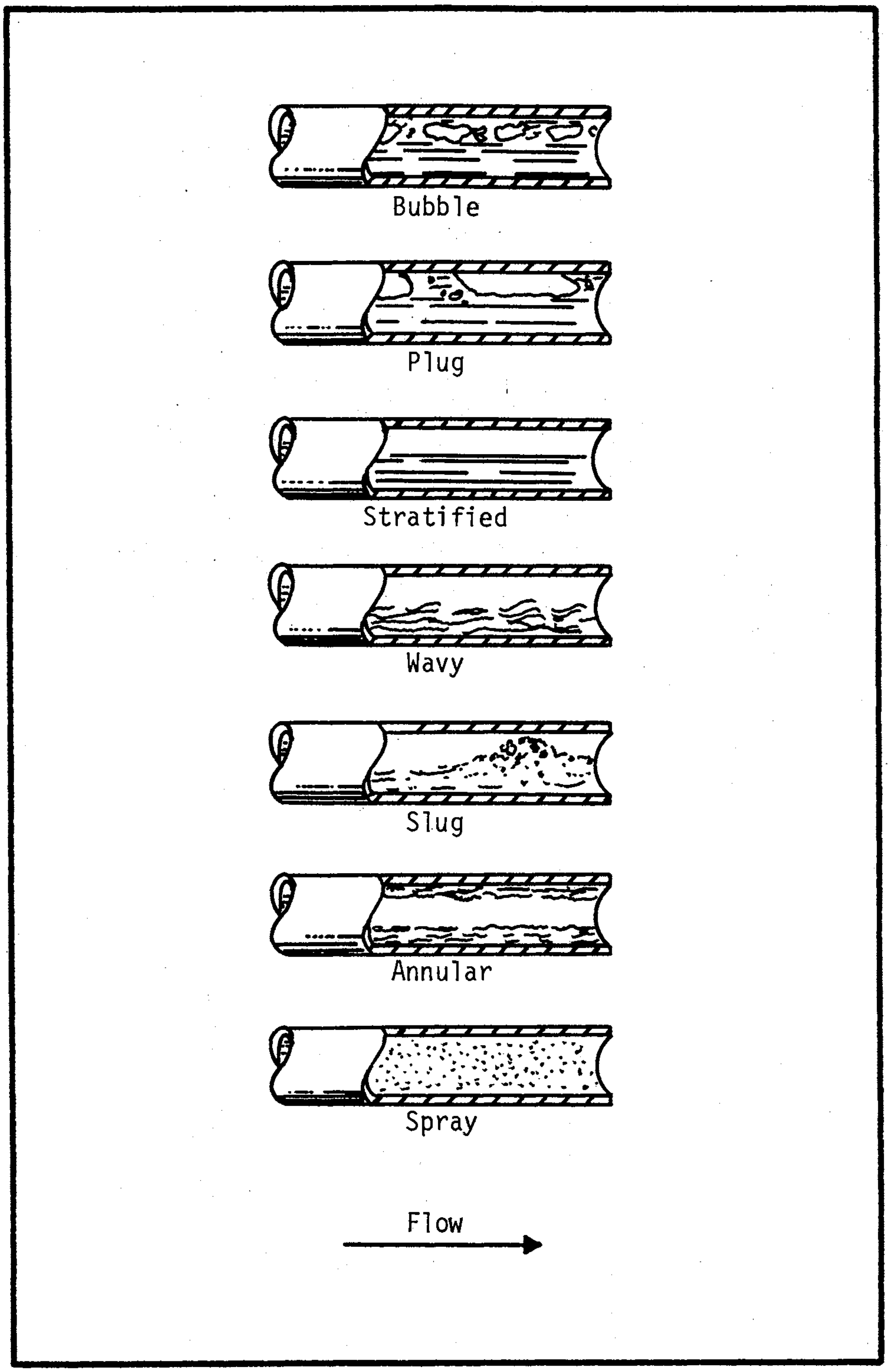

Figure 2. Flow Patterns in Horizontal Two-Phase Flow

required for the gas bubble to pass a certain point is very important, because it is during this time that the heat transfer coefficient is lowered considerably and the wall temperature will increase. If the transit time of the bubbles is long enough, burnout may occur.

Another type of flow pattern instability occurs when the flow condition is close to the point of transition from bubbly flow to annular flow. A temporary increase in the number of bubbles generated in the channel will change the flow regime to annular flow which has less pressure drop than bubbly flow. This reduction in pressure drop will cause the flow rate to increase. When the flow rate increases, the generated bubbles may not be sufficient to maintain the annular flow and the flow regime will change to bubbly-slug flow and the cycle will repeat.

It should be mentioned here that these types of instabilities can not be eliminated by inlet throttling because of the fact that formation of either slug flow, bubbly flow, or annular flow is primarily dependent on the flow rate and heat flux and independent of any external system characteristics.

2.4 Density Wave Instability

The origin of density wave oscillations can be clearly understood by considering a heated channel followed by a flow restriction. Assume that the heat flux is constant. For a constant pressure drop across the flow restriction, the volume flow rate through the restriction is inversely proportional to some power of the mixed fluid density entering the restriction. A small perturbation to a lower flow rate will cause more vapor to form in the heated section, which will decrease the density of the mixture and the less dense fluid will pass through the restriction very fast. This will increase the flow rate and less vapor will be formed in the channel and the density of the mixture will increase. The more dense fluid will pass through the restriction slowly and more vapor will be formed in the heated section. As soon as the less dense mixture reaches the restriction, the cycle starts over again. At any given point in the channel there is an oscillation in pressure, flow rate, and heat transfer coefficient.

These are low frequency oscillations in which the period of oscillation is approximately of the order of magnitude of the residence time of a fluid particle in the heater.

Density wave oscillations occur in the positive slope branch of the pressure drop versus mass flow rate, Figure 3. An inlet orifice in creases single phase pressure drop which is in phase with the change of inlet flow; and thus, it provides a damping effect on the increasing flow. Hence, these oscillations can be eliminated by providing sufficient inlet throttling.

2.5 Pressure Drop Oscillations

Pressure drop oscillations occur in systems having a compressible volume upstream of, or within, the test section such as a surge tank or gas pressurizer. When an attempt is made to operate on the negative slope region of the pressure drop versus flow rate curve, these oscillations will take place, Figure 3.

Consider a system which has a compressible volume upstream of the test section and in which supply pressure to the test section is a function of flow rate. If a small perturbation to a lower flow rate happens,

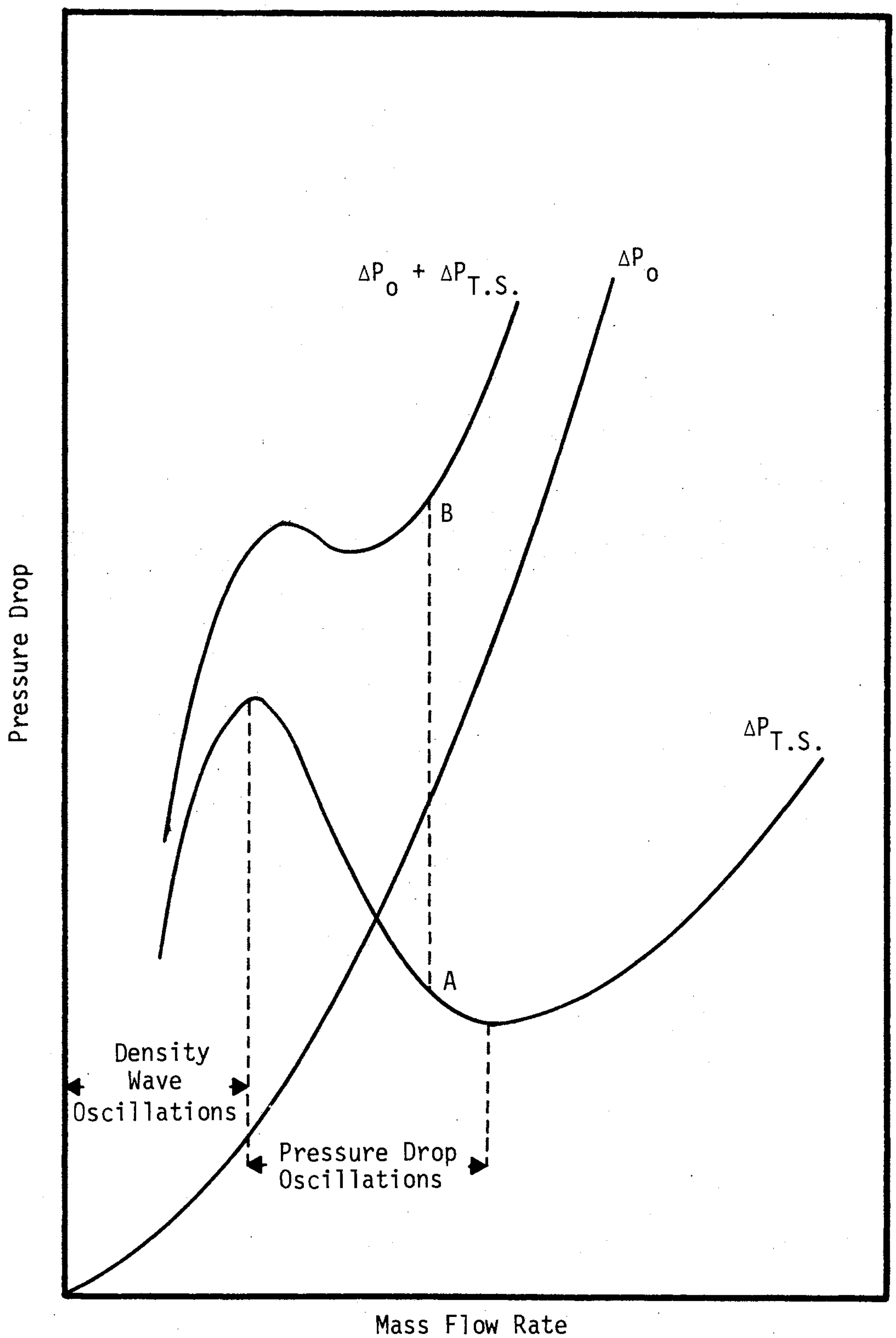

Figure 3. Density Wave and Pressure Drop Oscillations

the supply pressure to the test section will increase and at the same time the channel pressure drop will increase. This will cause the liquid to flow into the compressible volume until the supply pressure is not sufficient to drive any liquid into the compressible volume. At this point the flow rate into the test section will increase until it reaches the initial operating point. However, the inertia of the flow from the compressible volume will cause the flow in the test section to increase more and more and at the same time the supply pressure will decrease until the supply pressure is no longer sufficient to maintain the flow, and the flow rate to the test section will decrease and the cycle will start again.

The period of pressure drop oscillations is very much longer than the residence time of a fluid particle in the heater. Consider point A which is in the negative slope region of the pressure drop-flow rate curve, Figure 3. Operation at this point might be unstable. By imposing a sufficient inlet orifice pressure drop on this curve, the operation point will shift to point B which is in the positive slope region of the overall pressure drop-flow rate curve. Hence, these instabilities can be prevented by throttling the flow at the channel inlet.

These are the most important types of instabilities encountered in a forced-convection system with boiling; however, there are other types of instabilities which have been reported in literature and which will happen only in certain flow arrangements. Bumping, geysering, chugging, and acoustic instabilities are examples.

2.6 Instabilities in a Forced-Convection System

A forced-convection system with boiling might be subject to one or more types of the instabilities mentioned above. In the following sections, previous investigations on two phase flow instabilities in a forced-convection system will be reported. These investigations are divided into two major categories: 1) instabilities in a single heated channel, 2) instabilities in parallel heated channels.

2.7 Single Heated Channels

Ledinegg (2) in 1938 was the first to analyze the instability of a forced-convection system. He found that a channel may operate unstably if it is operating in the region where the steady state pressure drop versus flow rate curve has a negative slope. This behavior requires that the channel characteristic exhibits a region where the pressure drop decreases with increasing flow rate. More detailed treatment of this subject was presented by Chilton (3) and Markels (4). These analytical investigations are identical to Ledinegg's as far as the basic mechanism is concerned, but they contain detailed mathematical calculations.

Lowdermilk, et al. (5) investigated stable and unstable burnouts at low pressures in small diameter tubes. The effects of upstream throttling on a vertical tube were investigated. They found that it was always possible to stabilize the flow with enough inlet throttling.

Fraas (6) analyzed the flow instability in a forced-convection system with constant heat flux. According to his investigation, the negative slope region in the pressure drop versus flow rate curve increases with increasing degree of inlet subcooling and decreasing system pressure.

Blubaugh and Quandt (7) observed that a primary cause of flow oscillations are inlet subcooling and system pressure.

Mendler, et al. (8) carried out some experimental investigations under natural and forced-convection conditions using a rectangular channel as test section. They observed some flow fluctuations in two-phase natural circulation flow which were not present in forced-circulation flow at the same conditions. They also observed that these fluctuations increased at lower inlet temperatures and pressures.

Fraas (9) showed that in a vaporizer tube with constant heat flux, the stabilizing effect of inlet orificing increases with increasing the ratio of the orifice pressure drop to the pressure drop for the rest of the channel.

A theoretical approach of Jones (10) about instabilities of two-phase flow involves a point by point computer solution along the heated channel. He neglected the effects of subcooled boiling in his calculations, but considerable attention was given to all other two-phase flow calculations. His analysis appears to be the most precise which has been presented. However, the physical picture is lost in the mathematics and the application of his results is difficult.

Quandt (11) theoretically studied the instabilities in a heated channel. By assuming a homogeneous mixture of liquid and vapor, he started his analysis by formulating the four basic equations of two-phase flow: continuity, momentum, energy, and state. These equations then were written for small perturbations and the perturbed equations were integrated along the channel and the LaPlace transforms of the integrated equations were taken. Constant pressure drop and constant heat flux boundary conditions were applied. Two types of instabilities resulted from the analysis. One was flow excursion and the other was oscillatory instability. He further found out that if the system is operating at higher pressures, the oscillations have a tendency to damp out. The mathematical manipulation in his treatment is so complex that the physical picture is difficult to grasp.

Stenning (12) considered the flow of a boiling liquid in a channel and analyzed the problem analytically. He confirmed Lowdermilk's (5) observations and also showed that as long as the ratio of inlet density to exit density across the test section exceeds a critical value, the flow oscillations will exist in the system.

Stenning and Veziroglu (13) carried out some experimental investigations with boiling Freon-11 in a horizontal channel with constant heat flux. They observed two distinct modes of oscillations: density wave oscillations and pressure drop oscillations. They observed that these oscillations could be eliminated by providing sufficient orificing at the channel inlet provided that no cavitation occurs in the inlet orifice.

Stenning and Veziroglu (14) studied the density-wave type flow oscillations in boiling Freon-11 in a horizontal tube. They observed that these oscillations occur when the heat input exceeds a critical value for each set of operating conditions. They found out that an increase in the ratio of inlet to exit density across the evaporator decreases stability. They also studied the effect of subcooling on the density-wave oscillations and concluded that subcooling effects are extremely complex and an increase in subcooling may increase instability or decrease it depending on the conditions of the experiment.

Veziroglu and Lee (15) investigated the instabilities in a vertical single-channel forced-convection boiling upward flow with Freon-11. They studied experimentally the effect of flow rate, heat input and exit restriction on different types of oscillations. They identified two major modes of oscillations, namely density-wave and pressure drop oscillations. With regard to density-wave oscillations the following results were obtained:

1. Oscillations occur in the positive slope branch of the two-phase pressure drop versus mass flow rate curve.

2. An increase in mass flow rate increases stability.

3. An increase in heat input decreases stability.

4. Exit restrictions decrease stability.

With regard to pressure drop oscillations they found that:

1. Pressure drop oscillations occur on the negative slope portions of the pressure drop versus flow rate curve.

2. An increase in heat input decreases stability.

3. An increase in the negative slope of pressure drop versus flow rate curve decreases stability. They also observed that in general the vertical upward flows appear to be more stable than the horizontal flows.

Maulbetsch (16) studied pressure drop oscillations in considerable detail for subcooled boiling of water in horizontal channels. The effect of compressible volume on this type of instability was investigated. He found that:

1. Pressure drop oscillations are associated with operation on the negative slope region of the pressure drop flow rate curve.

2. In a single tube system, for a known supply system characteristic, and for a known amount of compressibility upstream of the heated

section, a critical slope of the overall pressure drop versus mass flow rate curve is required for the initiation of the pressure drop oscillations.

3. This critical slope increases with increasing the stiffness of the compressible volume.

4. In systems where the compressible volume has essentially zero stiffness, this critical slope is equal to zero and the oscillations initiate at the minimum point of the pressure drop versus mass flow rate curve.

5. When the compressible volume is external to the test section, this type of instability can always be prevented by sufficient throttling between the compressible volume and the heated section.

2.8 Parallel Heated Channels

Gouse and Andrysiak (17) studied the effect of subcooling on the flow oscillations in a system of three vertical heated channels. They reported that there was a range of subcooling within which the flow would oscillate, if the inlet subcooling were either greater or smaller than this range, the flow was steady. They also observed that an increase in the flow rate, with other variables held constant, increases stability.

Berenson (18) performed some experiments to investigate flow stability in a multitube forced-convection vaporizer. He used a five-tube horizontal boiler as test section with Freon-113 evaporating inside the tubes. The results of his experiments are:

1. An increase in inlet orifice pressure drop will increase stability.

2. An increase in entrance subcooling will increase stability.

3. An increase in the ratio of inlet density to exit density will decrease stability.

Schuster and Berenson (19) continued experimental investigation of Berenson (18) with the same loop and the same fluid test and confirmed the results of Berenson (18). The additional results of their experiments are:

1. The ratio of orifice pressure drop to two-phase pressure drop required to produce stable flow should be within a specific range (0.05 to 0.9). This range depends on the condition of the experiment.

2. Entrance subcooling tends to destabilize the flow up to a critical value (this critical value is dependent on the experiment condition); after this critical value, further subcooling increases stability.

3. Because of the coupling effect and phase relationship between tubes in a parallel tube boiler, flow oscillations out of the boiler are usually smaller than flow oscillations out of individual tubes.

Veziroglu and Lee (20) investigated the instabilities in a two-parallel-channel forced-convection boiling upward flow system using Freon-11. They observed the same two major modes of oscillations encountered in single-channel systems, namely the density wave oscillations and the pressure drop oscillations.

These two types of oscillations were encountered for all combinations of heat inputs whenever the flow rate through one channel was low enough to produce a relatively high inlet to exit ratio (15 or more).

With regard to the density wave type oscillations the following results were obtained:

1. Oscillations start when the density ratios (inlet to exit for one or both channels) are about 15 or more.

2. The period of oscillations is relatively low and is approximately in the order of magnitude of the residence time of a fluid particle in the heater.

3. Increasing the flow rate will increase the period of oscillations.

4. Decreasing the difference between the heat input into two channels will increase the period of oscillations. This means that the system is most stable when both channels receive the same amount of heat input.

5. An increase in total flow rate and inlet pressure drop increases stability.

With regard to pressure drop oscillations these results were obtained:

1. The oscillations occur when the pressure drop across the test section decreases with increasing flow rate.

2. The period of oscillations increases with increase in flow rate.

3. An increase in total flow rate and inlet pressure drop increases stability.

They also observed that the flow oscillations in the inlet plenum were smaller than those of individual channels. In general the system could be stabilized by introducing a pressure drop between the inlet plenum and any one of the channels, but not by introducing a pressure drop on the upstream side of the inlet plenum.

2.9 Closure

The literature review summarized above indicates that the problem of two phase flow instability is rather complex and a forced-convection system is subject to many different types of instabilities. Each type of instability is affected by numerous parameters. The following conclusions can be obtained from the literature:

1. The major part of instabilities in a forced-convection system is associated with the minimum point and negative slope region of steady state pressure drop-flow rate characteristic of the heated section.

2. The effect of inlet subcooling on the stability is not straightforward. An increase in subcooling can either increase or decrease stability. However, the experiments seem to indicate that there is a range of subcooling within which the flow would oscillate, if the subcooling is either greater or smaller than this range, the flow will be stable.

3. Heat flux has a destabilizing effect and increasing heat flux will increase instability.

4. The effect of system pressure on stability appears to be the most definite, because experiments have all shown that as the pressure is increased, holding other variables constant, the system becomes more stable.

5. The results of all experiments have shown that an increase in inlet orifice pressure drop will increase the stability.

6. The effect of mass flow rate on stability is that increasing the flow rate, with holding other variables constant, will increase stability.

CHAPTER III

EXPERIMENTAL APPARATUS

In this chapter the description, schematic diagrams, and photographs of the experimental facility which was used to obtain experimental data will be reported.

3.1 Hydraulic System

A schematic diagram of the apparatus which is of the closed loop type is shown in Figure 4. The pipings, fittings, and instruments were all built around a test bench which was constructed of plywood and slotted angle irons. All the tubing in the main loop was made of copper with ½ inch outside diameter and 0.032 inch wall thickness. The valves and fittings in the main loop were all brass for corrosion resistance. The test section line could be isolated from the main loop by means of two gate valves.

A survey of the characteristics of several fluids led to the selection of Freon-113 as the test fluid. It has low heat of vaporization, well established physical properties, and is relatively non-hazardous. Freon-113 was stored in an approximately 10 gallon cylindrical stainless steel supply tank. The supply tank was tested against pressure with hydraulic fluid up to 200 psi before installation. This tank was connected to the pressurized air line in the laboratory which had a pressure of approximately 160 psi. A pressure regulating valve was installed

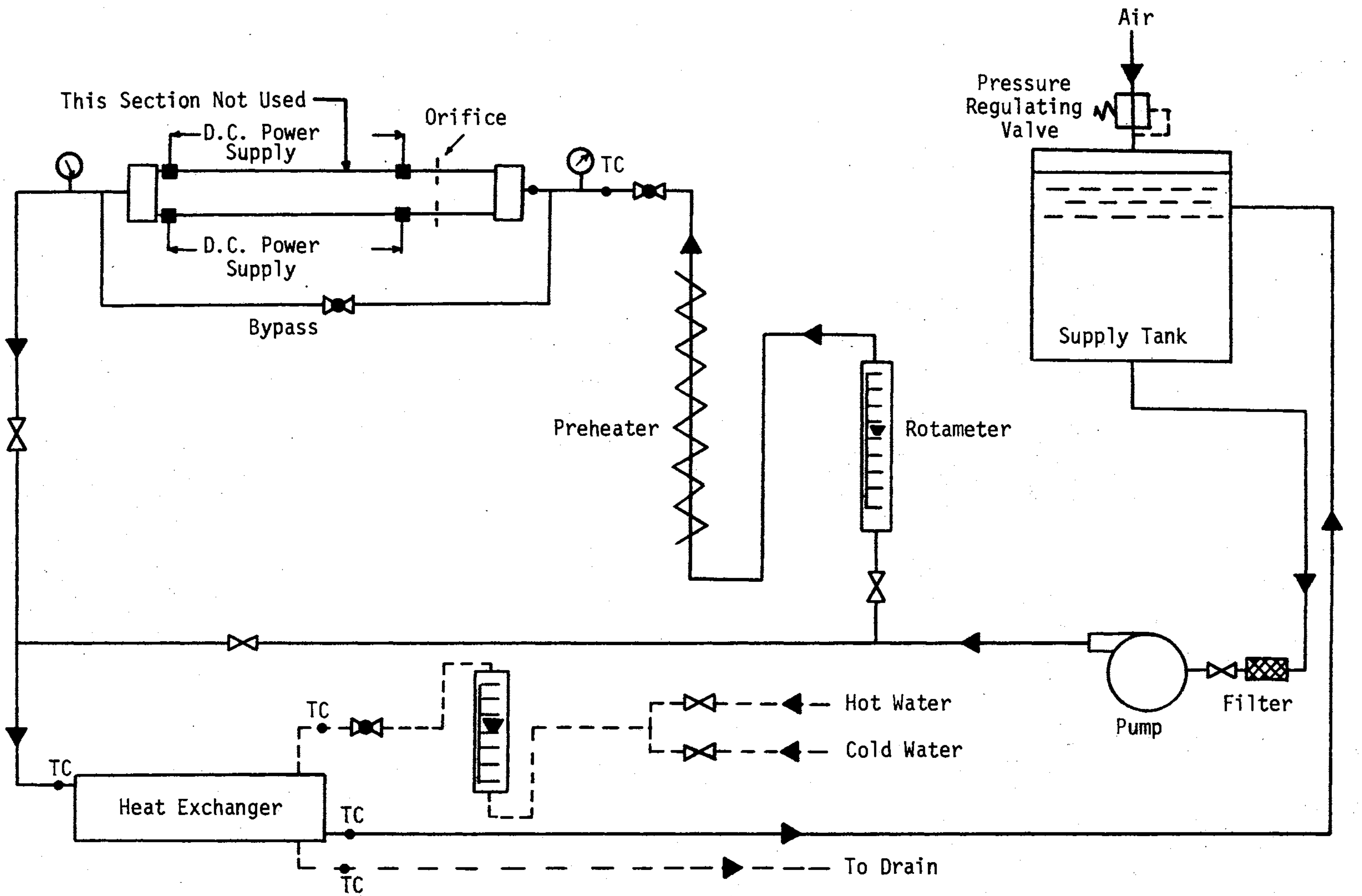

Figure 4. Schematic Diagram of the Loop

between the supply tank and the pressurized air line and by means of this valve the system pressure could be easily controlled.

Flow circulation was provided by a system of two pumps which were connected in series in such a way that it was possible either to use any one of them while the other one was shut-down, or to use both of them at the same time whenever high flow rates were required.

The first pump was a 1/3 horsepower centrifugal pump which was capable of handling 18 gallons per minute of water at zero head. The second pump was a 1/6 horsepower centrifugal pump with a capacity of 10 gallons per minute of water at zero head.

A filter made of wire mesh was installed just upstream of the pumping system to prevent external particles from entering into the main loop and the test section. A globe valve was installed on the downstream of each pump. This made it possible to control the flow rate in the main loop. The pumping system was connected to the main loop by a piece of short flexible stainless steel tube with an outside diameter of 5/8 inches. This arrangement was used to prevent transfer of the pump vibrations to the main loop.

The main loop also contained two Brooks flow meters for measurement of the flow rates. Two Briskeat electrically heated flexible heating tapes of approximately 900 watts were wrapped on the main loop tubing upstream of the test section to control the test section inlet temperature. The power output of these tapes were controlled in a continuous range from 0 to 900 watts by means of a variac mounted on the test bench.

The schematic diagram of the test section which was mounted on the top of the test bench is shown in Figure 5. The test section consisted

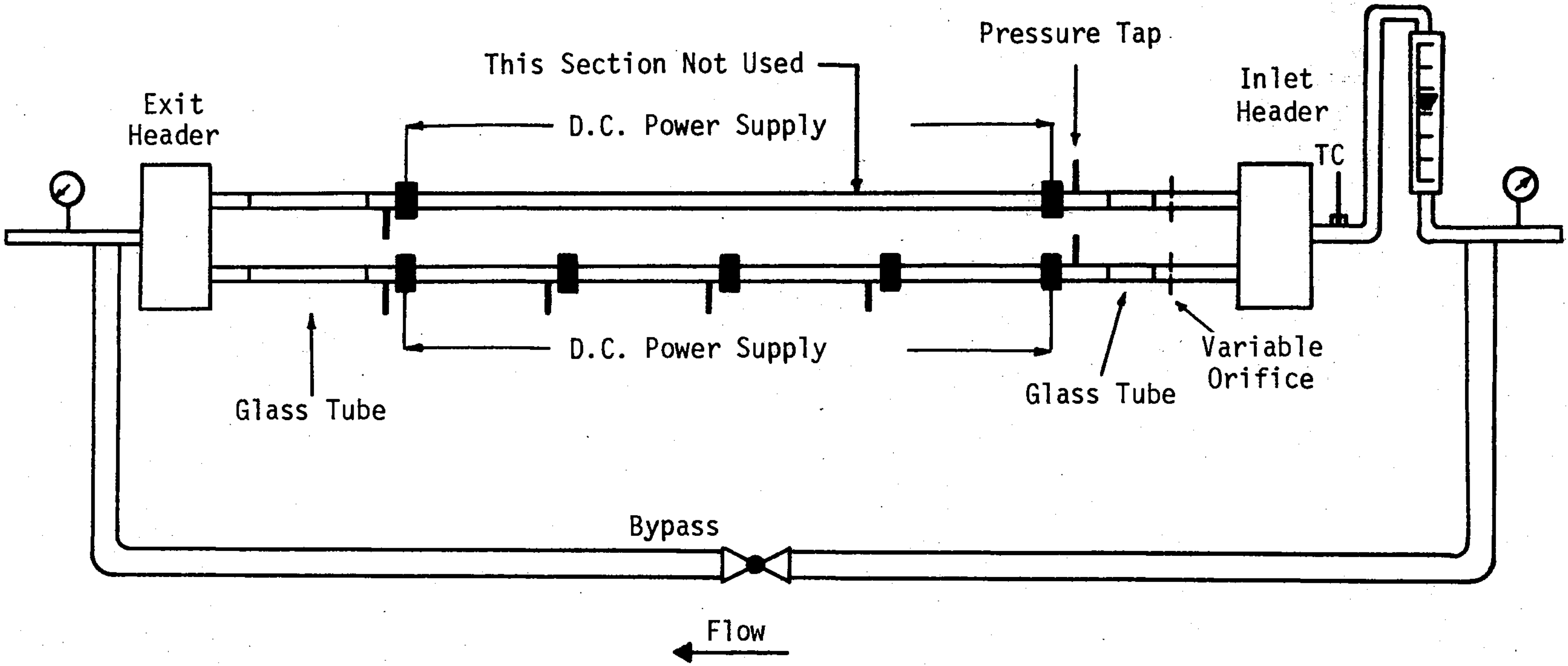

Figure 5. Schematic Diagram of the Test Section

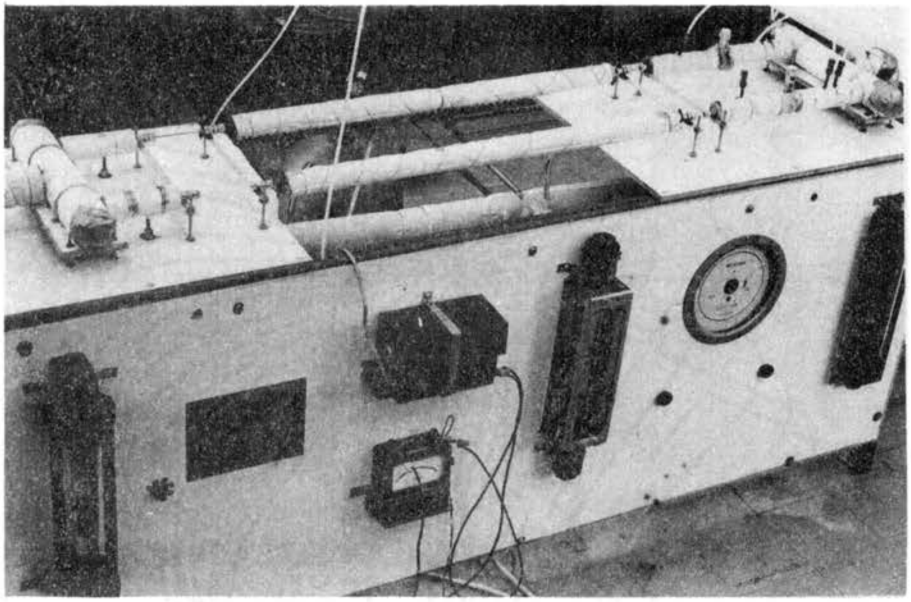

Figure 6. General Arrangement of Apparatus, Front View

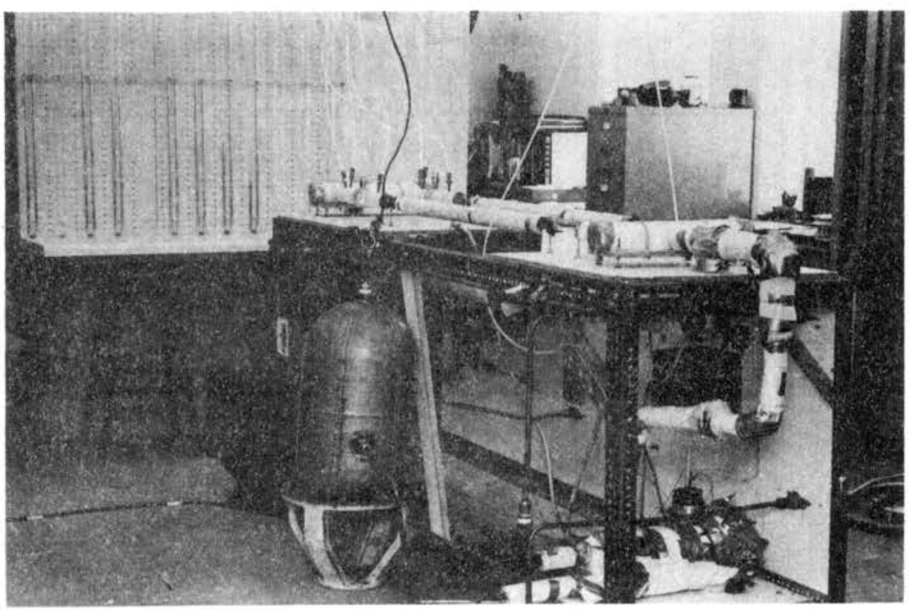

Figure 7. General Arrangement of Apparatus, Back View

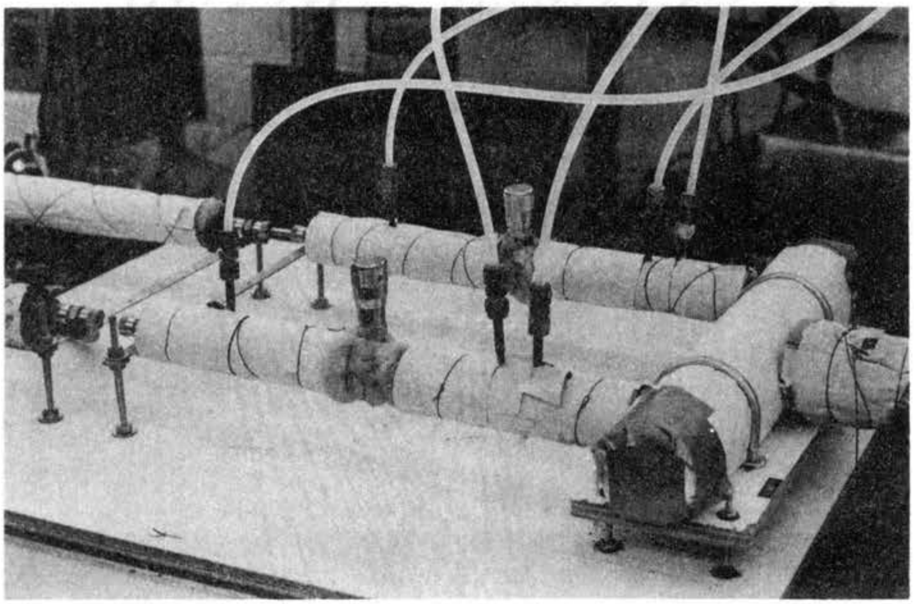

Figure 8. Inlet Header and Inlet Orifice Arangement

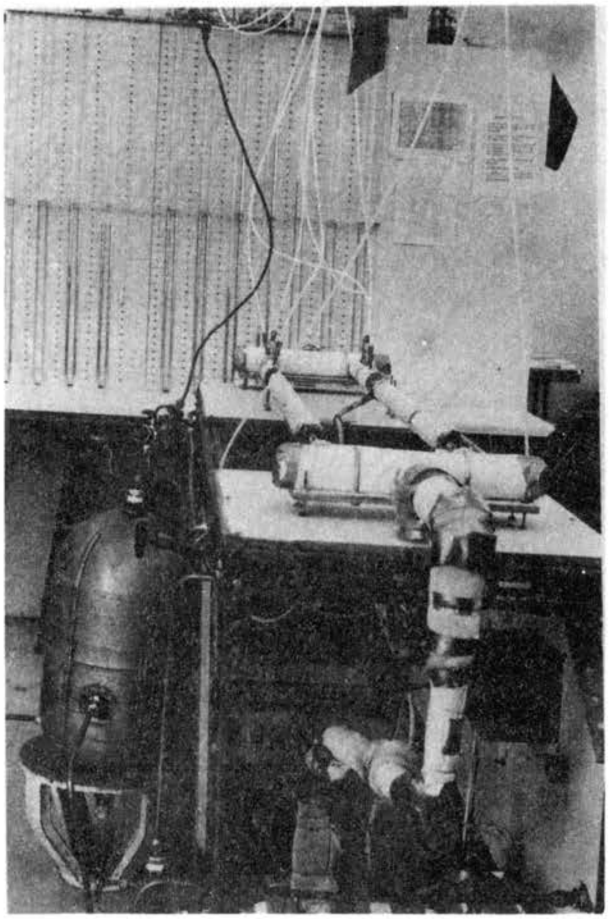

Figure 9. General Arrangement of Apparatus, Side View

of two horizontal parallel tubes between two large common inlet and exit headers with a large bypass around them, the two parallel tubes were 10 inches apart.

All the tubings and fittings in the test section were stainless steel for corrosion resistance except the bypass which was copper. The heater section was made of type 304 stainless steel with an outside diameter of 1/4 inch and an inside diameter of 0.176 inch. The inlet and exit headers were each 16 inches long and were made of a 2 inch nominal diameter, schedule 40 stainless steel pipe, and were tested against pressure with hydraulic fluid up to 200 psi before installation. The headers were mounted on two adjustable supports which made it possible to adjust the level of heaters and maintain a horizontal and parallel position. The test section flow rate was controlled by a 1/4 inch, Hoke 2300 series, globe pattern, stainless steel micro metering valve with 1/8 inch orifice. The 20 turn stem displacement from closed to open enabled this valve to give fine metering performance. This valve was set just upstream of the heater section.

Four different test sections were used with the same diameter, but different lengths, the complete dimensions of these test sections are given in Table I.

Since the system was a closed loop, the heat added to the test fluid Freon-113 was rejected to the city water in a Ross compact shell and tube heat exchanger with Freon in the shell side and water in the tubes.

Since the two flexible heating tapes which were wrapped on the tubes upstream of the test section to control the inlet temperature did not have sufficient power to raise the Freon temperature to high values, the Freon temperature was raised in the heat exchanger by increasing the water temperature in the tube side. To do so, the hot water line in the laboratory was connected to the cold water line. Two globe valves installed in each line provided sufficient control of the hot water and cold water flow rates and consequently, the inlet water temperature into the heat exchanger could be well controlled. The water flow rate was controlled by means of a globe valve set at the inlet to the heat exchanger. The water line also contained a Schutte-Koerting flow meter.

TABLE I

DIMENSIONS OF THE TEST SECTIONS

Test-section Identification	Inside Diameter inch	Heated length inch	Heated length to Diameter ratio
1	0.176	36	204
2	0.176	27	153
3	0.176	18	102
4	0.176	9	51

3.2 Power Supply

Power was supplied to the test section by means of a 9.6 KW Mallory D.C. power generator. The generator could deliver power in two different ranges. In the first range the generator was capable of delivering 800 amperes at 12 volts, and in the second range it could deliver 400 amperes at 24 volts. A switch on the generator made it possible to regulate the power output in 8 equal discrete steps from zero up to the maximum power. The generator was driven by a 220 volt, 3 phase motor.

A Mullenbach variable resistor, installed in series with the test section, made it possible to dissipate the excess power of the generator whenever it was desired and at the same time made it possible to regulate the power input into the test section.

The test section tube was used as the electrical resistance for providing a uniform heat input. Five copper bus-bars were silver soldered on the test section. At the upstream and downstream sides of the test section, the ends of the cable assembly were clamped to the bus-bars.

The heater tube was electrically insulated from the rest of the loop by two pieces of glass tube on the upstream and downstream of the test section. The glass tube on the upstream side was 2 inches long and the one on the downstream side was 5 inches long. These were Corning precision bore Pyrex glass tubing and had the same inside and outside diameters as the test section. The use of the glass tube for electrical insulation of the test section made it possible to check and make sure that no evaporation started in the liquid before entering the heater.

The glass tubes were connected to the stainless steel tubing of the test section by means of four 1/4 inch Cajon ultra-torr stainless steel unions. The special feature of these unions were that they permit the thermal expansion of the heater tube.

3.3 Instrumentation

Instrumentation was provided to measure the Freon and water flow rates and their temperatures at different locations as well as the test section pressure drop, test section exit pressure, and the test section heat input. A total of six thermocouples were used for temperature measurements, two were installed upstream of the test section, one at the test section exit and upstream of the heat exchanger, one at the downstream of the heat exchanger. These four thermocouples were used to measure Freon temperature. Two more thermocouples were installed at the upstream and downstream of the heat exchanger on the water line to measure the inlet and exit water temperature to and from the heat exchanger. The thermocouples were iron-constantan and were made of 30-guage wire. At the point of each thermocouple installation a hole was drilled in the tube and a short piece of brass tubing which had a blind end was inserted into the hole such that the blind end was approximately at the center of the tube. The brass tube was then silver soldered on the outside to the main tube. The brass tube had an outside diameter of 1/8 inch and an inside diameter of 0.058 inch. The thermocouple junction was then inserted into the brass tube such that the thermocouple junction was always in touch with the blind end of the brass tube.

When the thermocouples were installed, they were calibrated by bleeding steam through the tube. Due to the conduction losses, all the thermocouples showed a temperature less than that of the steam. The maximum temperature difference was less than 1 °F. This temperature deviation was proportional to the temperature difference between the thermocouple junction temperature and the ambient temperature. For actual runs, the loop was operating at temperatures much less than 212 °F., thus, the temperaturé deviations from the actual values were much less than 1 °F.

Because of this slight temperature deviation, no corrections were made for the temperature readings. A cold junction was maintained by an ice-water mixture in a small flask and the thermocouple junctions were all submerged in a glycerine-filled test tube which minimized fluctuations in cold junction temperature during ice renewal. The thermocouples were attached to a Digitec potentiometer by a switch which had six positions.

The potentiometer was also calibrated by a galvanometer and the accuracy of the potentiometer was within 0.01 millivolts.

A Wallace-Tiernan pressure gage was used to measure the test section exit pressure with an accuracy of 0.05 psi. This pressure gage was calibrated by a mercury manometer before installation, the calibration curve is given in Appendix C.

The test section flow rates were measured by three rotameters, a Brooks rotameter was used to measure the high flow rates, and a Cox rotameter and a Fischer-Porter rotameter were interchangeably used to measure the low flow rates. These rotameters were all calibrated for water flow rates and the sizing factors of each rotameter was calculated at different temperatures. To obtain the equivalent Freon flow rate of each rotameter at a specific temperature, the equivalent water flow rate of that rotameter was divided by the sizing factor of the rotameter at that temperature.

The water flow rates into the heat exchanger were measured by a Schutte-Koerting rotameter which was calibrated before installation. The calibration curves for all rotameters are given in Appendix C.

The test section pressure drops were measured by means of a mercury manometer system. Basically, it consists of two 48-inch U-tube Meriam manometers. The manometer lines could be freed from trapped air through appropriate valves. An approximate check on the manometer readings could be obtained from the pressure gage. The pressure gage was connected to two pressure taps, one at the test section exit and the other one at the upstream of the inlet header by two 1/4 inch plastic tubing; and a valve was installed on each line. By closing one valve and opening the other one, it was possible to obtain an approximate test section pressure drop. A better way to find out whether the manometer system was working properly or not, was to determine if, under isothermal conditions, pressure level alone had no effect on the pressure drop.

A total of six pressure taps was installed on the test section, at each location a 1/32 inch hole was drilled in the test section tube, and the pressure tap tubes were silver soldered on the outside of the test section tube. The pressure tap tubes were made of brass and had an outside diameter of 1/8 inch and an inside diameter of 0.058 inch. Any burrs inside the tube were removed before the installation of the test section.

The heat input to the test section was computed from measurement of the voltage drop across the heated section and the current to the test section. The voltage drop was read on a Digitec, multirange D.C. voltmeter with an accuracy of $\pm$ 0.1% of full scale and the same voltmeter was used to measure the current to the test section by reading the voltage drop across a shunt which was in series with the test section.

Fiberglass insulation was wrapped around the tubing in order to minimize the heat losses to the surroundings. Most of the components in the loop were cleaned with acetone first and then with the water before installation.

It should be mentioned here that the system of two identical parallel test sections which were installed between the inlet and exit headers were designed for other studies, in this study only one of the test sections was used while the other one was removed from the loop.

CHAPTER IV

EXPERIMENTAL PROCEDURE

4.1 Range of Experimental Parameters

The design of the experimental apparatus provided a rather wide choice of variables for studying the system behavior. The final selection of the range of the variables was based on the equipment availability.

Table II shows the range of experimental parameters.

TABLE II

RANGE OF EXPERIMENTAL PARAMETERS

Parameter	Range
Inlet Temperature	85 - 120° F
Exit Pressure	25 - 70 psia
Mass Flow Rate	0.5 - 13 lb_m/min
Heat Flux	0.0 - 50,000 BTU/hr-ft^2
Length to Diameter Ratio of Heated Section	51 - 204

4.2 Operation Procedure and Data Taking

After the loop assembly was completed, it was hydrostatically tested by pressurizing the Freon-filled loop to 70 psia. The leaks were detected by a Freon leak detector and all of them were stopped.

The data was obtained at constant heat flux, constant exit pressure and constant inlet temperature while varying the mass flow rate.

At the beginning of each run, the system was pressurized and the vents were opened for the air to escape. When the system was free of air, the pump was turned on and the water line was opened for water to flow through the heat exchanger. Before turning on the generator and the preheaters, the flow rate was set to a constant value and the test section pressure drop was read from the manometer at the same flow rate but at different exit pressures under isothermal conditions. Since the pressure drop is independent of the pressure level under isothermal conditions, the pressure drops measured for the same flow rate but at different pressure levels should be the same. If this were the case, then the manometers were working properly and no air was trapped in the manometer lines; but if this were not the case, the lines were bled and similar runs were repeated until constant pressure drop was obtained for the same flow rate at different pressure levels.

When the manometer system was working properly, the generator and the preheaters were turned on. It was necessary for the generator to work 1½ hours in order to warm up and maintain a steady voltage. At the end of this time, the heat flux, exit pressure, and inlet temperature were set to desired values and the flow rate was set to a high value and the testing began.

Freon inlet and outlet temperatures, water inlet and outlet temperatures, room temperature, Freon exit temperature from the heat exchanger, Freon and water flow rates, voltage drop across the test section, current through the test section, test section exit pressure, and the test section pressure drop were all recorded. The flow rate was then lowered to a new value. As soon as the flow rate was changed, the test section exit pressure and the Freon inlet temperature were also changed. The pressure regulator on the pressurized air line and the preheaters power output were adjusted to maintain the desired values of exit pressure and inlet temperature.

It was very difficult and time consuming to maintain a constant inlet temperature, so a deviation of $\pm$ 1 °F from the desired value in the inlet temperature was permitted.

The flow rate was further decreased until a further decrease in the flow rate increased the pressure drop. Since the location of the minimum point in the pressure drop-flow rate curve was one of the objectives of this study, more data was taken in the neighborhood of this point. The flow was further decreased and the pressure drop increased, indicating that the system was operating in the negative slope region of the pressure drop-flow rate curve. Operation in this region was unstable and the pressure drop started to oscillate. This could be seen from the oscillation of the mercury level in the manometer tube. To obtain a steady operation the flow was throttled upstream of the test section by micrometering valve. When the system became steady, see Figure 3, the data taking procedure started again. The flow rate was further decreased until a further decrease in the flow rate resulted in a decrease in the pressure drop. A number of points were taken in the vicinity of this maximum point and the flow rate was again decreased. For low heat fluxes the flow was decreased as low as it could be read from the rotameters, but for high heat fluxes the flow was lowered to the point where all the Freon was vaporized in the test section. The flow rate was not decreased beyond this point to avoid burnout.

When the system was operating at low flow rates, it was noticed that the power input into the test section was changed. This was because at low flow rates the wall temperature increased and this changed the electrical resistance of the test section. In such cases the power output of the generator was changed to maintain a constant heat flux into the test section.

For the large test section (L/D = 204) when the system was working in the negative slope region of the pressure drop-flow rate curve it was not always possible to maintain steady state operation by throttling the flow upstream of the test section. This happened especially when the system was working at high heat fluxes, low exit pressures, and high inlet temperatures. In such cases the flow was throttled as much as possible, this throttling reduced the amplitude of the pressure drop oscillations and then the average test section pressure drop was recorded. For other test sections, the system was always stabilized by upstream throttling.

Every day, before data taking started, the atmospheric pressure was read from a Fortin-type barometer and was corrected for the effect of room temperature and Stillwater altitude. The effect of altitude and room temperature was also applied to obtain specific gravity of mercury. These informations were later used to convert the pressure drop from inches of mercury to psi and to convert psig to psia.

At shutdown, the generator was first turned off and then the preheaters. The cold water line was fully opened and all the valves in the main loop were opened and the system was allowed to operate for 15 minutes at zero power. At the end of this time, the system was completely cool and the pump was turned-off and all the valves were closed.

The experimental procedure which was explained above was repeated for all the runs.

4.3 Test Section Heat Balance

After the loop assembly was completed and before the actual data taking started, several runs were made to calculate heat losses at various pressures, heat fluxes, and inlet temperatures. The heat losses for highest heat flux and highest inlet temperature was always less than 2%. For lower heat fluxes, the losses were always much smaller than 2%. Due to the fact that heat losses were very small, they were neglected.

CHAPTER V

EXPERIMENTAL RESULTS AND DISCUSSION

5.1 Pressure Drop Flow Rate Curve

The results for the heated section pressure drop versus mass flow rate are given in Figures 10 through 38. These results suggest that there are five regions of pressure drop in the pressure drop-flow rate curve. The first region is that of pure forced-convection and the flow rate is so high that no evaporation occurs in the heated section. The pressure drop in this region is smaller than that of the isothermal case, and this is due to the variation in fluid properties especially the viscosity with heat addition.

As the flow rate is decreased, the second region begins, which is characterized by formation of small bubbles. In this region which can be called "partial subcooled boiling" or "highly subcooled" region, only few nucleation sites are active and small bubbles grow and collapse while they are still attached to the heated surface and do not penetrate into the subcooled flow. The growth and collapse of the bubbles will cause the slope of the pressure drop-flow rate curve to decrease. It is in this region that the pressure drop-flow rate curve intersects the liquid isothermal pressure drop curve. A further decrease in the flow rate will cause the pressure drop still to decrease; however, the slope of the pressure drop-flow rate curve continues to decrease and the pressure drop is larger than that of the isothermal liquid case.

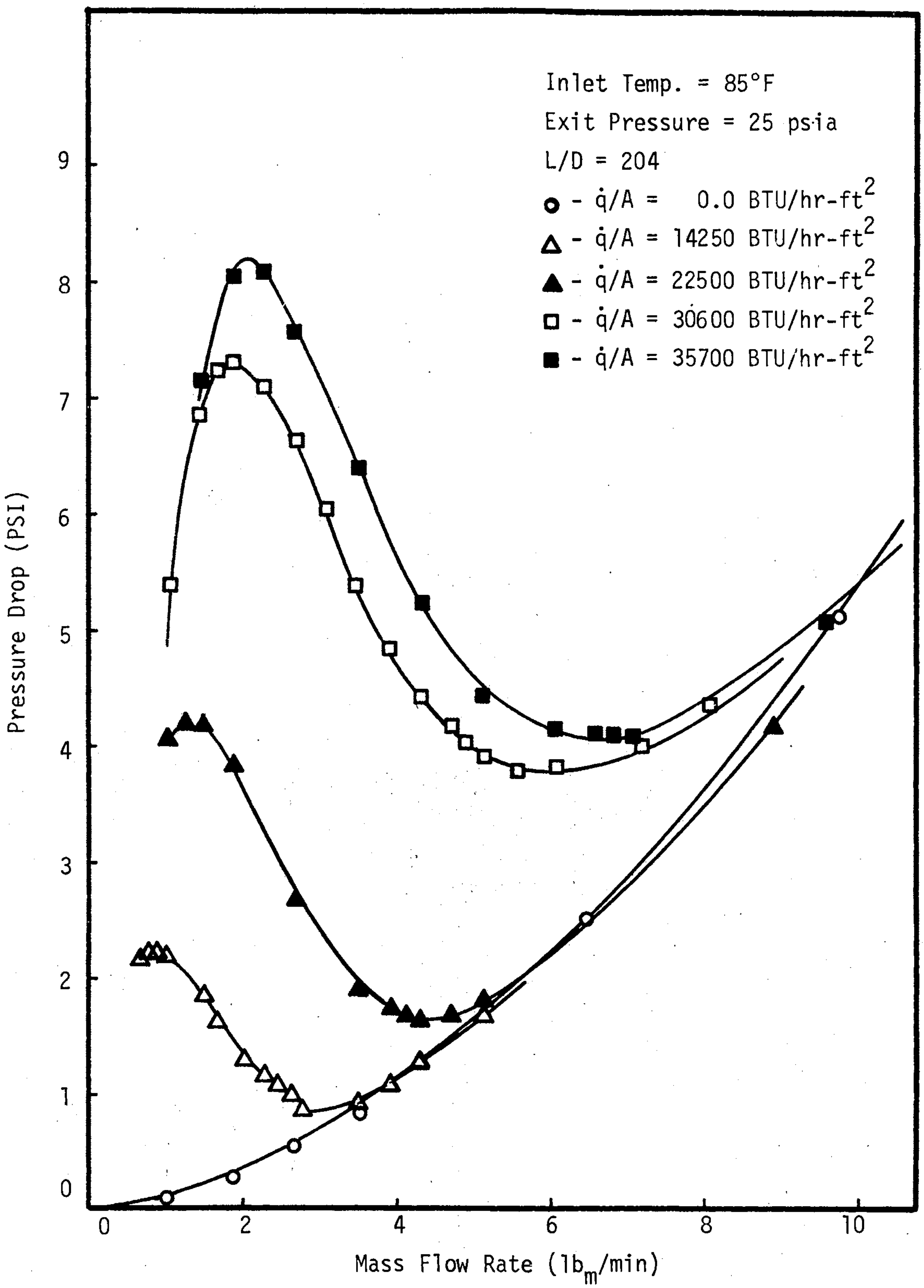

Figure 10. Test Section Pressure Drop Versus Mass Flow Rate

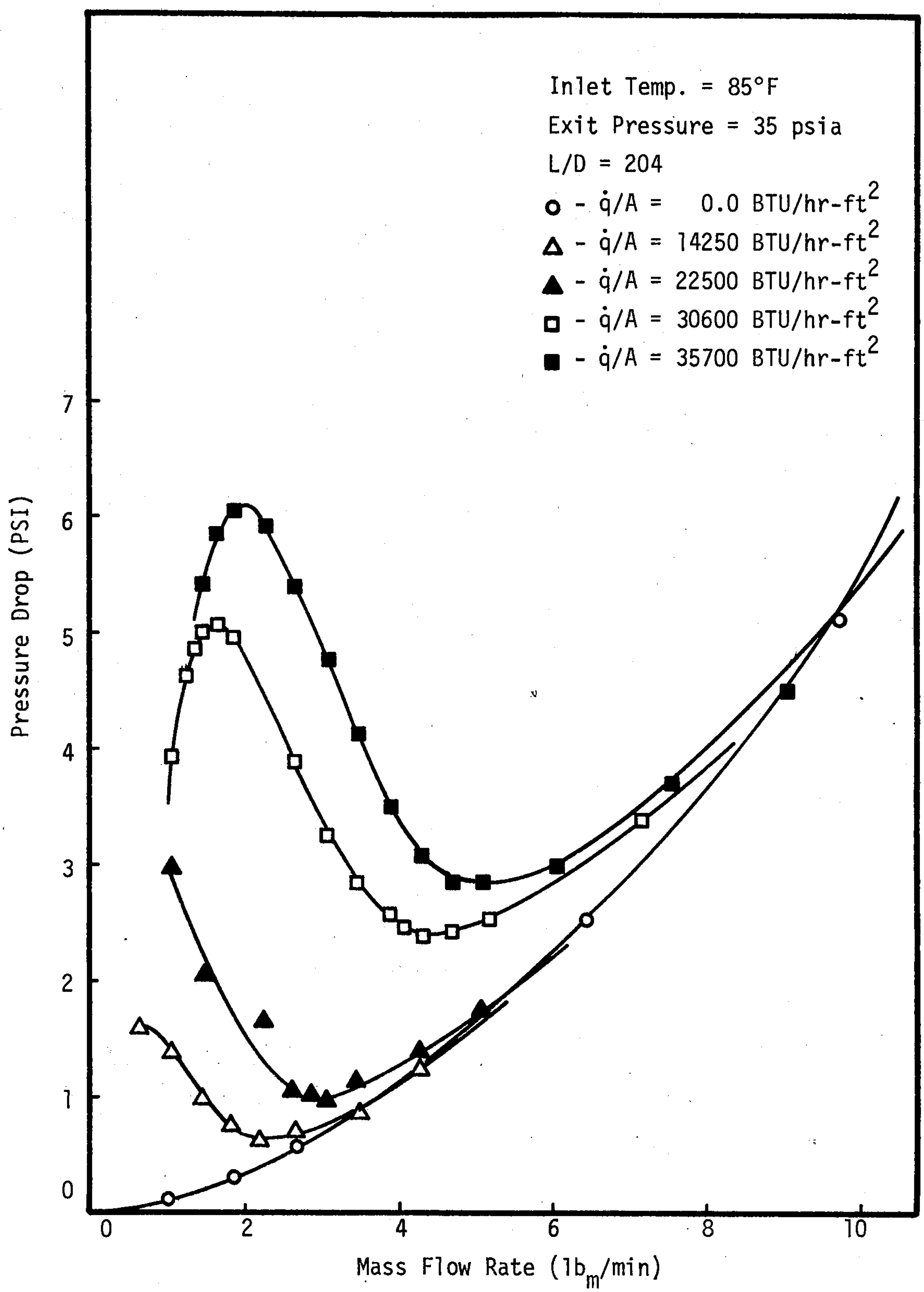

Figure 11. Test Section Pressure Drop Versus Mass Flow Rate

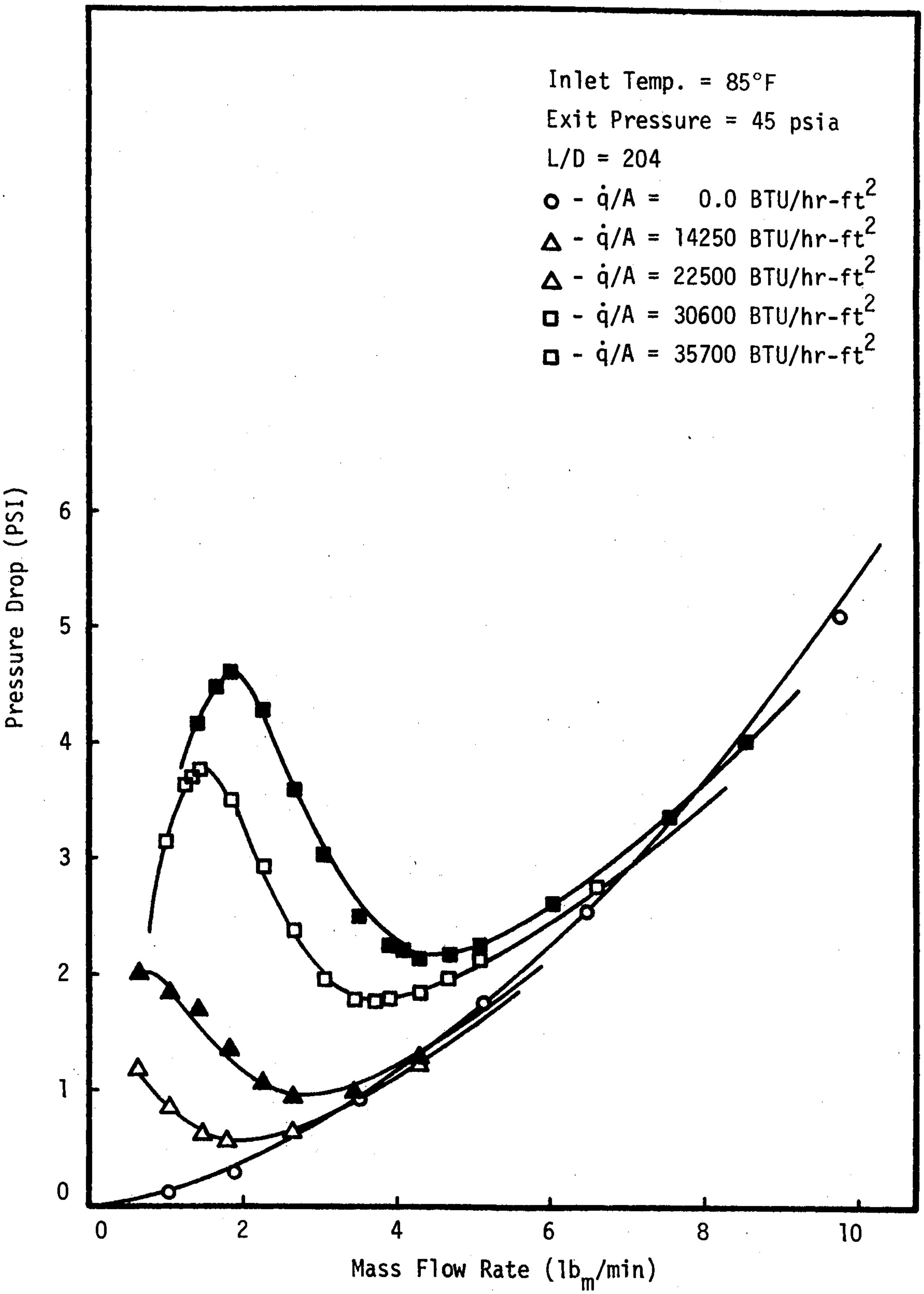

Figure 12. Test Section Pressure Drop Versus Mass Flow Rate

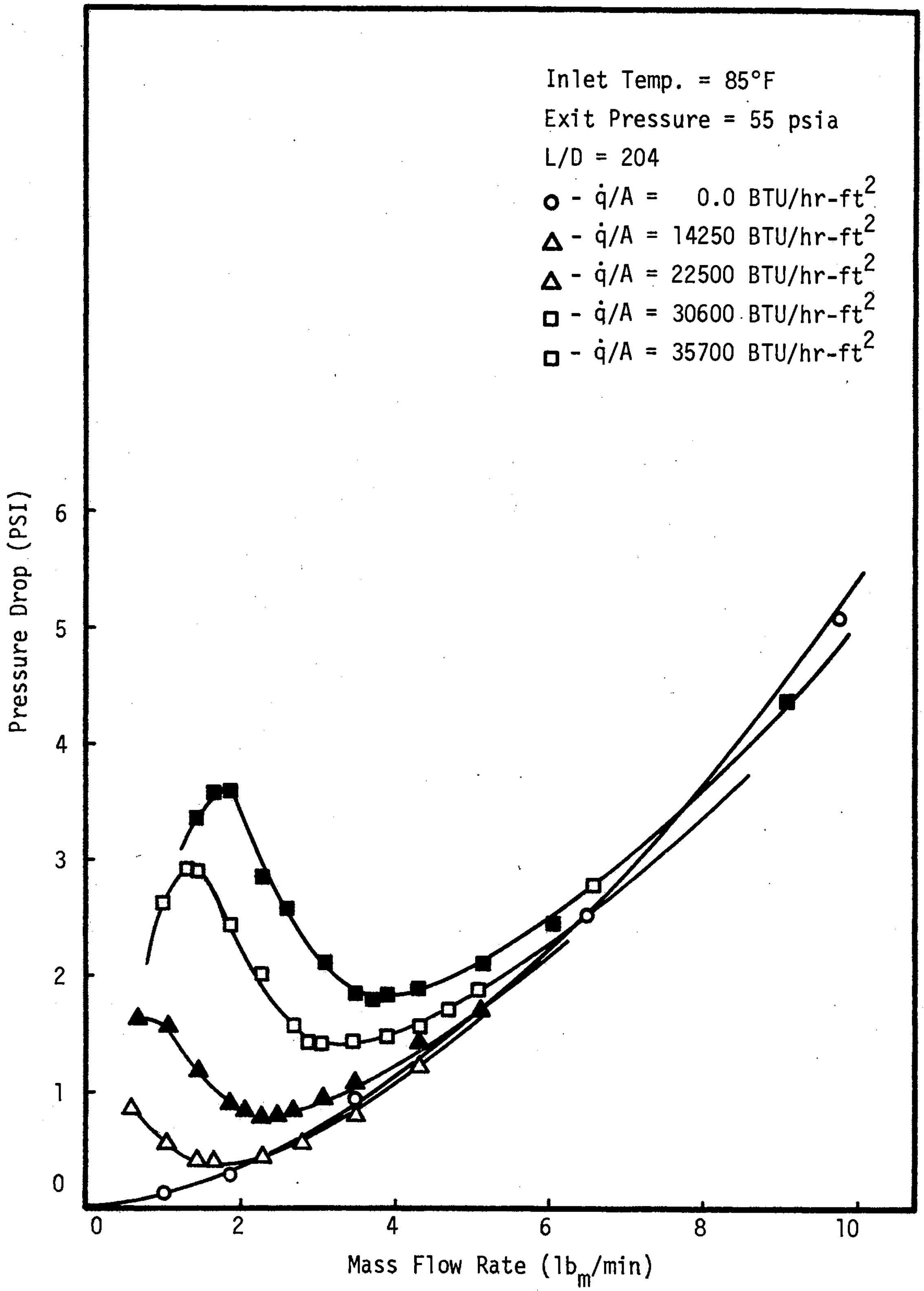

Figure 13. Test Section Pressure Drop Versus Mass Flow Rate

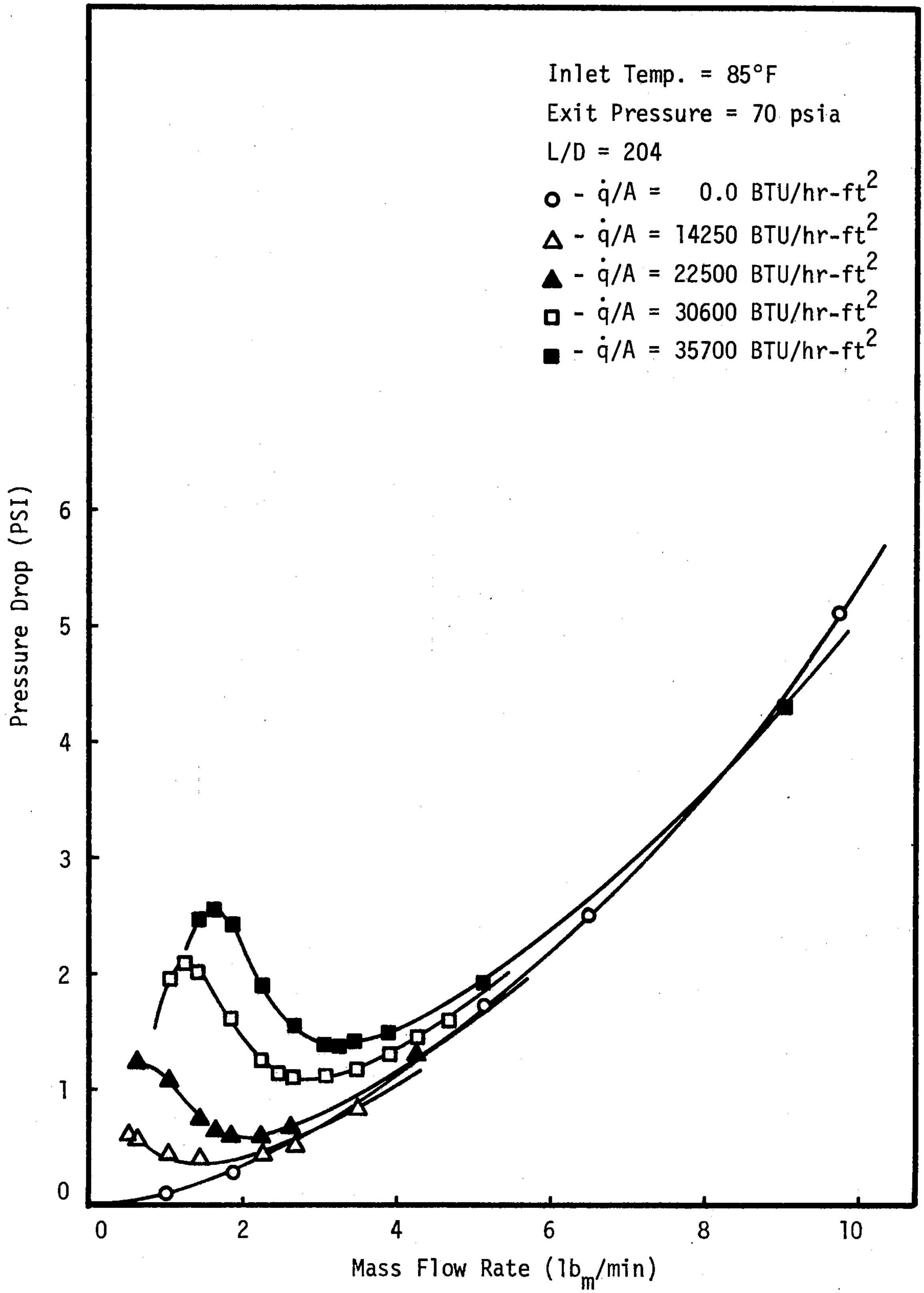

Figure 14. Test Section Pressure Drop Versus Mass Flow Rate

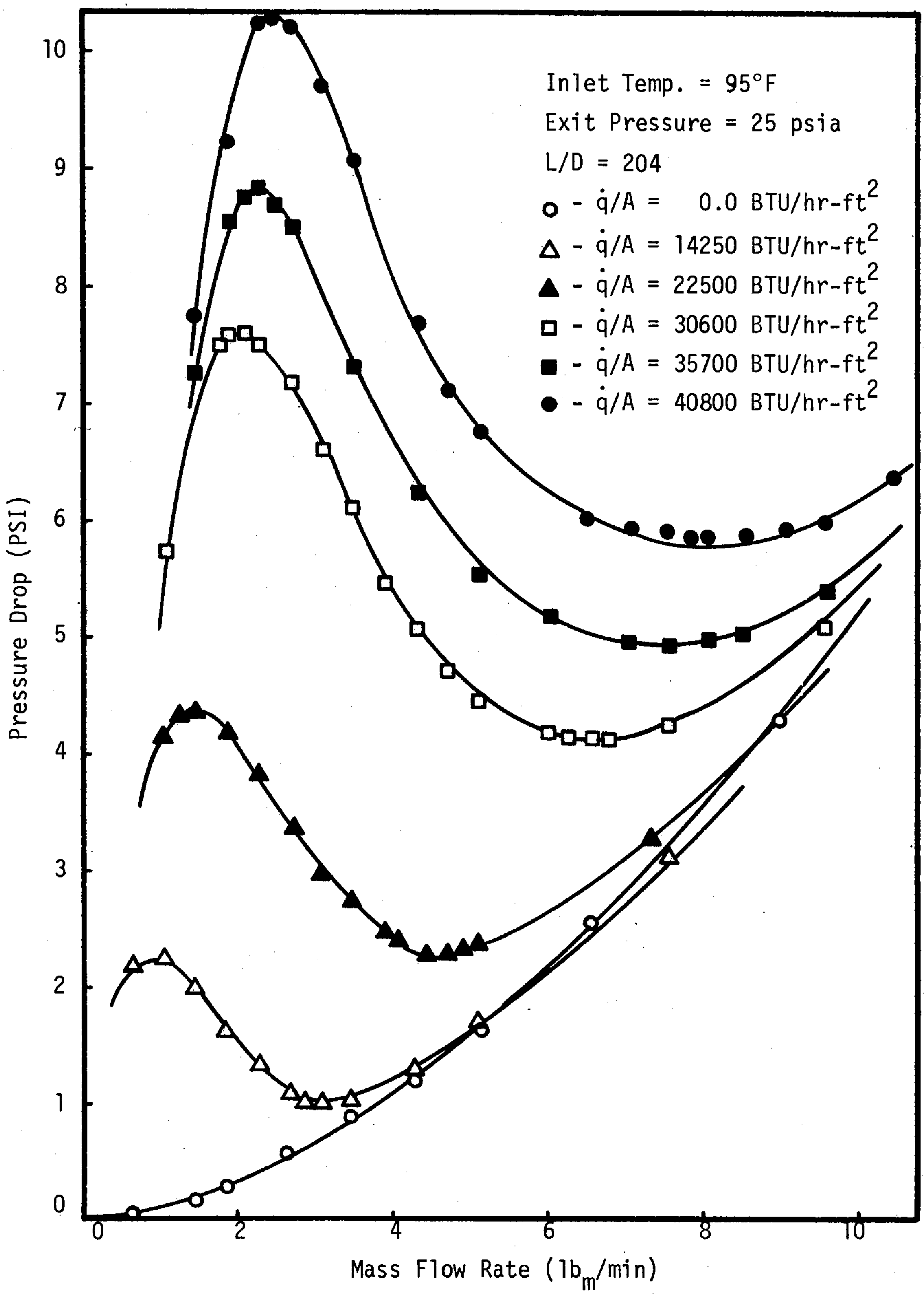

Figure 15. Test Section Pressure Drop Versus Mass Flow Rate

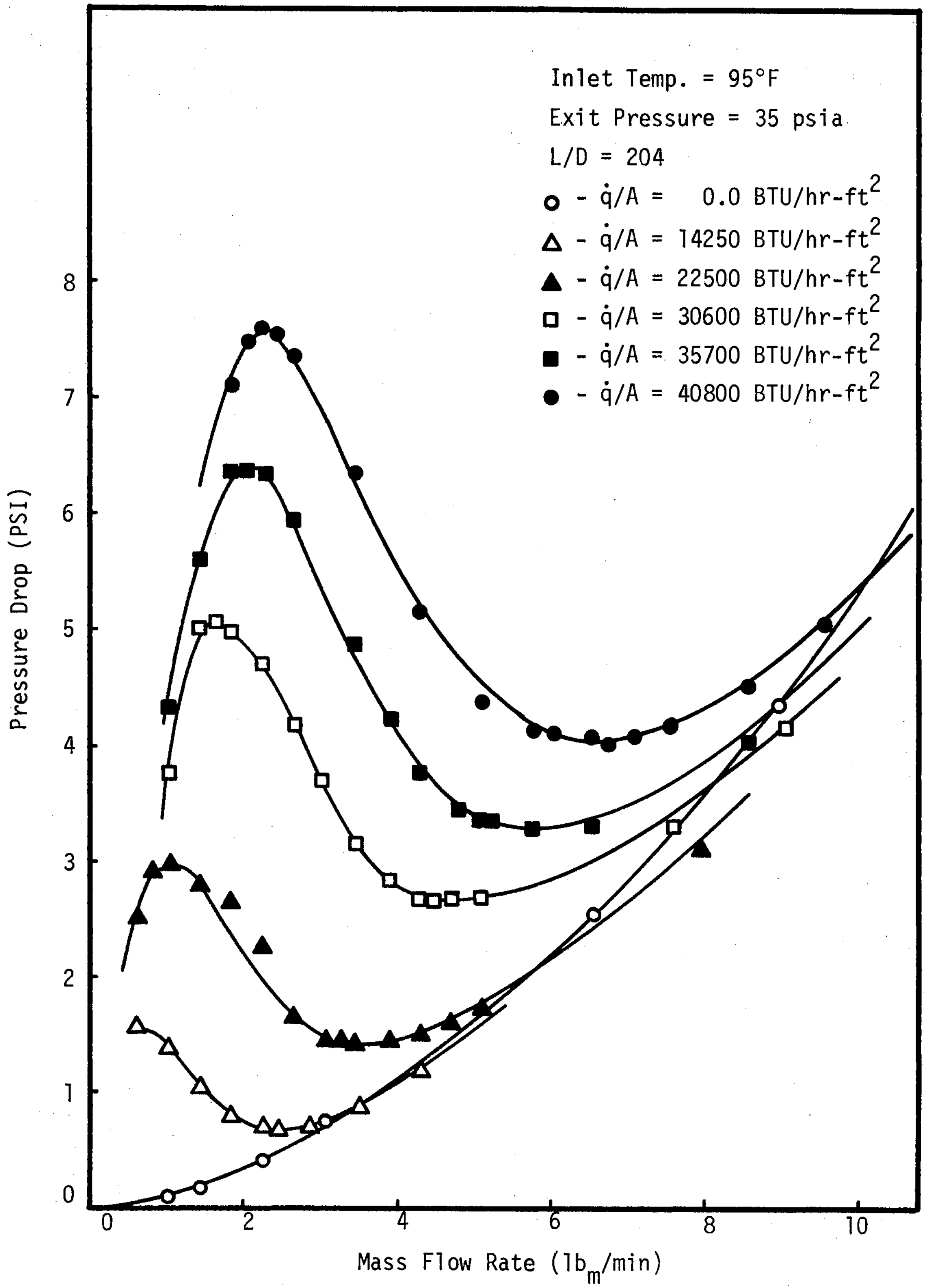

Figure 16. Test Section Pressure Drop Versus Mass Flow Rate

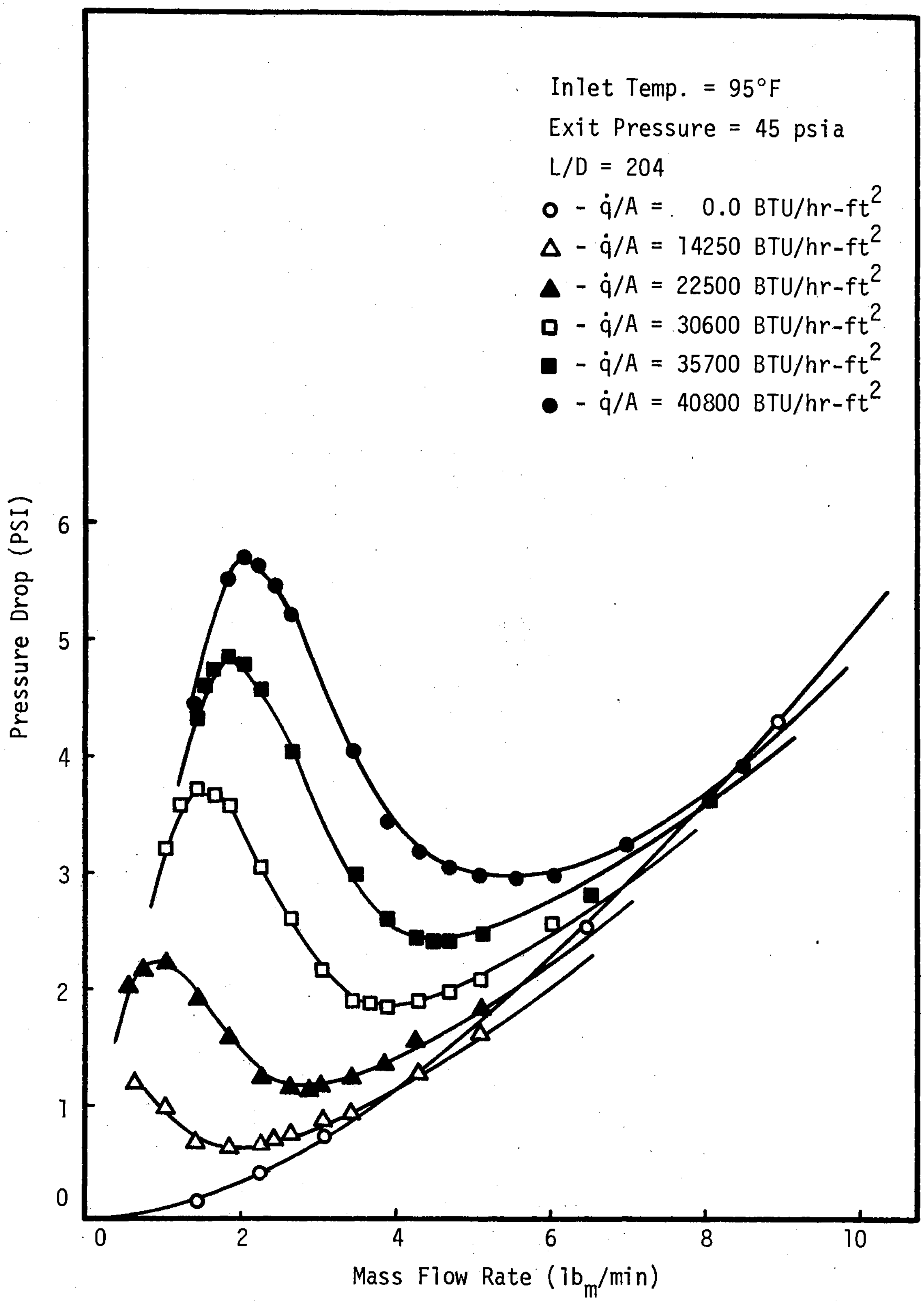

Figure 17. Test Section Pressure Drop Versus Mass Flow Rate

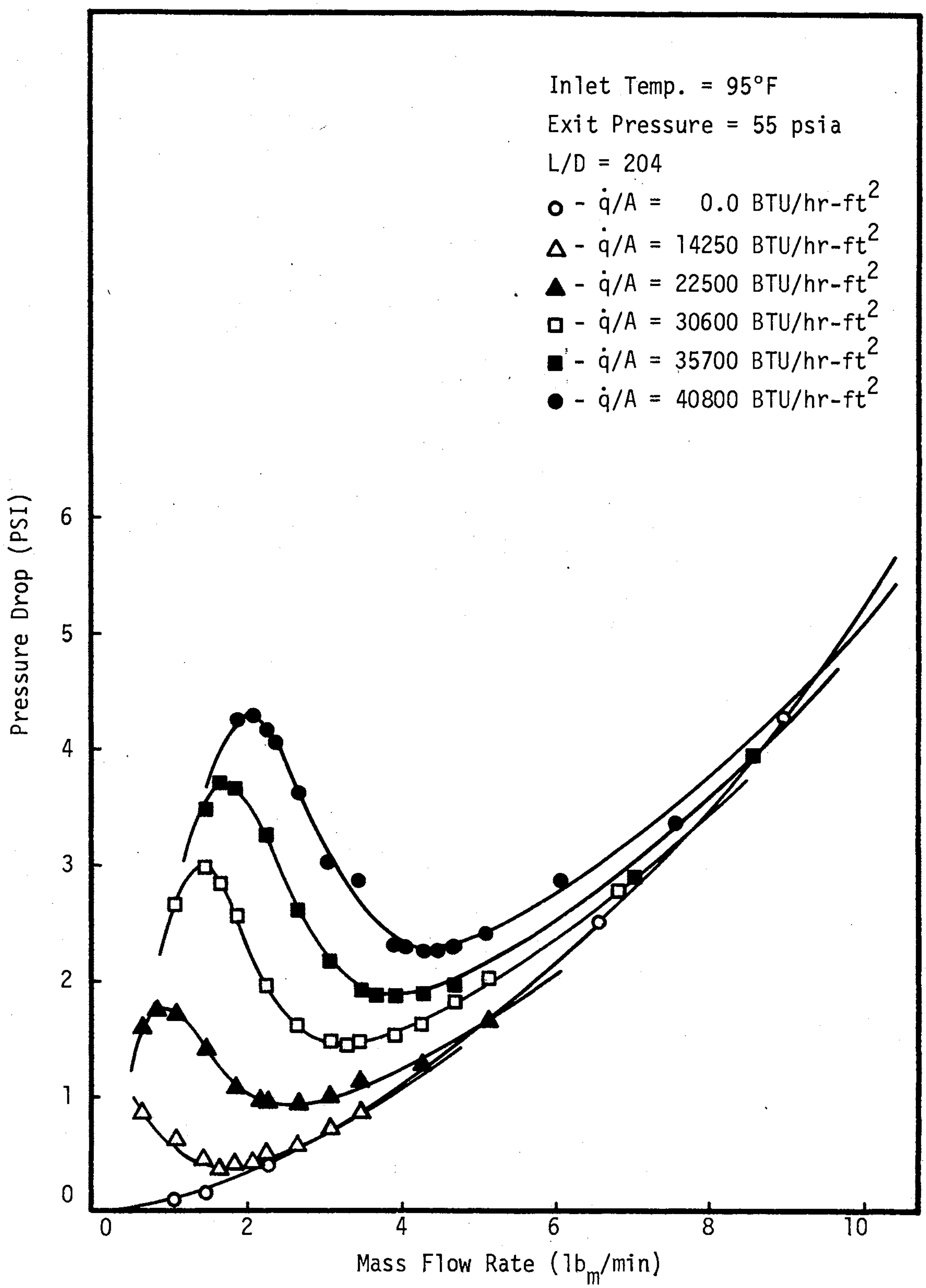

Figure 18. Test Section Pressure Drop Versus Mass Flow Rate

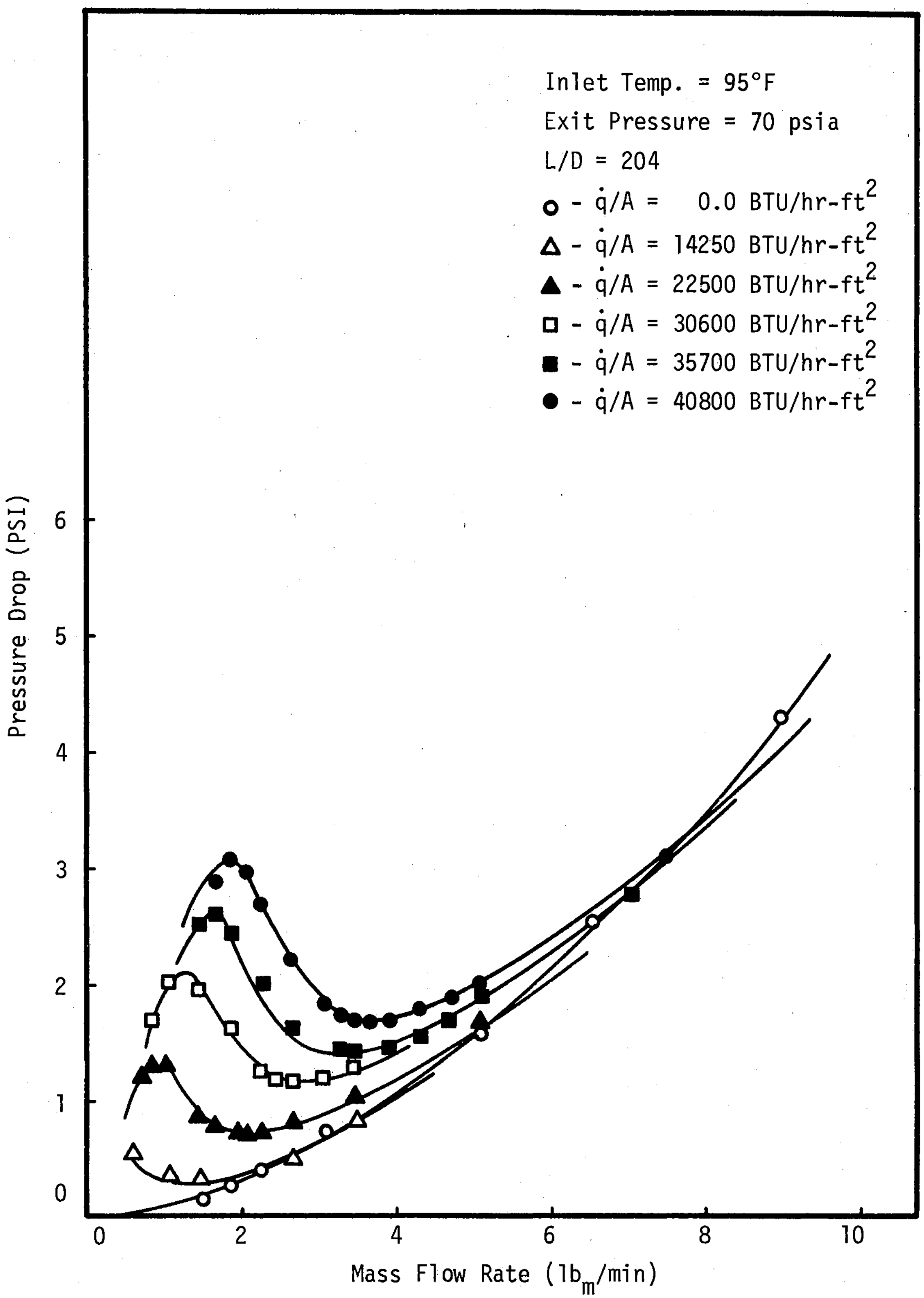

Figure 19. Test Section Pressure Drop Versus Mass Flow Rate

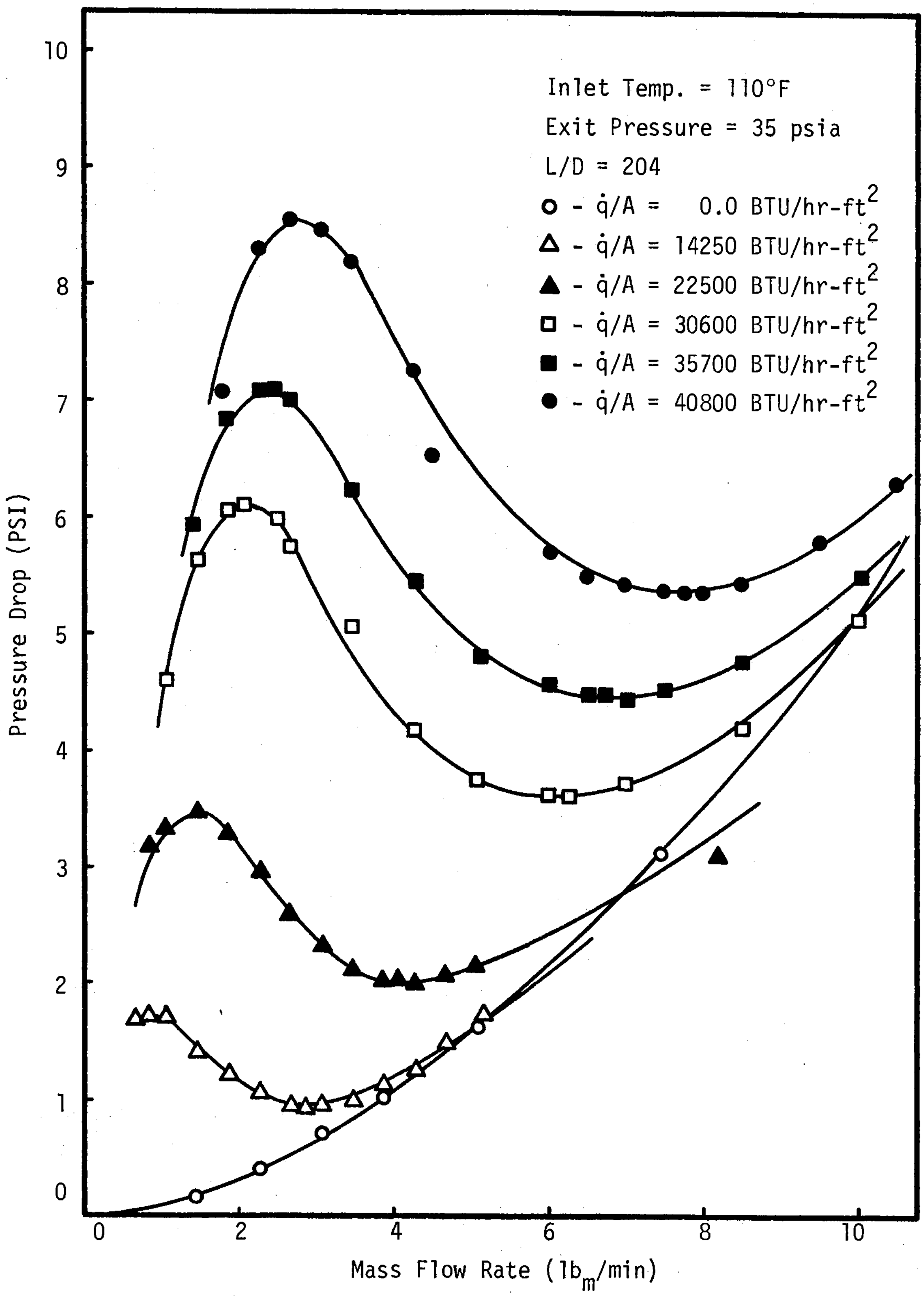

Figure 20. Test Section Pressure Drop Versus Mass Flow Rate

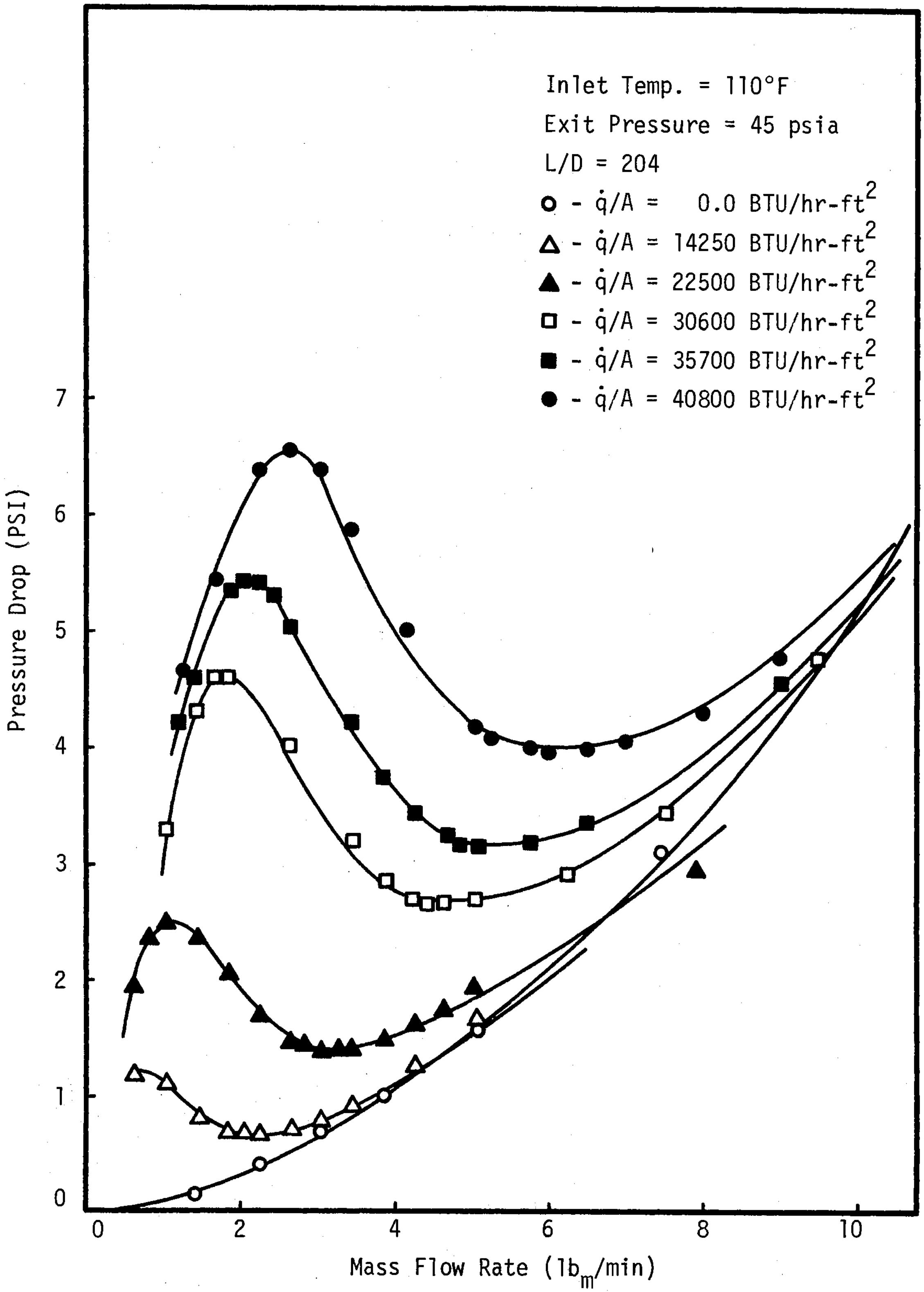

Figure 21. Test Section Pressure Drop Versus Mass Flow Rate

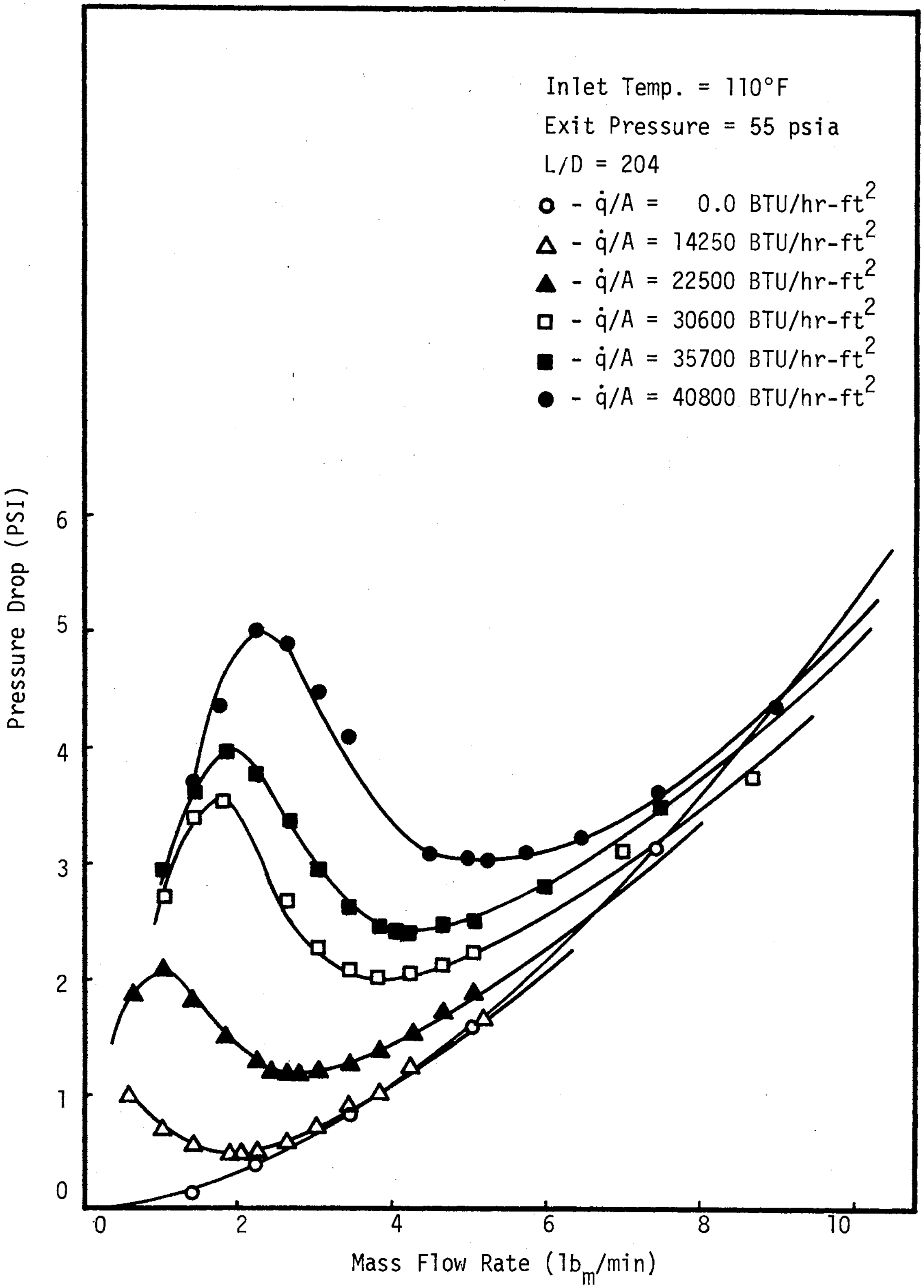

Figure 22. Test Section Pressure Drop Versus Mass Flow Rate

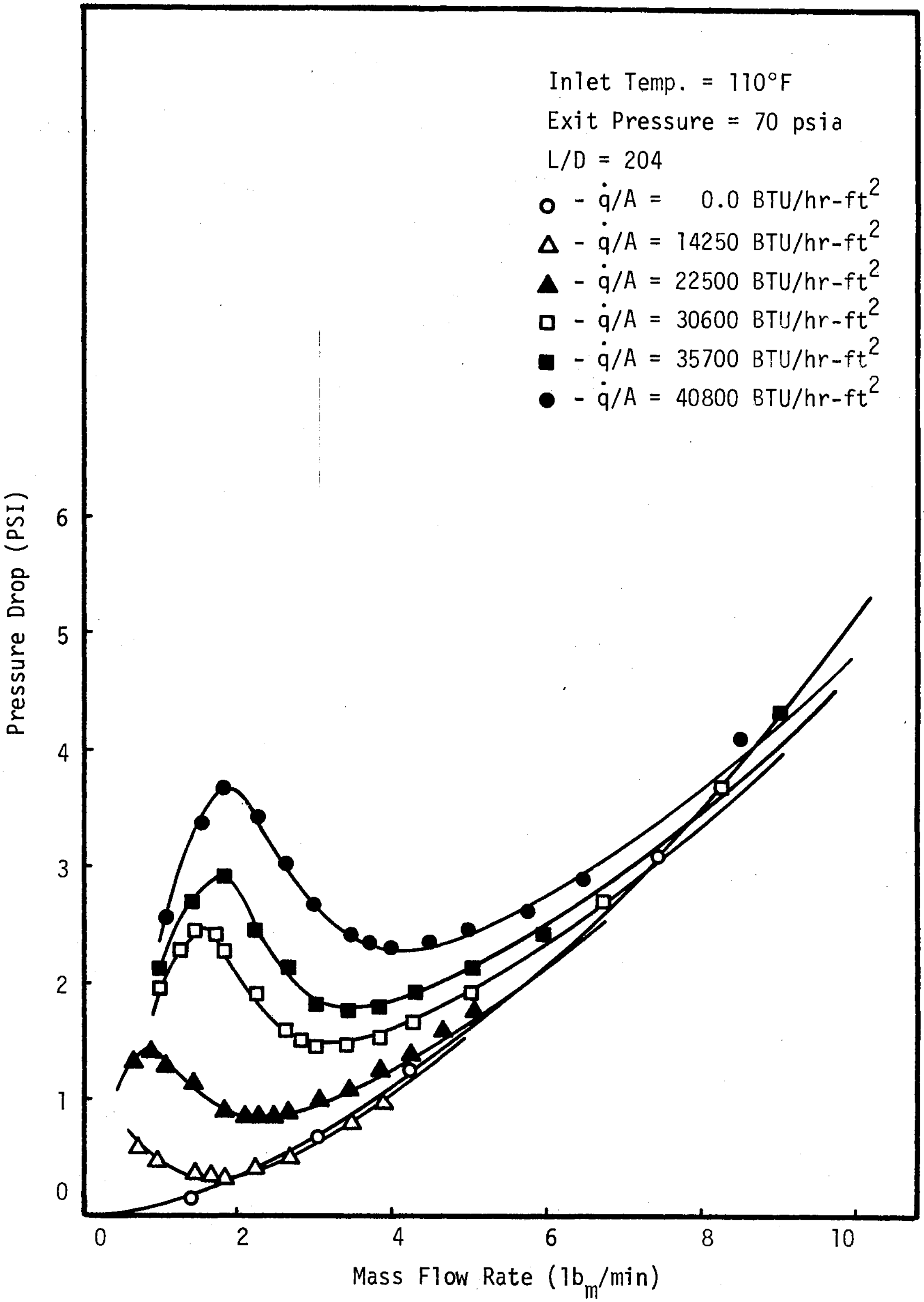

Figure 23. Test Section Pressure Drop Versus Mass Flow Rate

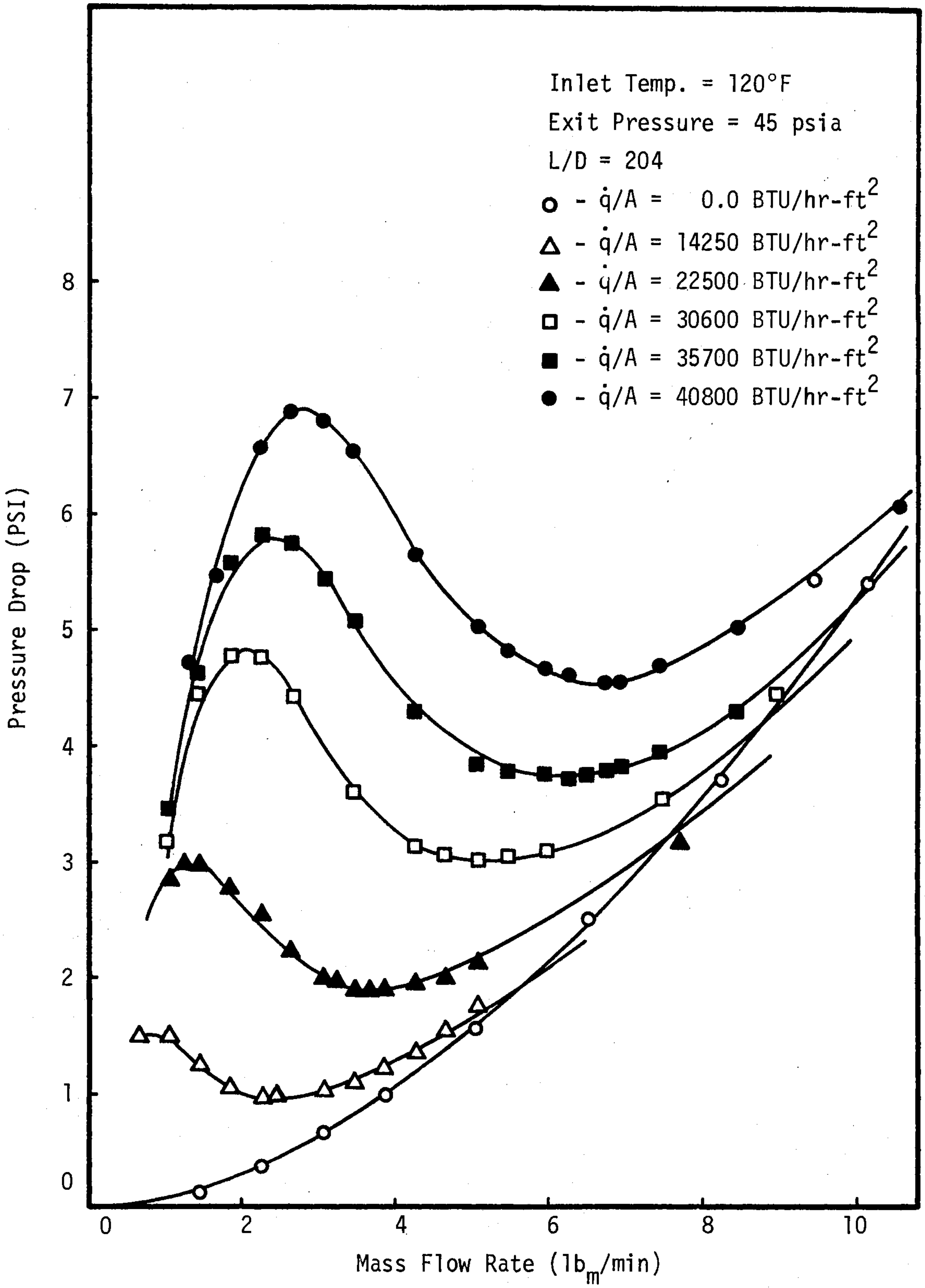

Figure 24. Test Section Pressure Drop Versus Mass Flow Rate

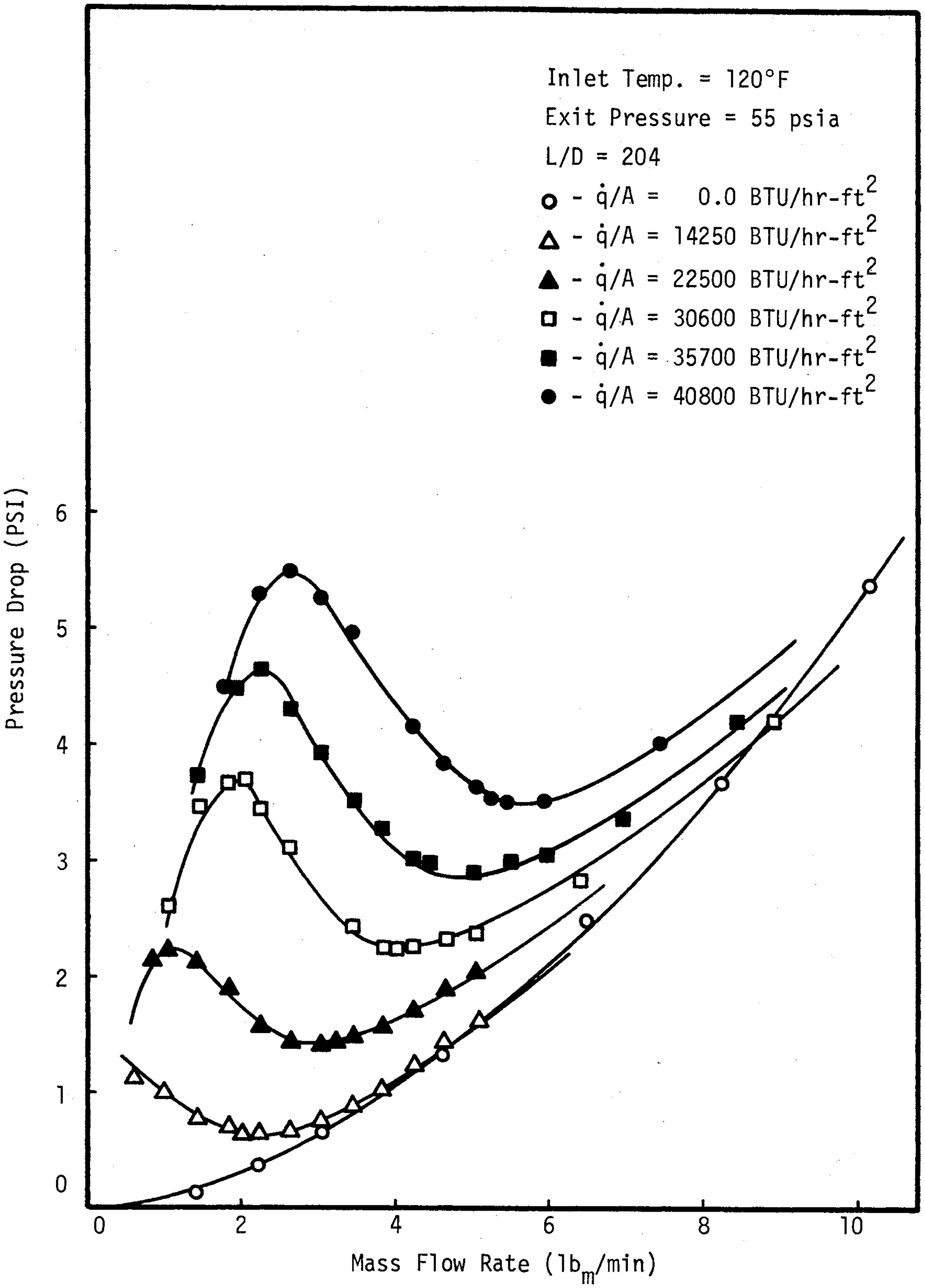

Figure 25. Test Section Pressure Drop Versus Mass Flow Rate

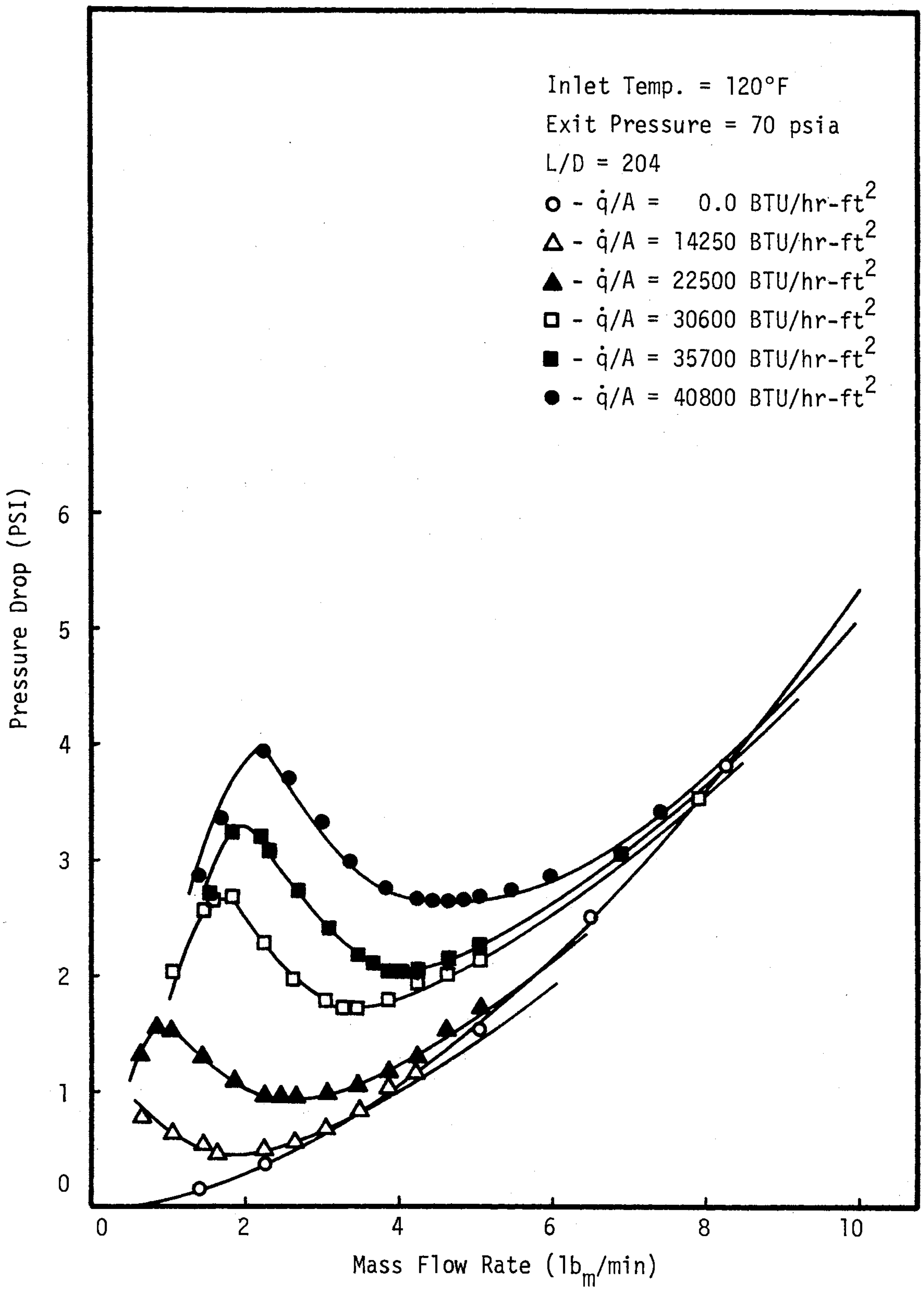

Figure 26. Test Section Pressure Drop Versus Mass Flow Rate

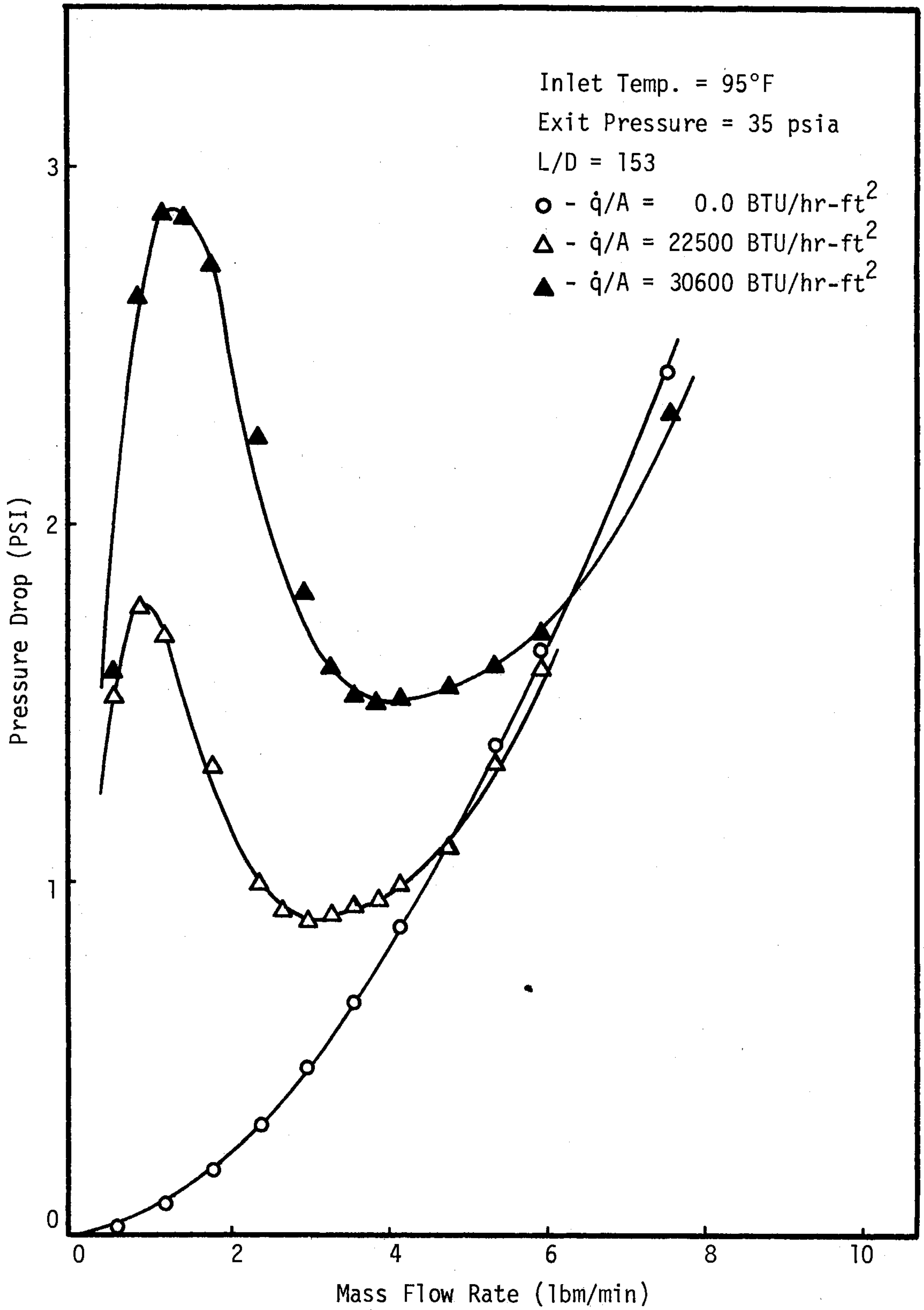

Figure 27. Test Section Pressure Drop Versus Mass Flow Rate

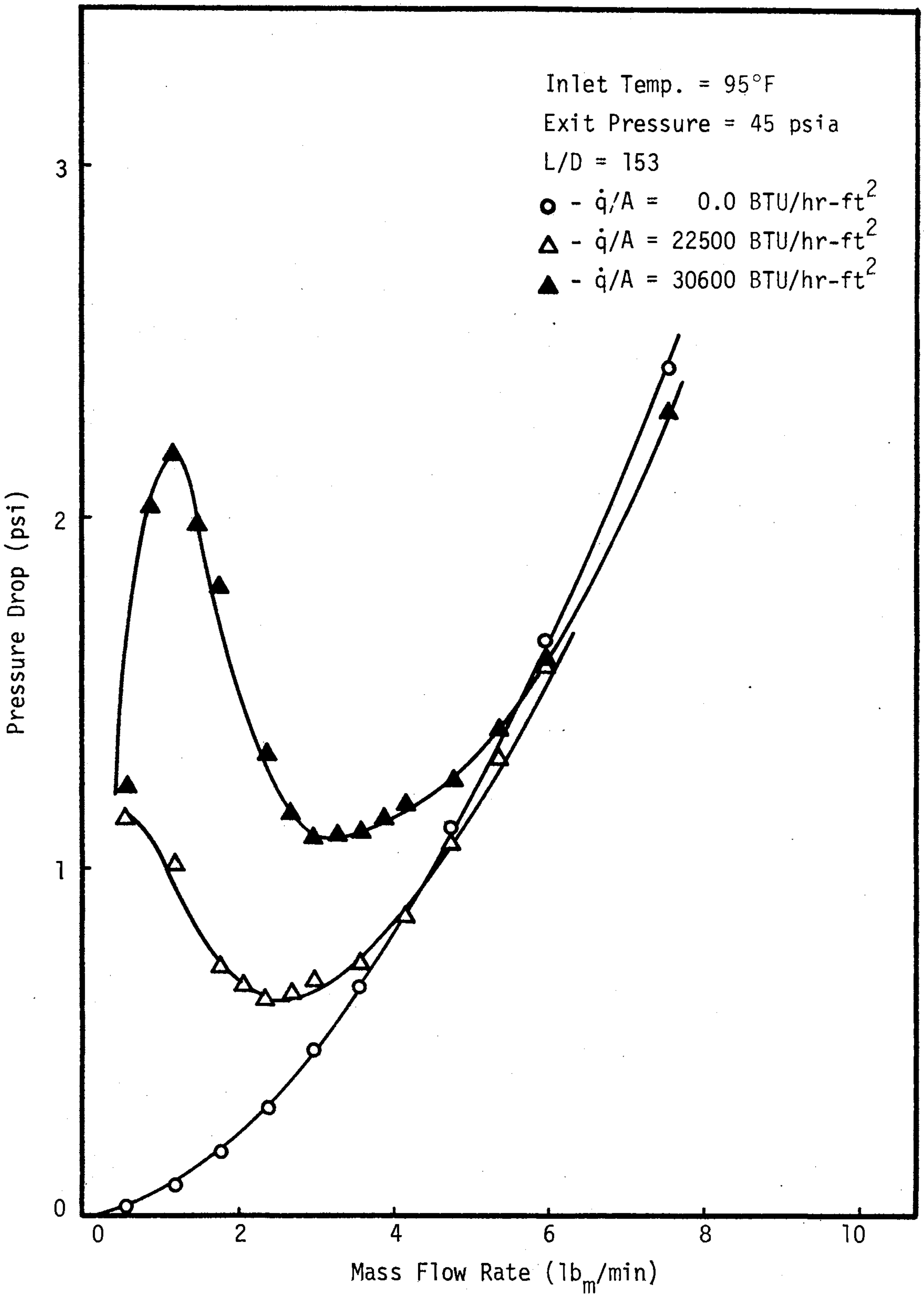

Figure 28. Test Section Pressure Drop Versus Mass Flow Rate

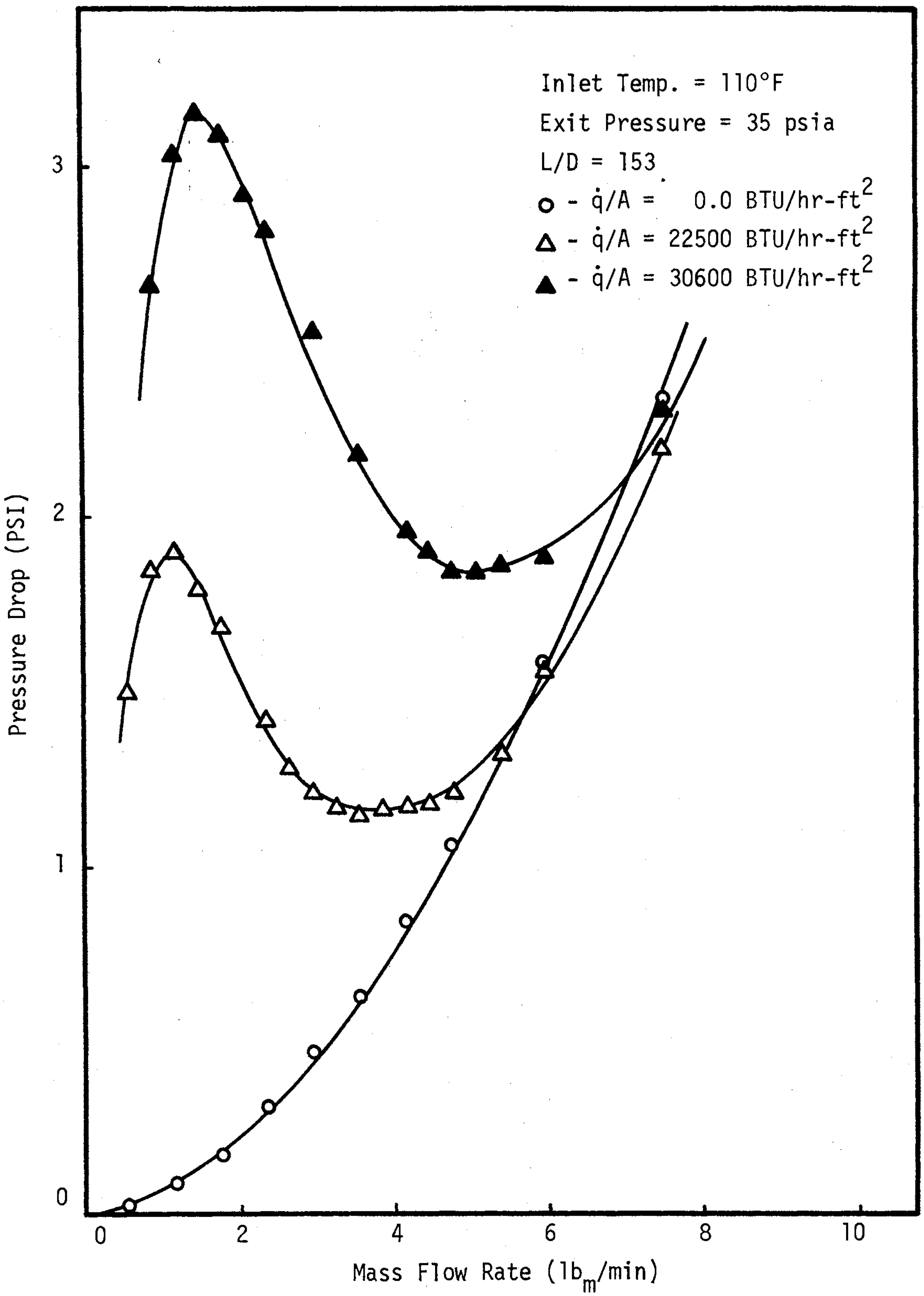

Figure 29. Test Section Pressure Drop Versus Mass Flow Rate

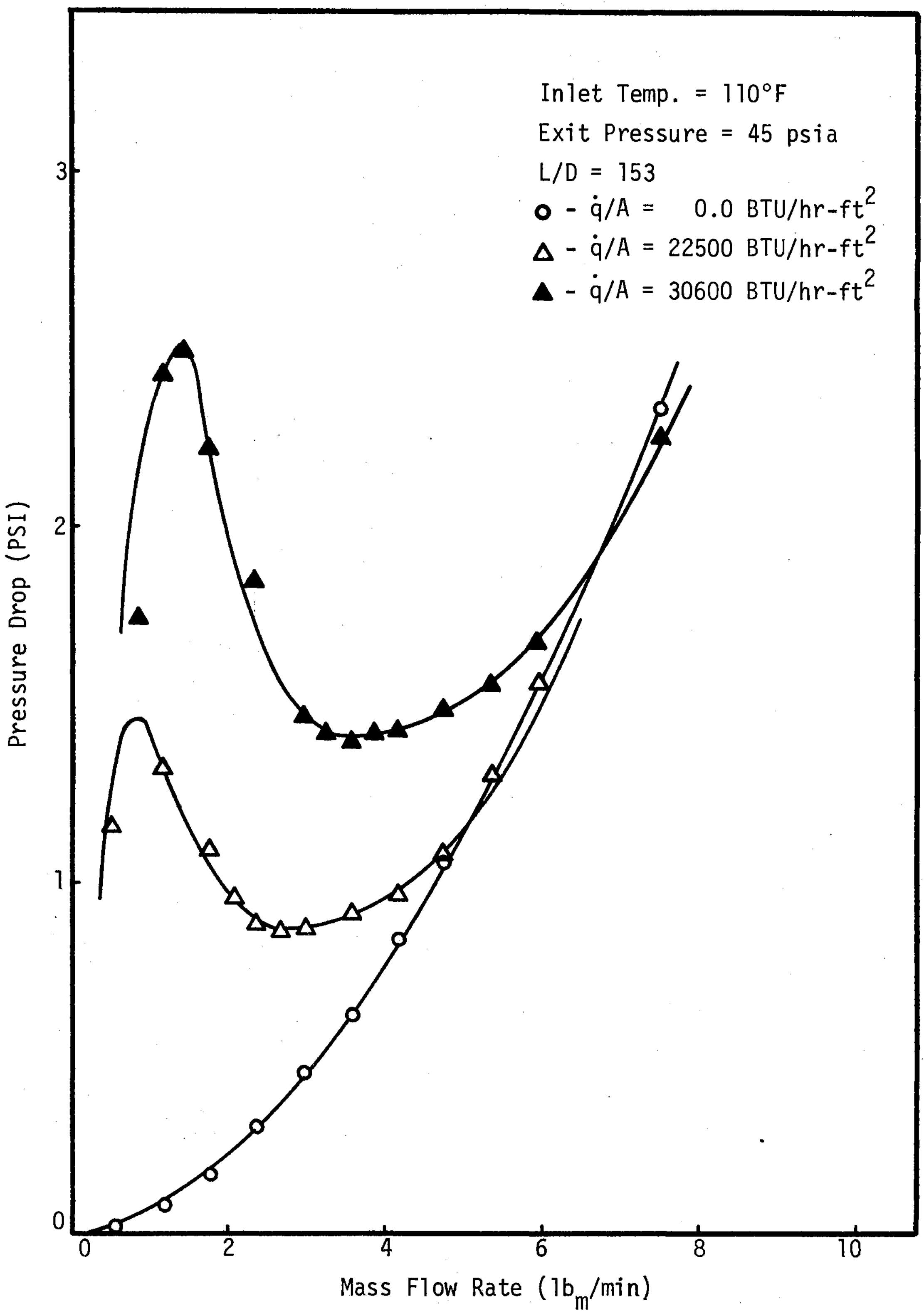

Figure 30. Test Section Pressure Drop Versus Mass Flow Rate

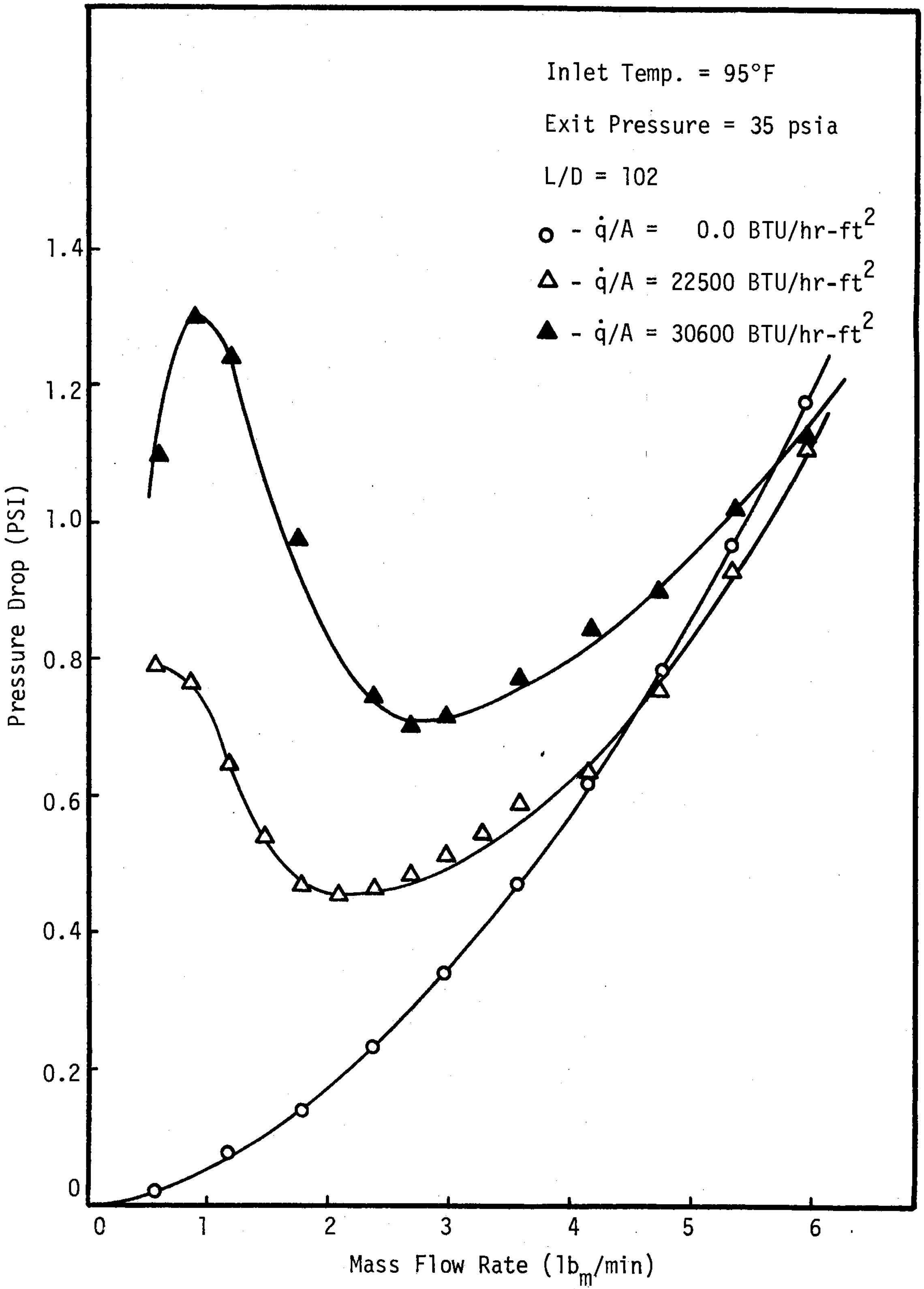

Figure 31. Test Section Pressure Drop Versus Mass Flow Rate

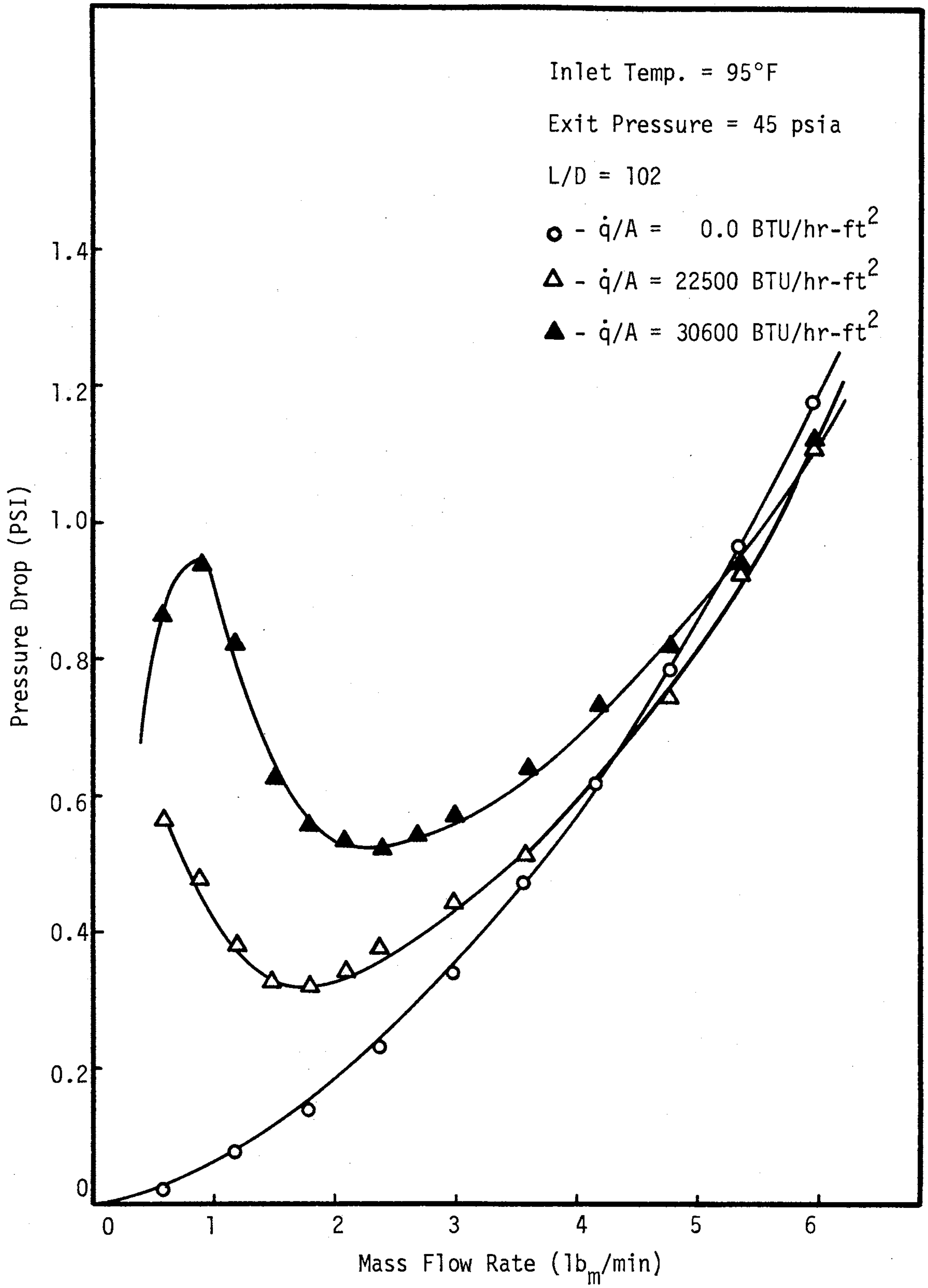

Figure 32. Test Section Pressure Drop Versus Mass Flow Rate

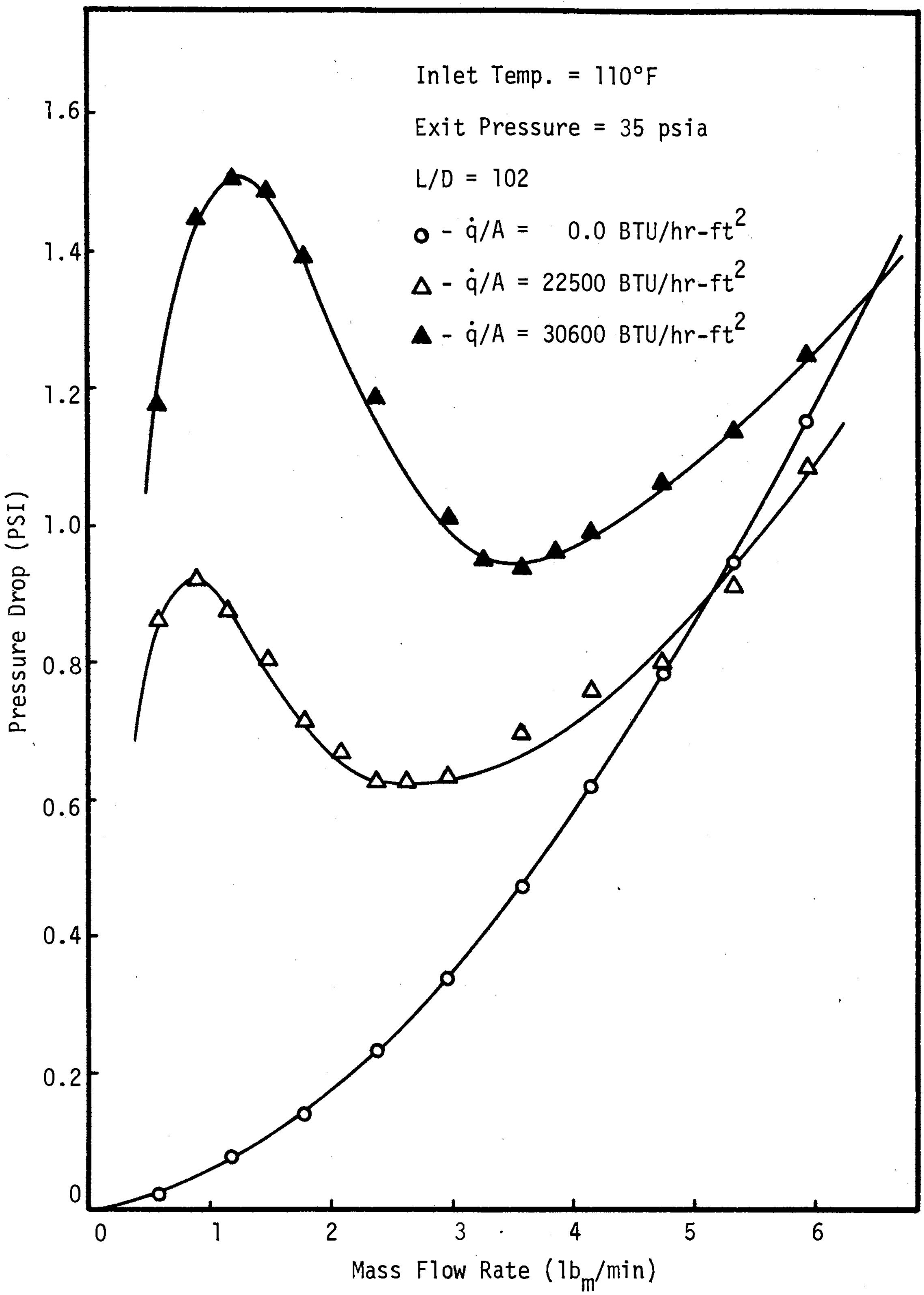

Figure 33. Test Section Pressure Drop Versus Mass Flow Rate

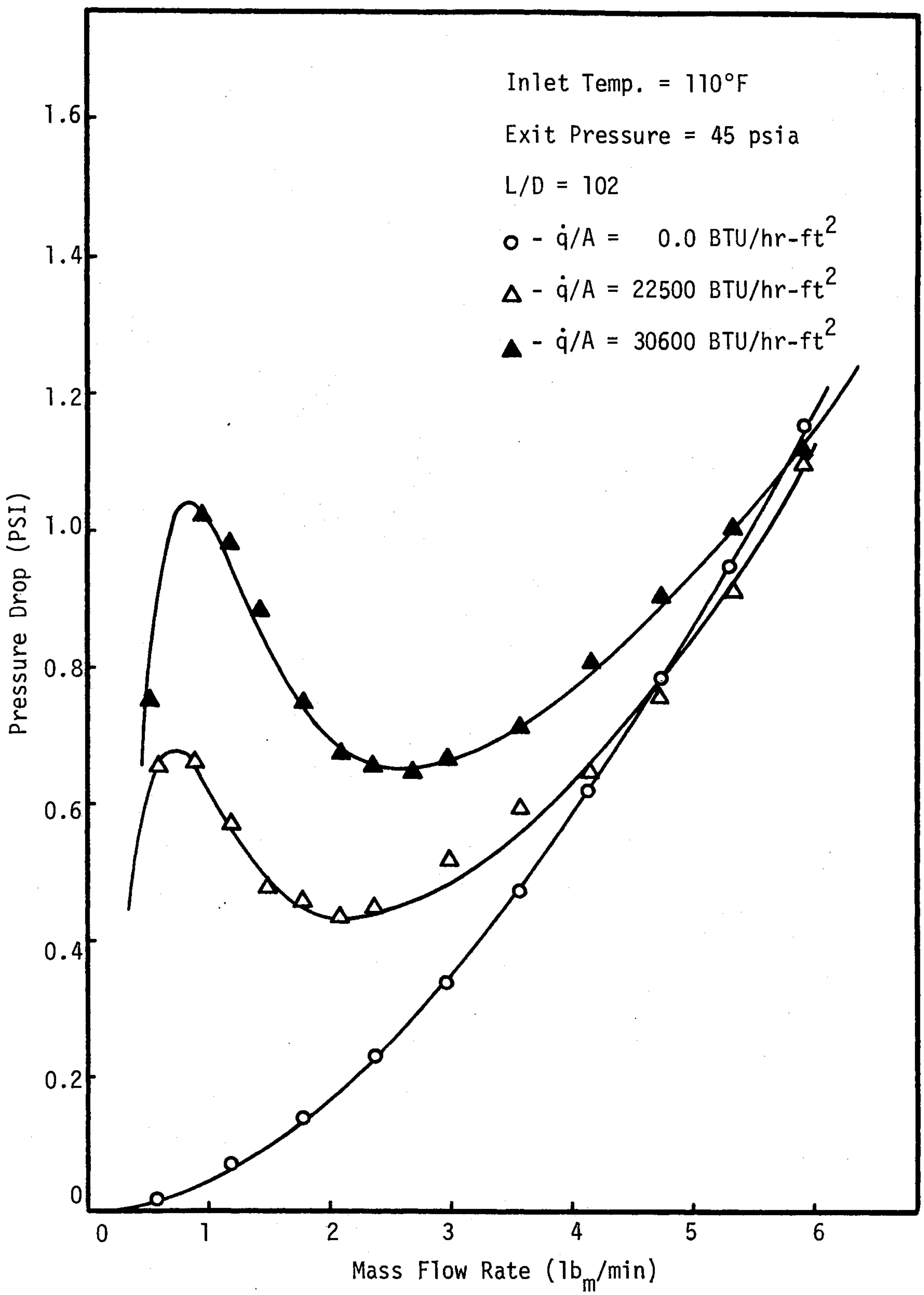

Figure 34. Test Section Pressure Drop Versus Mass Flow Rate

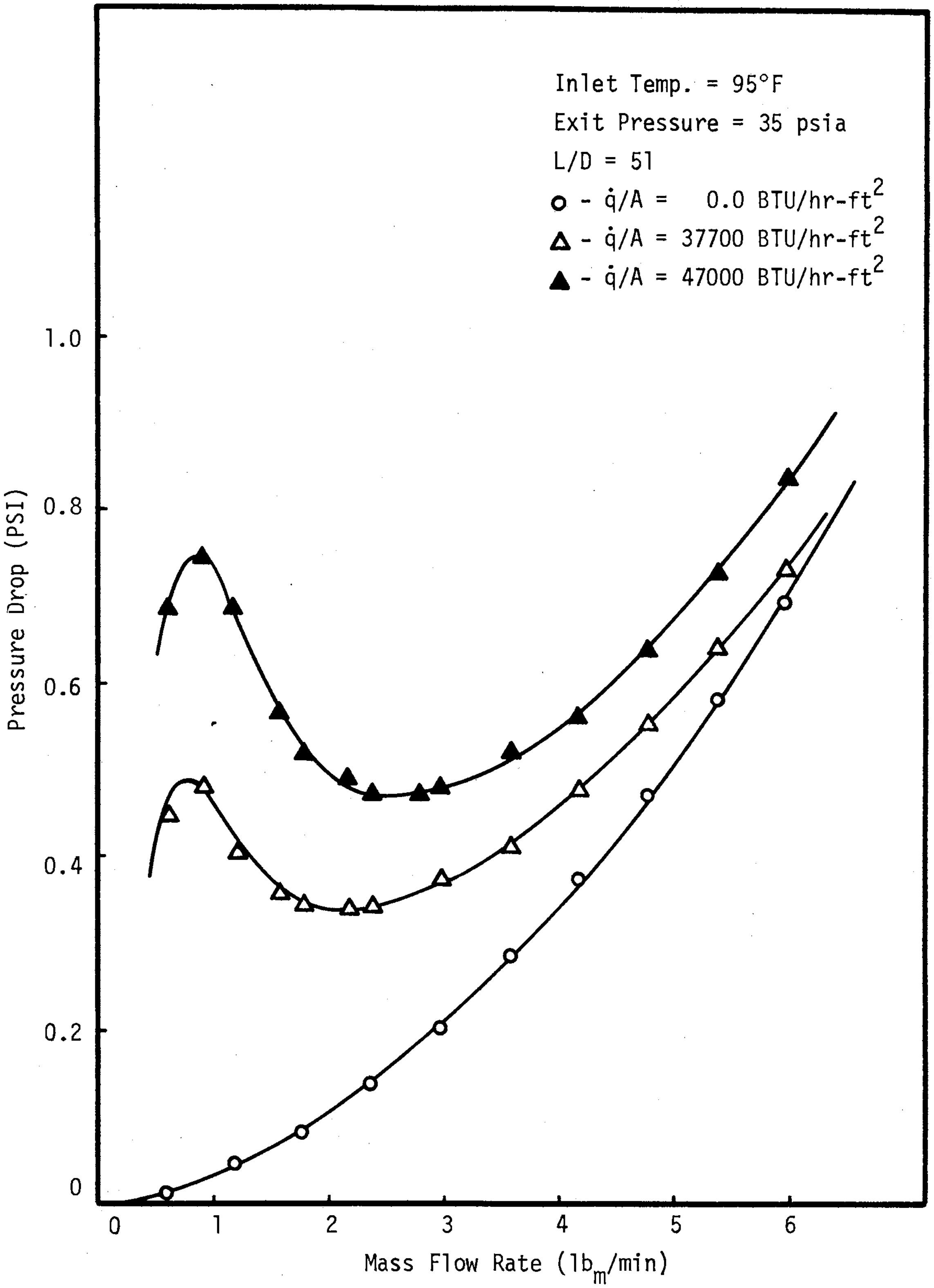

Figure 35. Test Section Pressure Drop Versus Mass Flow Rate

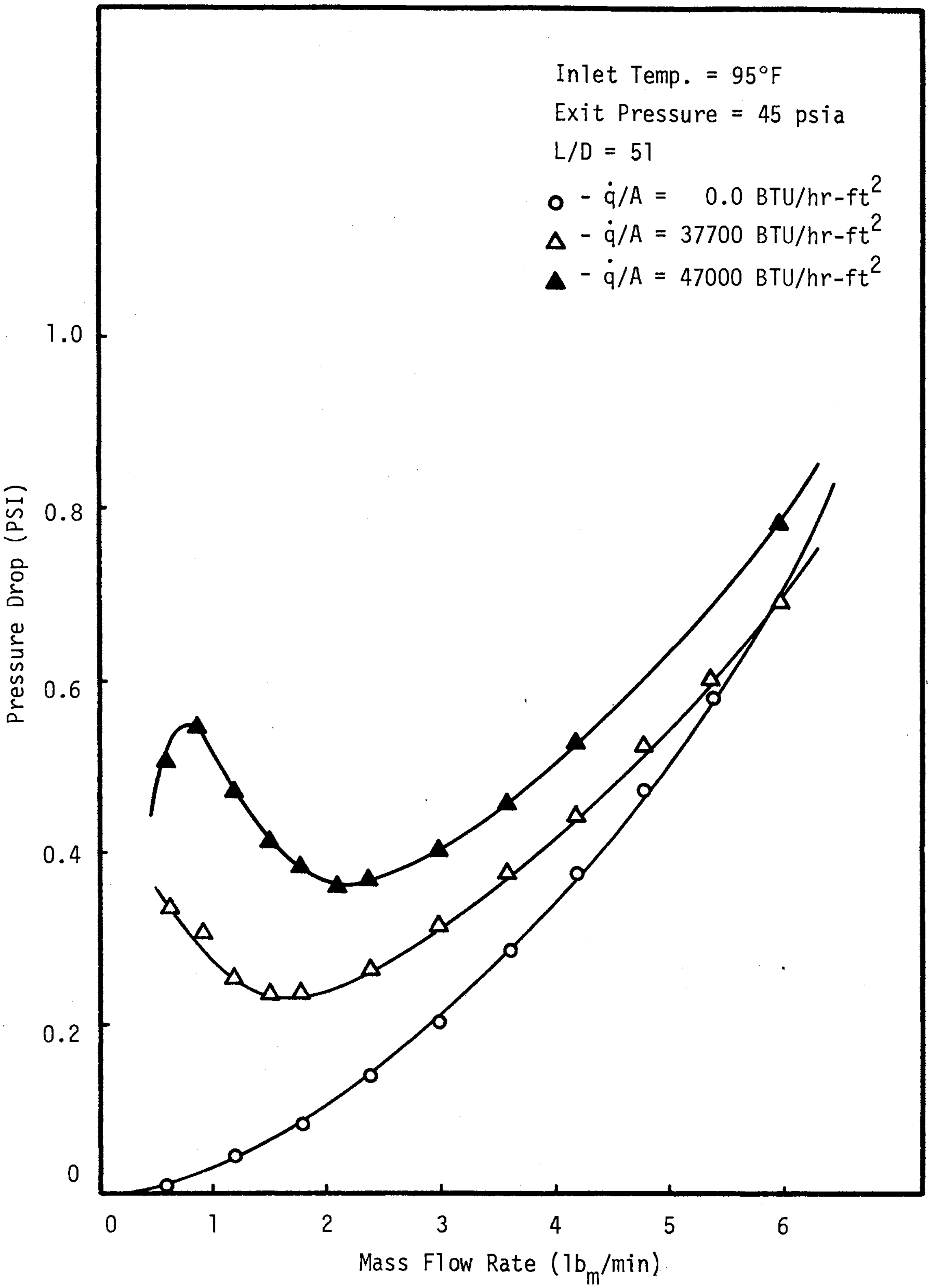

Figure 36. Test Section Pressure Drop Versus Mass Flow Rate

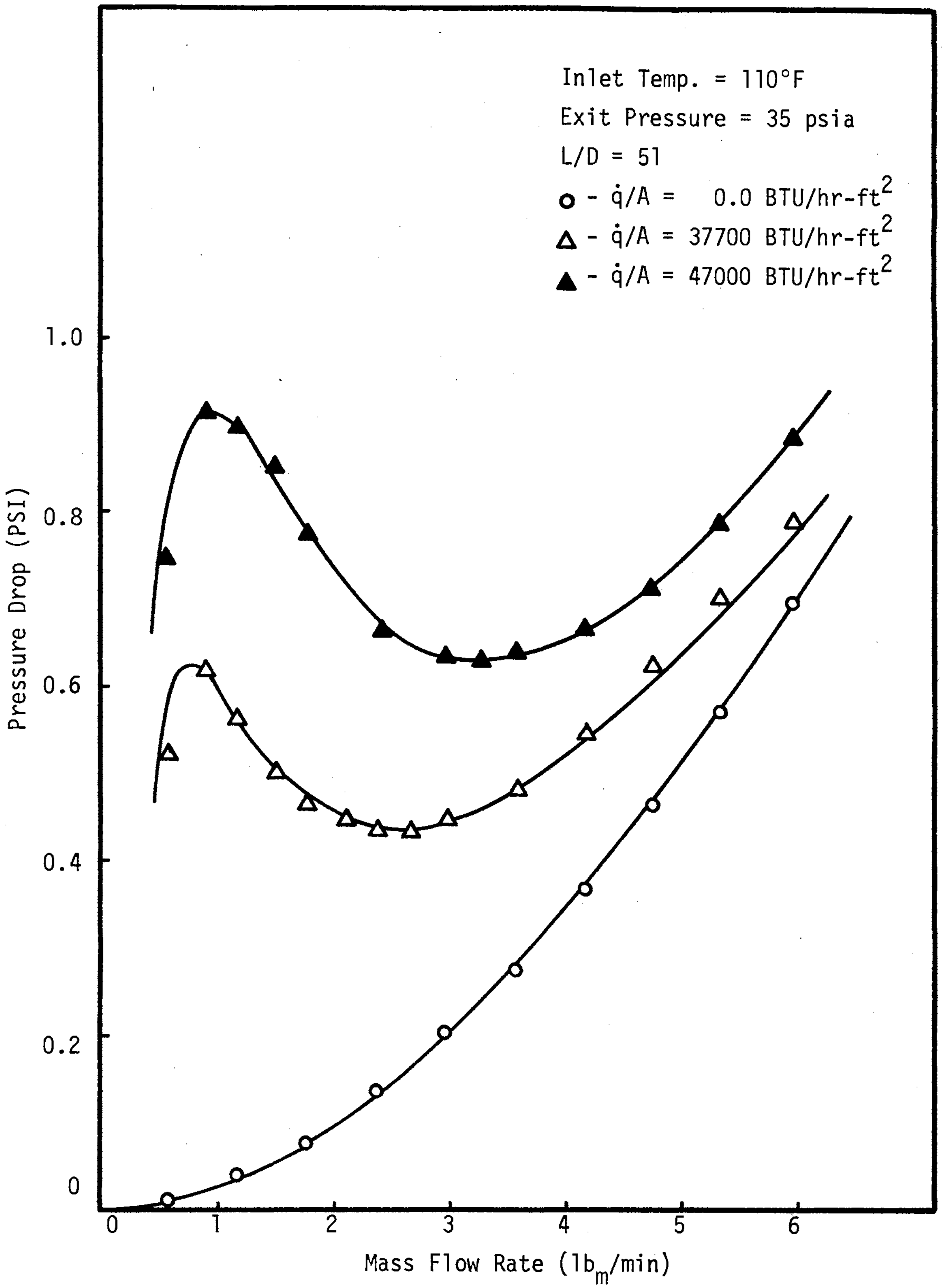

Figure 37. Test Section Pressure Drop Versus Mass Flow Rate

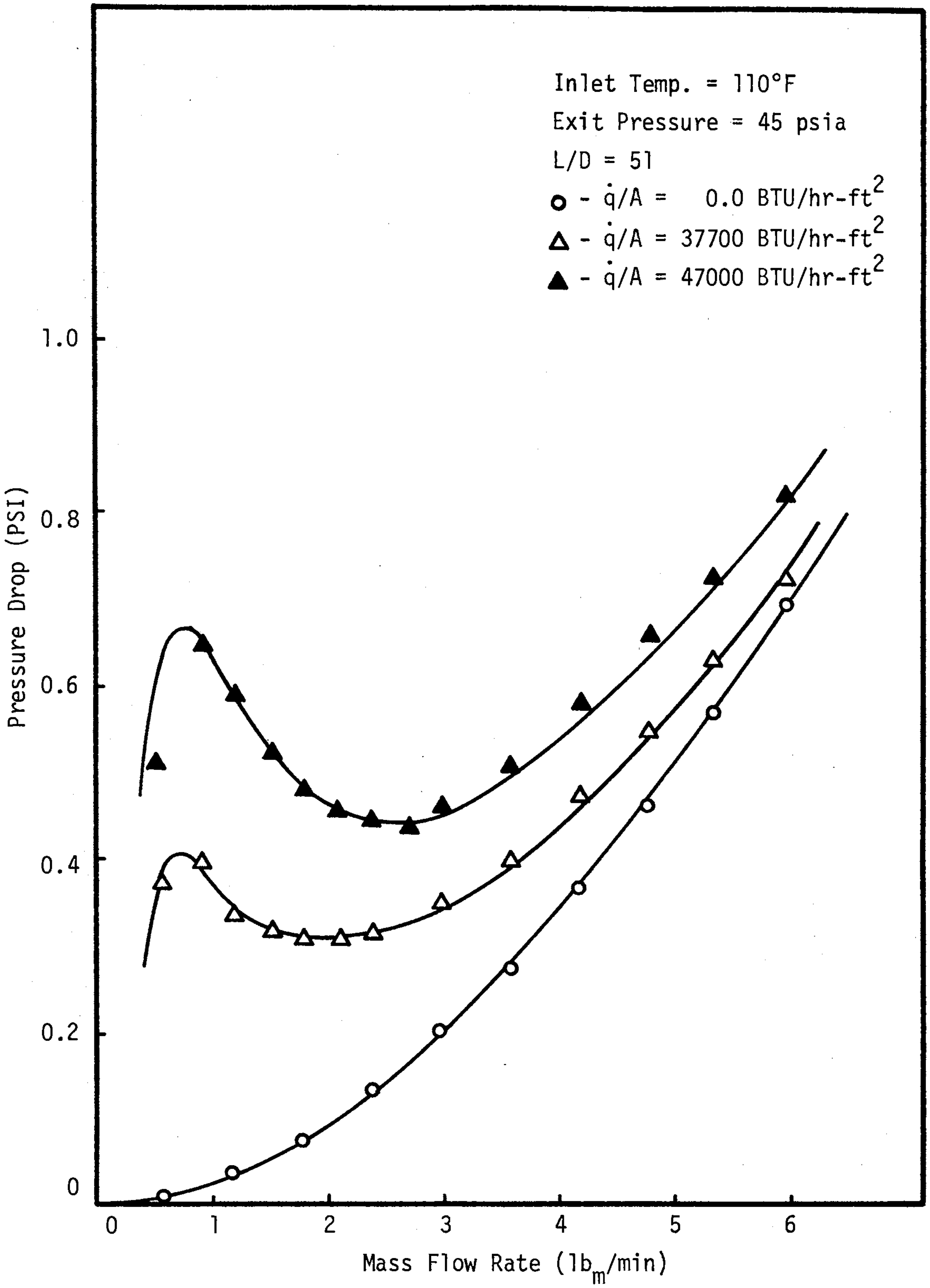

Figure 38. Test Section Pressure Drop Versus Mass Flow Rate

The third region begins with a further reduction in the flow rate and it is called "fully developed subcooled boiling" or the "low subcooled" region.

In this region the number of nucleation sites increase and more bubbles grow at the heating surface. These bubbles detach from the wall, and they condense slowly as they pass through the slightly subcooled liquid. The void fraction in this region rises sharply, and this will cause a sharp increase in the pressure drop. It is in this region where the pressure drop-flow rate curve passes through a minimum pressure drop.

As the flow rate is decreased, the fourth region or "saturated nucleate boiling" region begins. In this region the liquid temperature will reach to the saturation temperature and bulk boiling starts. A further decrease in the flow rate will increase the vapor quality. The pressure drop continues to increase due to the acceleration of the mixture along the tube. Further reduction of the flow rate will increase the vapor quality until all the liquid evaporates, and the fifth region begins. This region, like the first region, is that of pure forced-convection, and further reduction in the flow rate will decrease the pressure drop. It is between the fourth and fifth region where the pressure drop-flow rate curve passes through a maximum. The above five regions are shown in Figure 39.

To check on the reproducibility of the data, ten different runs from the longest test section (L/D = 204) were repeated after twenty days. The maximum deviation was about $\pm$ 6% while most of the data was close to $\pm$ 2% which was considered acceptable.

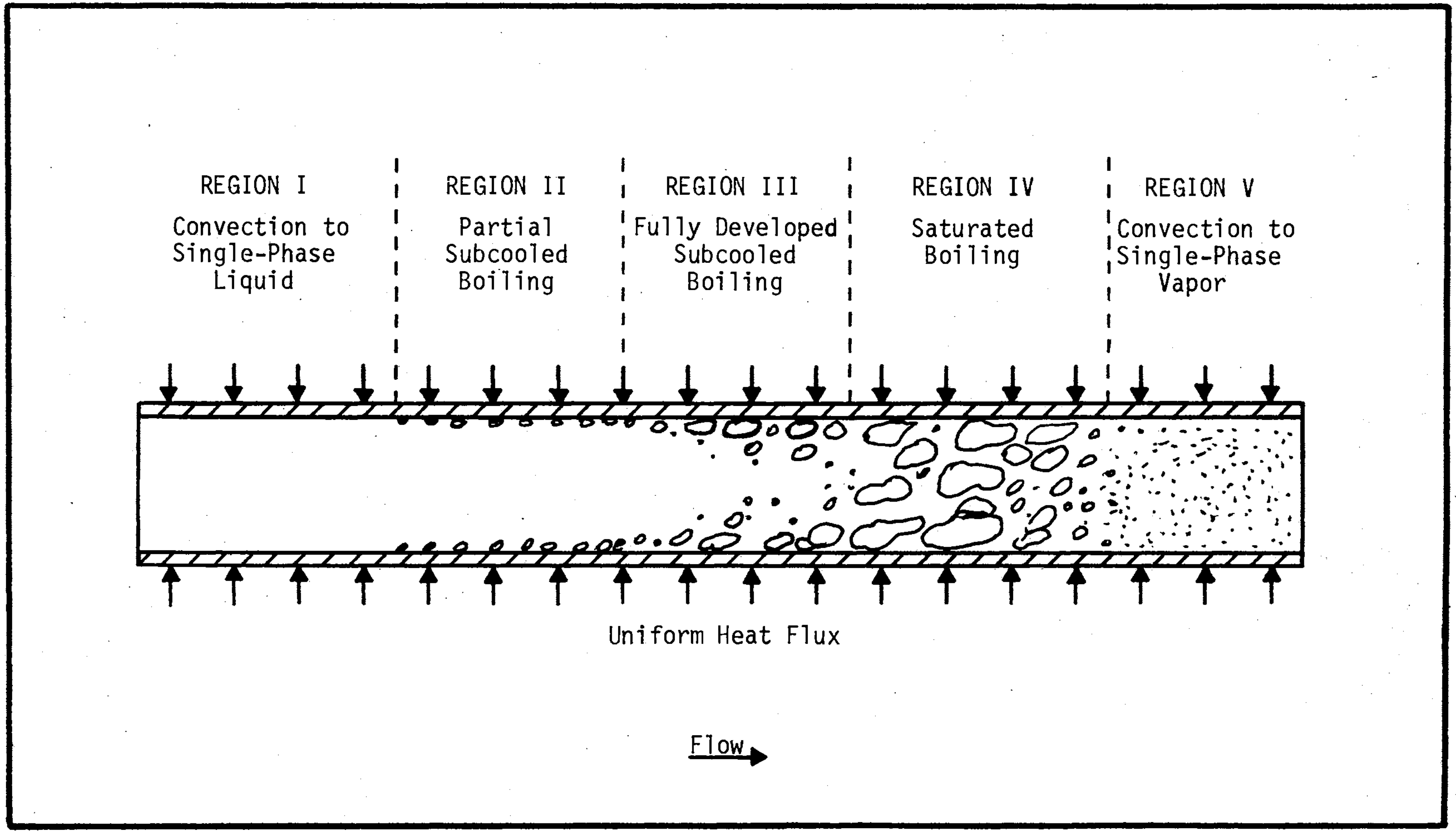

Figure 39. Regions of Pressure Drop in Forced-Convection Boiling With Inlet Subcooling

5.2 Effect of Various Parameters

In the following sections the effect of various parameters on the pressure drop-flow rate curve will be discussed and their effect on the excursive instability will be analyzed.

5.3 Inlet Subcooling

A study of the experimental data presented in Figures 10 through 38 indicated that decreasing the inlet subcooling while holding the other variables constant, shrinks the first region (forced-convection region) of the pressure drop flow rate curve. Consequently, the second and third regions begin at higher mass flow rates and the curve will pass through the point of minimum pressure drop at higher values of mass flow. This means that increasing the inlet subcooling increases the range of the stable operation. Maulbetsch (16) also obtained the same result.

The review of literature shows that the effect of inlet subcooling on the oscillatory instability is complex, and it might have a stabilizing or destabilizing effect. In excursive instability this does not appear to be the case.

5.4 Pressure

The effect of the system pressure on the pressure drop-flow rate curve is that it expands the forced-convection region on the liquid side due to the fact that increasing the pressure will increase the saturation temperature and will cause the minimum pressure drop to occur at lower flow rates. Also, increasing the system pressure will increase the vapor density; and consequently, the range of the negative slope region of the pressure drop-flow rate curve will decrease. Thus, increasing the system pressure increases the range of the stable operation.

This result, without any exception, is in agreement with all the previous investigations on the effect of system pressure on the stability.

5.5 Heat Flux

The data has been presented in such a way that the effect of heat flux can be seen in each figure. At high mass flow rates where no vapor is present, increasing the heat flux will reduce the pressure drop. This is due to the fact that viscosity near the wall will decrease with increasing temperature. However, increasing the heat flux will contract the single phase region on the liquid side; and consequently, the second and third regions will start at higher mass flow rates, which in turn, causes the point of minimum pressure drop to occur at high mass flow rates. Increasing the heat flux will increase the test section total pressure drop in the "highly subcooled" region, "low subcooled" region, and "saturated nucleate boiling" region. Also, an increase in the heat flux will increase the negative slope region of the pressure drop flow rate curve. This shows that increasing the heat flux decreases the range of the stable operation. This result is in agreement with the result of the other investigators.

5.6 Length to Diameter Ratio

An extensive investigation of pressure drop for subcooled boiling of water was carried out by Dormer and Bergles (21). They found that as long as the length to diameter ratio remains constant, the diameter has a very small effect on the pressure drop and that the length to diameter ratio is of prime importance. This is supported by the results of Maulbetsch (16).

It was mentioned in section 5.1 that the pressure drop flow rate curve passes through the point of minimum pressure drop in the subcooled boiling region. At the minimum of each curve, a heat balance was performed to find out the condition of the flow at the channel exit. It was found out that without exception, this minimum occurs at exit conditions which are subcooled. However, it was noticed that degree of subcooling at the channel exit corresponding to the condition of the point of minimum pressure drop varies with the length to diameter ratio.

For the large length to diameter ratios the degree of subcooling at the channel exit for the minimum is less than those for the small length to diameter ratios.

In two test sections with different L/D, which are operating under the same heat flux, inlet subcooling, and system pressure, the minimum in the larger test section occurs at the higher mass flow rates than that in the smaller test section. This is due to the fact that the total heat flow rate into the larger test section is more than that for the smaller test section. Thus, increasing the length-to-diameter ratio decreases the range of the stable operation provided that heat flux, inlet subcooling, and system pressure in both cases are the same.

This result can be justified by the following discussion. Location of the point of minimum pressure drop on the pressure drop-flow rate curve is strongly dependent on the onset of subcooled nucleate boiling, due to the fact that the point of minimum pressure drop occurs somewhere in the subcooled boiling region.

The results obtained by Bergles and Rohsenow (22), Bowring (23), and many other investigators show that the onset of subcooled nucleate boiling is a function of heat flux and pressure.

Now, consider two test sections with different length-to-diameter ratios operating under the same heat flux, system pressure, inlet subcooling, and mass flow rate. If the mass flow rate in both test sections is reduced slowly, the wall temperature will start to increase until at a specific value of mass flow rate the wall superheat will reach to a value which is sufficient to initiate surface boiling. The point of initiation of the subcooled boiling is at the same distance from the test section inlet for both of the test sections. This is obvious from a heat balance. The distance between this point and the channel exit is larger for the test section with larger L/D; and consequently, the temperature of the liquid at the channel exit with larger L/D will be more than the liquid exit temperature in the channel with smaller L/D. Thus, the exit subcoolings for the test sections with small L/D are higher than those corresponding to the test sections with large L/D.

5.7 Inlet Orificing

After the data taking was finished and the pressure drop-flow rate curves were plotted, three different types of orifice pressure drops were imposed on these curves. For each inlet temperature the pressure drop-flow rate curve for each test section under isothermal conditions was obtained. Three different orifices were assumed to have pressure drop-flow characteristics as:

$$\frac{\Delta P_o}{\Delta P_{adb}} = 0.5, \; \frac{\Delta P_o}{\Delta P_{adb}} = 1.0, \; \frac{\Delta P_o}{\Delta P_{adb}} = 2.0.$$

Where ΔP_o is the orifice pressure drop for a given inlet temperature and test section, ΔP_{adb} is the test section pressure drop at the same inlet temperature under adiabatic conditions.

It was found that inlet orifice pressure drop will shift the point of minimum pressure drop to lower mass flow rates and at the same time reduces the negative slope region of the pressure drop-flow rate curve. Consequently, the inlet orificing has a stabilizing effect on the instability. This has been obtained by many other investigators and accepted as an established fact for many years.

A typical effect of inlet orificing is shown in Figure 40.

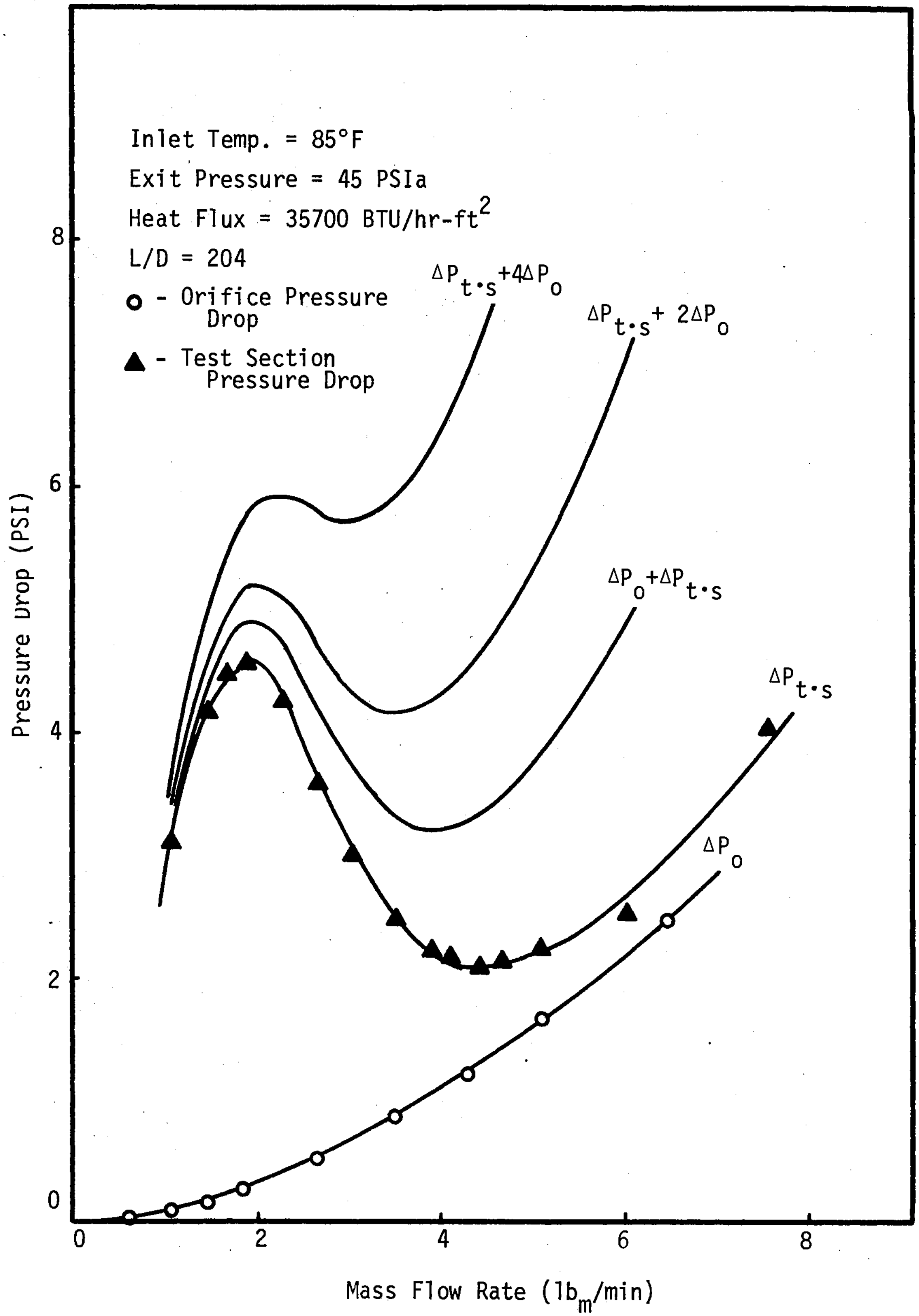

Figure 40. Effect of Inlet Orificing on the Pressure Drop-Flow Rate Curve

CHAPTER VI

CORRELATION OF THE RESULTS

In flow stability problems, as well as other heat transfer and fluid mechanics problems, it is very important to reduce the variables to a set of dimensionless groups. The use of dimensionless groups has many advantages:

1. The number of variables is reduced.

2. The results of different investigations can be compared more easily.

3. Simulation of the practical problem is possible with more convenience in the laboratories.

The literature review revealed that the most important parameters affecting the two-phase flow stability are: inlet subcooling, pressure level, heat flux, inlet orificing, mass flow rate, and geometry. The effect of inlet subcooling is best described by the ratio of the heat required to raise the fluid to the saturation temperature to the heat required for vaporization. Therefore, the dimensionless parameter $C_p(T_s-T_i)/h_{fg}$ was selected to describe the effect of inlet subcooling. C_p and T_i are the specific heat and inlet temperature of the fluid and T_s and h_{fg} are the saturation temperature and heat of vaporization at the condition of the channel exit. Since T_s and h_{fg} are dependent on the system pressure, the above dimensionless group will also reflect the effect of the system pressure. The effect of the system pressure can also be described by the ratio of the vapor density to the liquid density (ρ_v/ρ_ℓ). It was found that the effect of the pressure on the dimensionless parameters $C_p(T_s-T_i)/h_{fg}$ and ρ_v/ρ_ℓ is approximately the same and that $C_p(T_s-T_i)/h_{fg}$ can describe the effect of the pressure as well as ρ_v/ρ_ℓ.

This is justified by the fact that the value of the dimensionless parameter $(\rho_v/\rho_\ell)C_p(T_s-T_i)/h_{fg}$ (which is similar to Jakob number) is insensitive to the pressure.

The primary objective of this chapter is to find a correlation for the points of the minimum pressure drop on the pressure drop-flow rate curves.

Maulbetsch (16) found that the point of the minimum pressure drop occurs in the subcooled nucleate boiling region. Whittle and Forgan (24) suggested that this point is very close to the point of the bubble detachment from the heated surface and Bowring (23), Levy (25), and Staub (26) found that the point of bubble detachment is in the subcooled boiling region. The results of this study also showed that this point is in the subcooled boiling region. It can be concluded that the point of the minimum pressure drop is closely associated with the point where the subcooled nucleate boiling first starts. The onset of subcooled nucleate boiling is dependent on the heat flux and the saturation temperature and the density ratio does not have a significant effect on this point. For these reasons, the dimensionless parameter $C_p(T_s - T_i)/h_{fg}$ was selected to describe the effects of the inlet subcooling and the pressure at the same time.

The second dimensionless parameter is selected to be $\dot{q}/A/Gh_{fg}$, where $\dot{q}$ is the heat flow rate and G is the mass velocity. This parameter will describe the effects of the heat flux and the mass flow rate. The effect of the orifice pressure drop can be expressed in dimensionless form by dividing it by the adiabatic pressure drop of the test section, thus $\Delta P_o/\Delta P_{adb}$ was selected to be another dimensionless parameter. The last dimensionless parameter is L/D which describes the effect of the geometry.

At the point of minimum pressure drop on the pressure drop-flow rate curve, the above dimensionless parameters were calculated and the results are presented in Figures 41 through 44.

For the large test section (L/D = 204) each data point represents the average of five measured points. Since these five points are very close to each other only the average is shown.

The effect of inlet subcooling, system pressure, heat flux, inlet orificing, mass flow rate, and geometry on the excursive instability can be clearly seen from these curves.

Figure 41 can be used as a prediction of the onset of excursive instability in parallel channel systems, where the external system pressure drop is independent of the flow rate (constant pressure-drop supply system). Also, Figure 41 is useful in prediction of the location of the minimum pressure drop on the pressure drop-flow rate curve for single channels.

With a given inlet temperature, exit pressure, heat flux, mass flow rate, and L/D it is possible to predict whether the system is in the stable region or unstable region. If the point of operation happens to be in the unstable region and if the system is a constant pressure-drop supply system, burnout will occur. If the system is not a constant pressure-drop supply system, operation will be in the negative slope

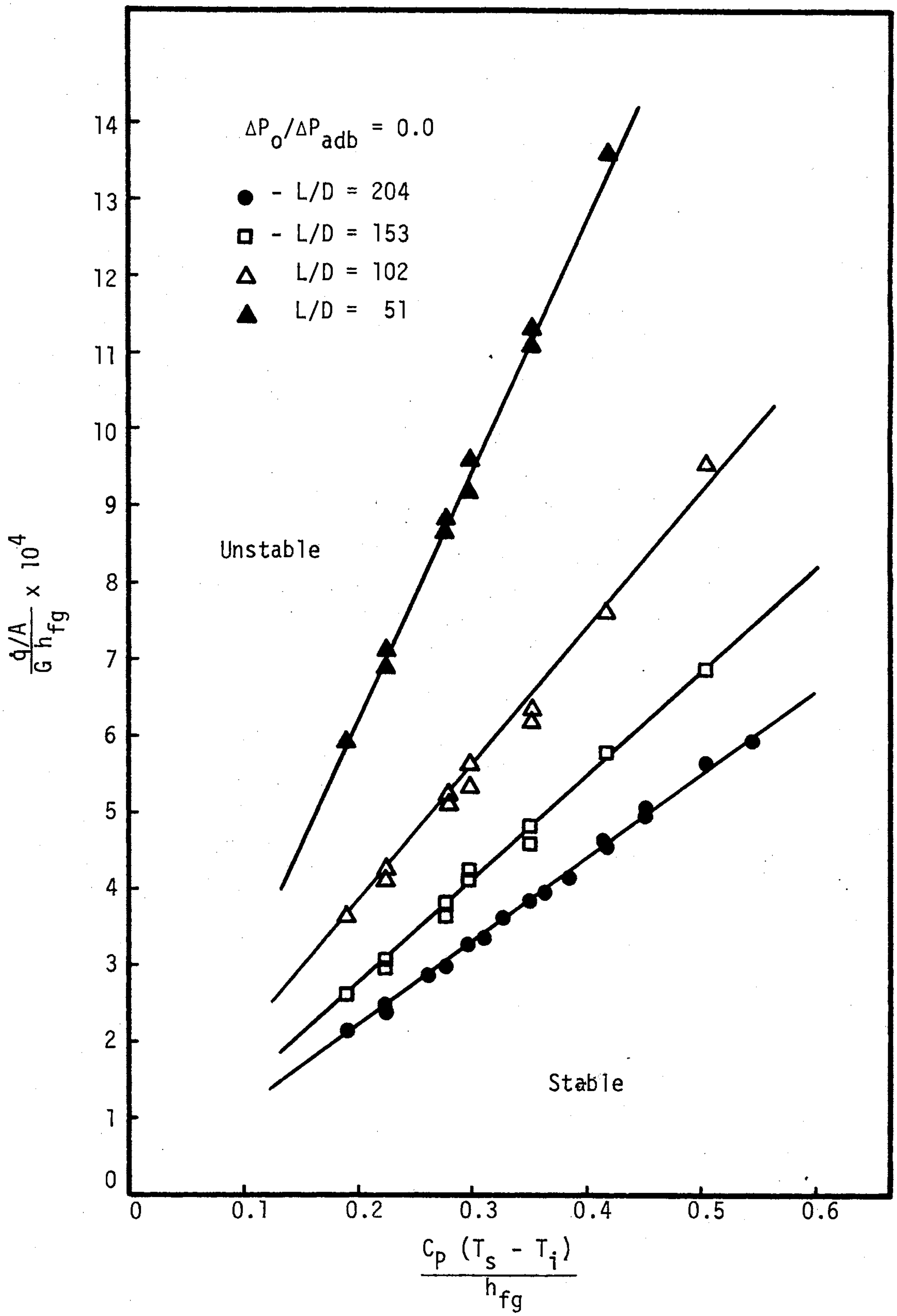

Figure 41. Correlation of Data

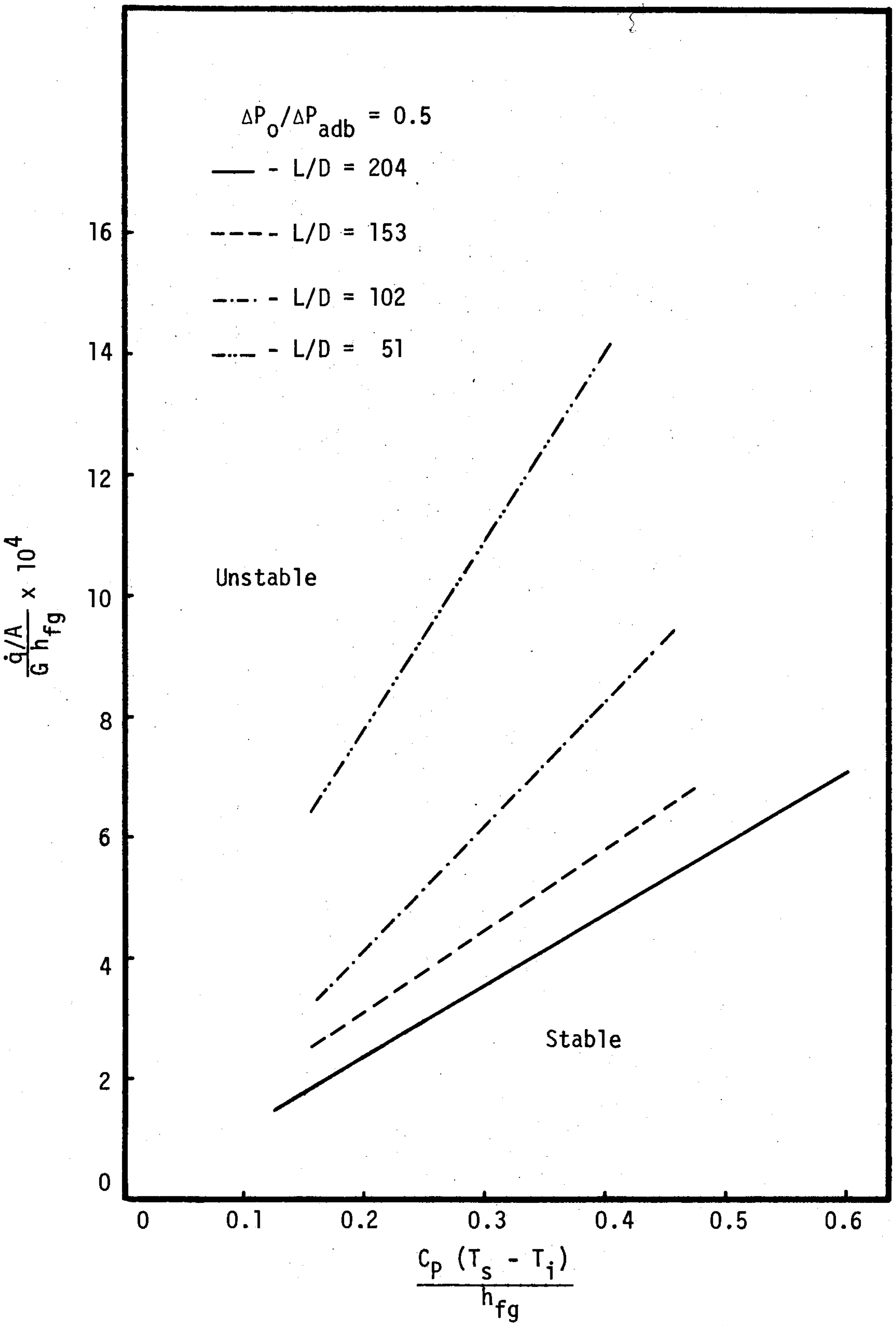

Figure 42. Correlation of Data

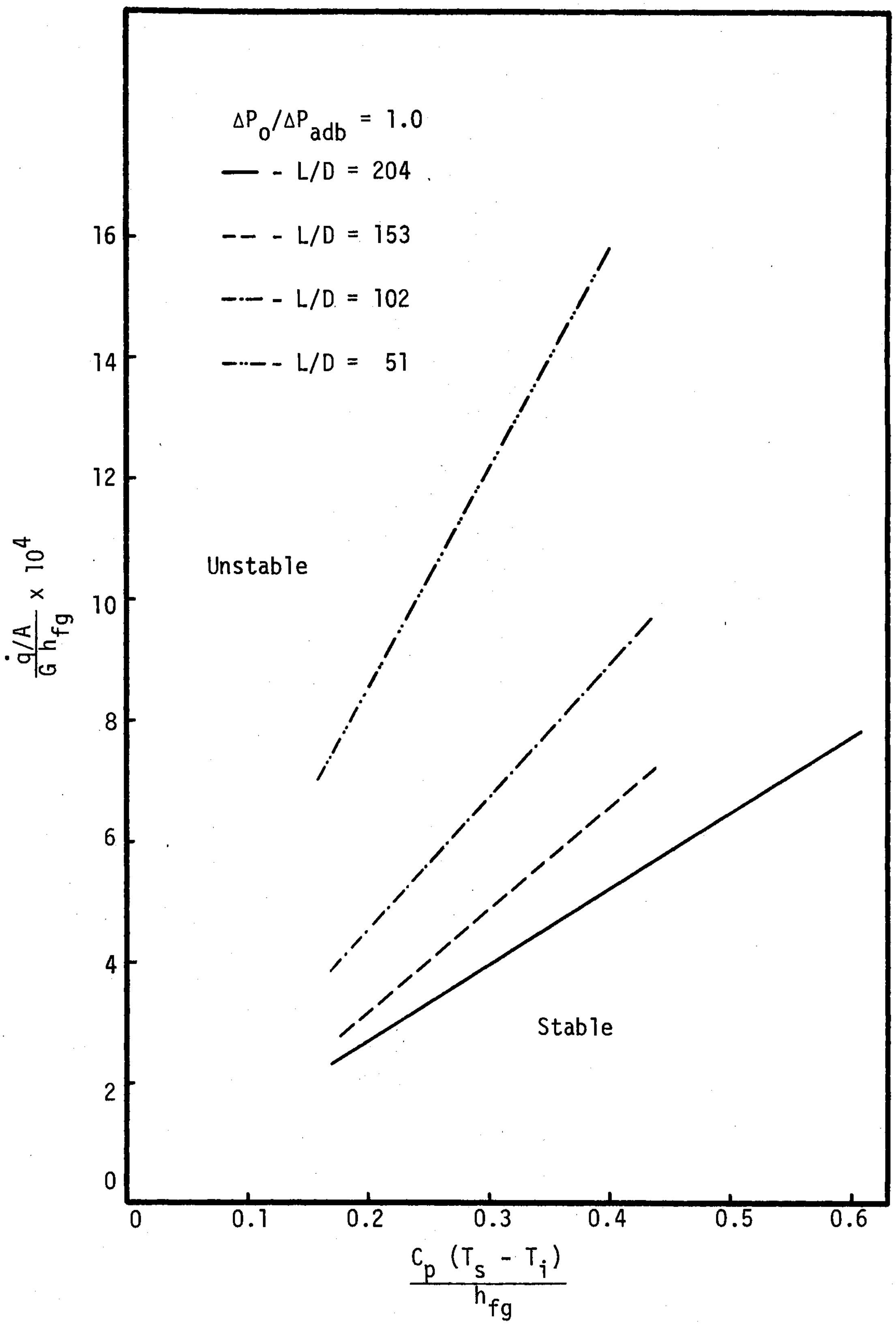

Figure 43. Correlation of Data

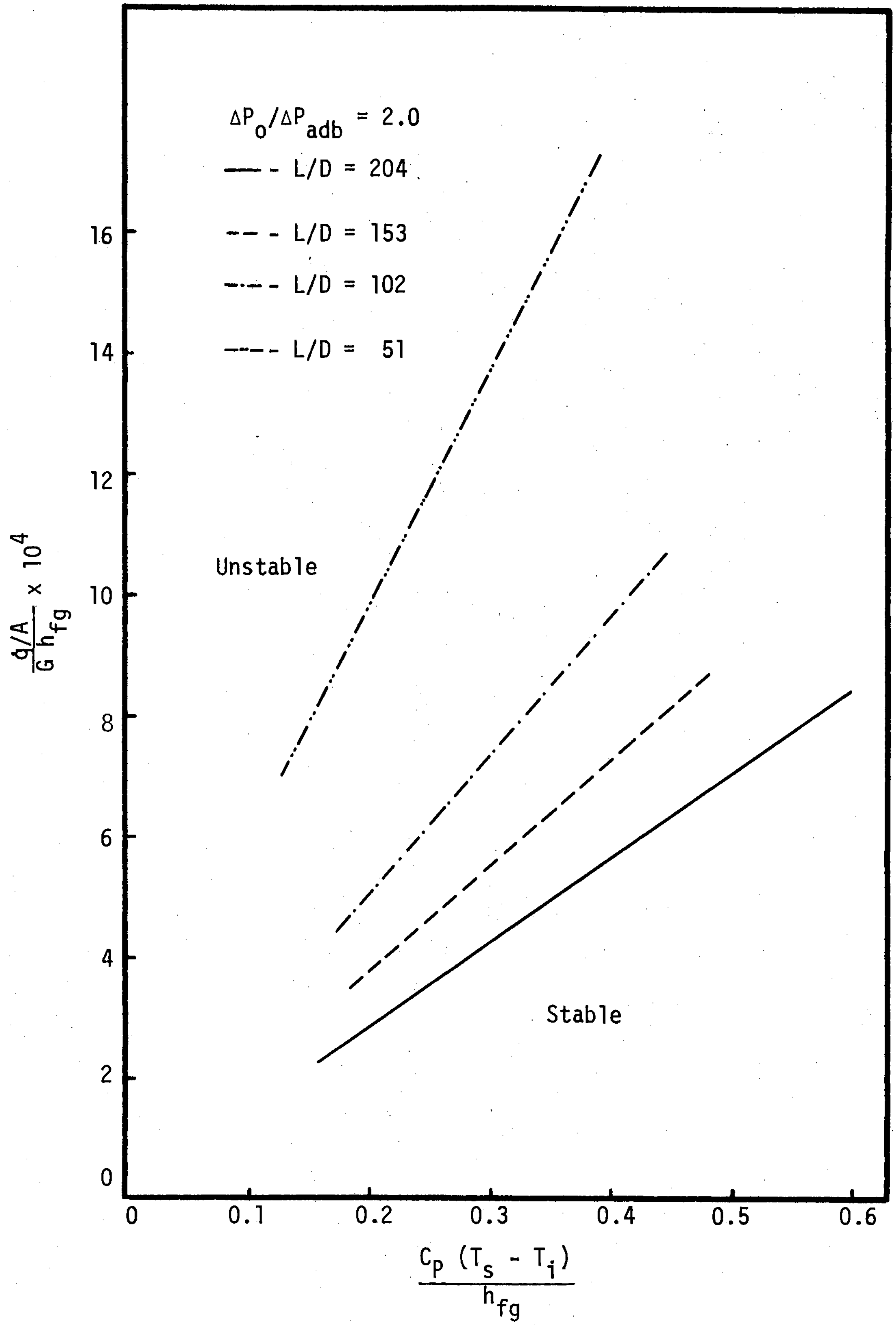

Figure 44. Correlation of Data

region of the pressure drop-flow rate curve and the system will be subject to the pressure drop oscillations. This might or might not lead to the burnout, depending on the external supply system. In such cases, by changing one or more of the above parameters, the operation point can be shifted from the unstable region to the stable region. However, if due to the design considerations it is not possible to change any of the above parameters, the only way to operate in the stable region is by providing a sufficient inlet orificing.

In such cases, Figures 42 through 44 can be used depending how much orifice pressure drop can be used.

From Figures 41 through 44 it can be seen that the data points corresponding to the onset of excursive instability for a given orifice pressure drop fall on a straight line and the slope varies only with the length-to-diameter ratio.

The slope of each line is $\dot{q}/A/C_pG(T_s-T_i)$, where (T_s-T_i) is the difference between the inlet temperature and the saturation temperature at the condition of the channel exit. This slope can be written in the following form: $(\dot{q}/\dot{q}_{se})$ $(1/4L/D)$ where $\dot{q}$ is the actual heat flow rate into the test section and $\dot{q}_{se}$ is the heat flow rate which is required to obtain a saturation condition at the test section exit.

For each test section the value of L/D is constant. For a given test section the value of $\dot{q}/\dot{q}_{se}$ at the point of minimum pressure drop is constant, and the value of this constant changes only with length-to-diameter ratio.

This result has been previously noted by Maulbetsch (16). From this result it seems that it is possible to use L/D as a parameter for correlating $\mathring{q}/\mathring{q}_{se}$ and obtain a stability map. To do so, at the points of the minimum pressure drops the values of $\mathring{q}/\mathring{q}_{se}$ were calculated and the average values of $\mathring{q}/\mathring{q}_{se}$ for each L/D were obtained. The results are shown in Figure 45. Maulbetsch (16) obtained pressure drop-flow rate curves for water flowing inside small diameter tubes up to the point of the minimum pressure drop. To compare his results with the results from this study, the values of $\mathring{q}/\mathring{q}_{se}$ at the points of minimum were calculated and the results are shown in Figure 45. It can be seen that there is a good agreement between the two results. This gives more confidence in the experimental results and the fact that a proper set of dimensionless groups was selected.

Similar curves were obtained with imposing different orifice pressure drops on the pressure drop-flow rate curves and the results are shown in Figure 46.

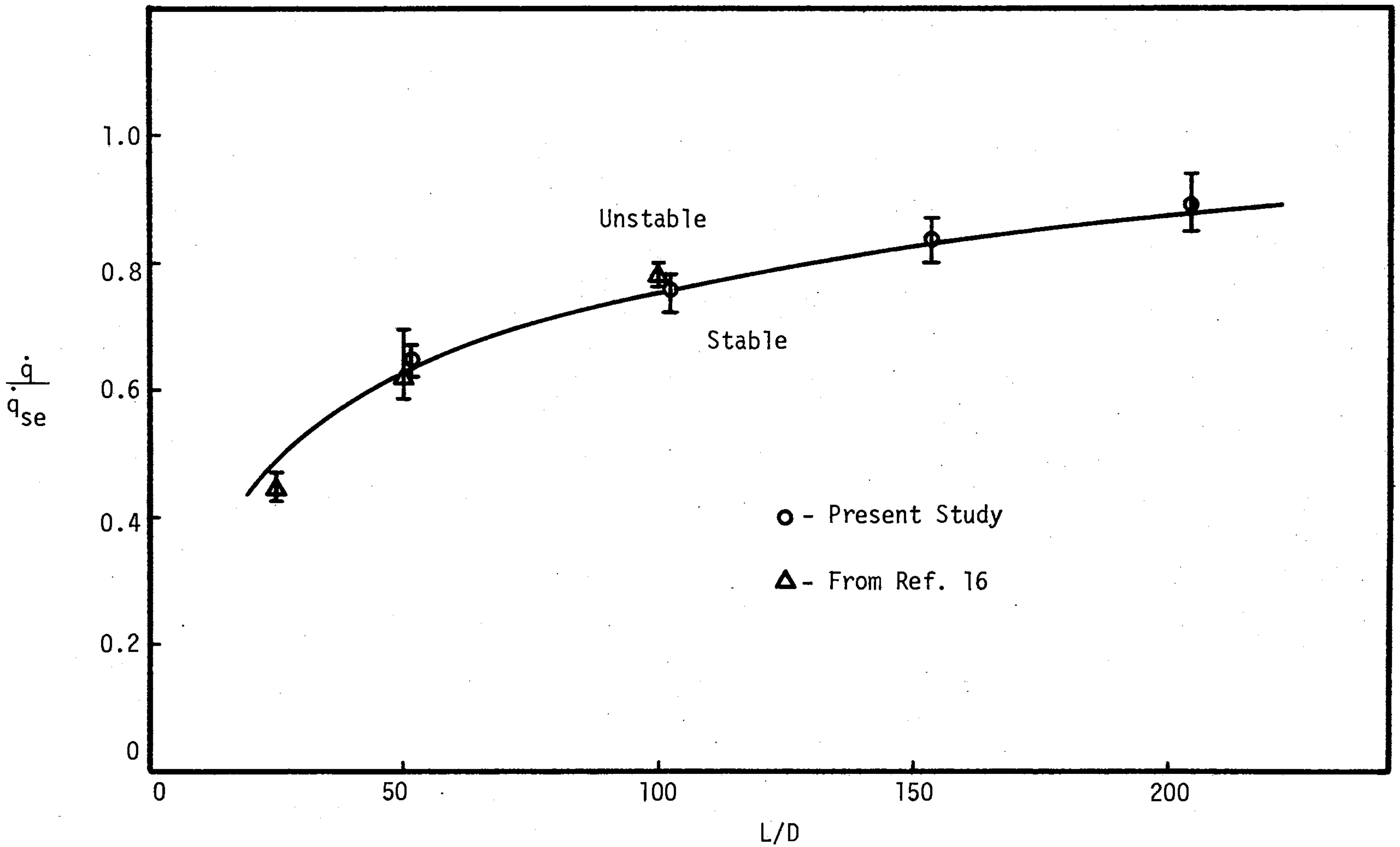

Figure 45. Correlation of Data

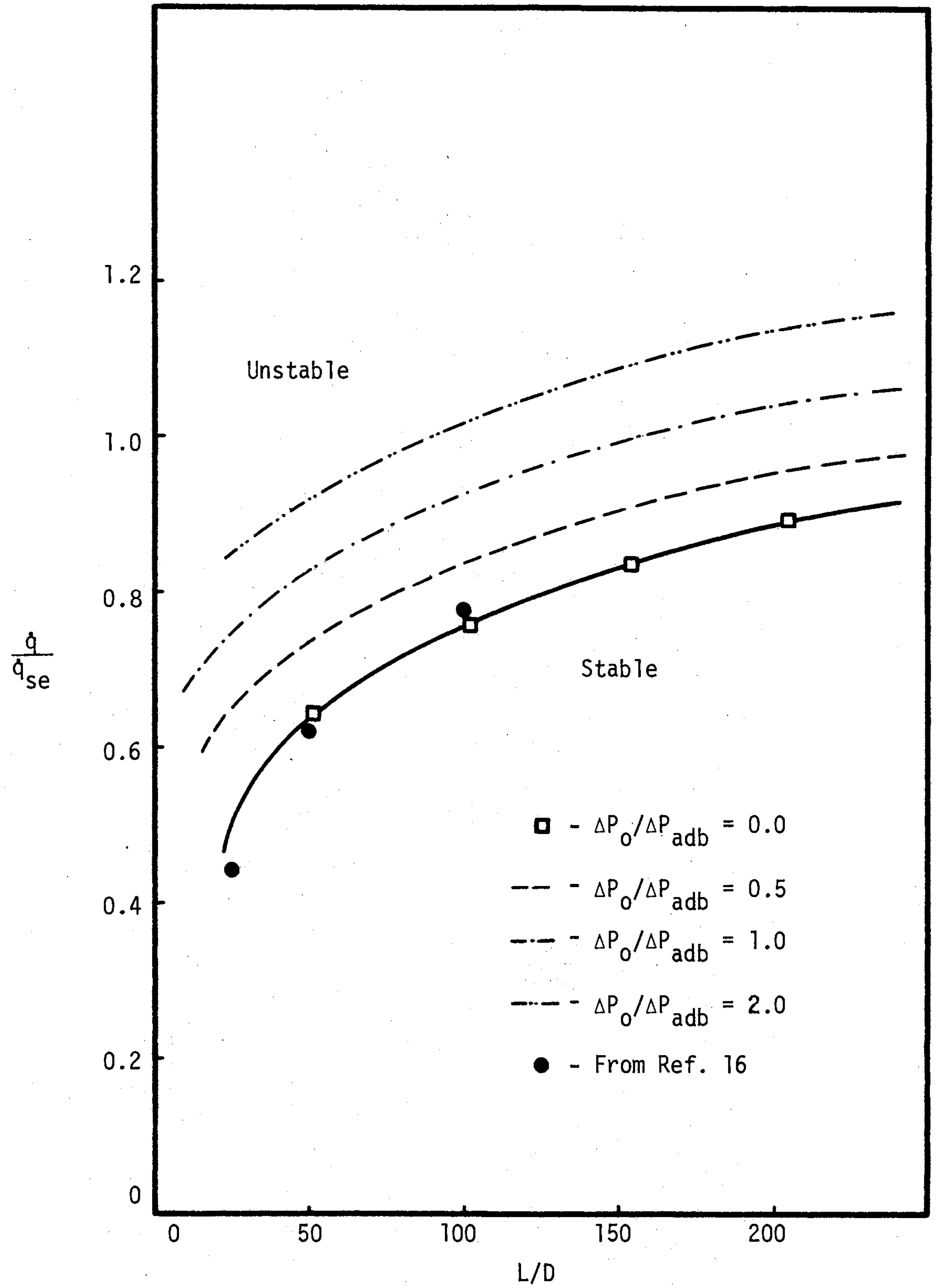

Figure 46. Correlation of Data

CHAPTER VII

CONCLUSIONS AND RECOMMENDATIONS

Two-phase flow stability was studied in horizontal channels by steady-state measurements of the pressure drop versus flow rate curve. The effects of inlet subcooling, system pressure, heat flux, inlet orificing, and geometry on this curve and particularly on the point of minimum pressure drop were investigated.

The conclusions which have been reached in this investigation can be summarized as follows:

1. In the range of the variables studied, the pressure drop-flow rate curves have distinct minima and maxima.

2. The point of the minimum pressure drop on the pressure drop-flow rate curve occurs in the subcooled boiling region where the void fraction rises sharply.

3. Increasing the inlet subcooling increases the range of stable operation by shifting the point of the minimum pressure drop towards the lower mass flow rates. Decreasing the inlet subcooling will shift the point of the minimum pressure drop towards the higher mass flow rates and hence decreases the range of stable operation.

4. Increasing the system pressure increases the range of stable operation and reduces the size of the negative slope region of the pressure drop-flow rate curve.

5. Increasing the heat flux will decrease the range of stable operation and will increase the size of the negative slope region of the pressure drop-flow rate curve.

6. Increasing the inlet orifice pressure drop will increase the range of the stable operation and reduces the size of the negative slope region of the pressure drop-flow rate curve.

7. Decreasing the length to diameter ratio while holding the inlet subcooling, inlet orificing, system pressure, and heat flux constant will increase the range of the stable operation. However, decreasing the length to diameter ratio while holding the inlet subcooling, inlet orificing, system pressure, and heat flow rate constant will decrease the range of stable operation.

8. At the point of the minimum pressure drop the ratio of the actual heat flow rate to the heat flow rate required to obtain saturated liquid at the channel exit is a constant value and the value of this constant is dependent only on the length to diameter ratio.

9. The results of this investigation have been correlated and shown in Figures 41 through 46. The correlation curves should be useful in the design of heated parallel channels with a constant pressure-drop supply system. The curves show the safe and unsafe regions with respect to excursive instability. For such systems, this instability may lead to burnout at a heat flux well below the stable critical heat flux. If the system is not a constant pressure-drop supply system, for example, if the system has only a few channels, the curves give conservative answers, and may also be useful to predict whether the operation point is in the negative slope region or not.

10. The results obtained in this study are applicable to horizontal, smooth tubes and their validity is not assured in other situations.

The following suggestions are recommended to extend the range of applicability of the results obtained in this study:

1. Similar experimental data are needed for short test sections (L/D<50) and for large test sections (L/D>200) in order to extend the range of applicability of the correlation curves.

2. In Figure 45 it can be observed that the slope of the correlation curve will decrease with increasing length-to-diameter ratio. It seems that at higher length-to-diameter ratios, the slope of this curve will finally reduce to zero. It would be of particular interest to find the value of L/D at which the slope of the curve becomes zero and also to find the value of $\frac{\dot{q}}{\dot{q}_{se}}$ corresponding to this L/D.

A SELECTED BIBLIOGRAPHY

(1) Boure, J. A., A. E. Bergles, and L. S. Tong. "Review of Two-Phase Flow Instability." ASME Paper No. 71-HT-42, 1971.

(2) Ledinegg, M. "Instability of Flow During Natural and Forced Circulation." Die Warme, Vol. 61, 1938, pp. 891-898.

(3) Chilton, H. "A Theoretical Study of Stability in Water Flow Through Heated Passages." Journal of Nuclear Energy, Vol. 5, 1947, pp. 273-284.

(4) Markels, M. "Effects of Coolant Flow Orificing and Monitoring on Safe Pile Power." Chemical Engineering Progress Symposium Series, No. 19, Vol. 52, 1956, pp. 73-85.

(5) Lowdermilk, W. H., C. D. Lanzo, and B. L. Siegel. "Investigation of Boiling Burnout and Flow Stability for Water Flowing in Tubes." National Advisory Committee for Aeronautics, Technical Note No. 4382, 1958.

(6) Fraas, A. P. "Flow Stability in Heat Transfer Matrices Under Boiling Conditions." Oak Ridge National Laboratory Report No. 59-11-1, 1959.

(7) Blubaugh, A. L., and E. R. Quandt. "Analysis and Measurement of Flow Oscillations." United States Atomic Energy Commission Report, Series WAPD, No. AD-TH538, 1960.

(8) Mendler, O. J., A. S. Rathbun, N. E. Van Huff, and A. Weiss. "Natural Circulation Tests with Water at 800 to 200 psia Under Nonboiling, Local Boiling, and Bulk Boiling Conditions." Journal of Heat Transfer, Trans. ASME, Series C, Vol. 83, 1961, pp. 261-273.

(9) Fraas, A. P. "Flow Stability in Heat Transfer Matrices Under Boiling Conditions." Oak Ridge National Laboratory Report No. 59-11-1, 1961.

(10) Jones, A. B. "Hydrodynamic Stability of a Boiling Channel." Knolls Atomic Power Laboratory Report No. 2170, 1961.

(11) Quandt, E. R. "Analysis and Measurement of Flow Oscillations." Chemical Engineering Progress Symposium Series, No. 32, Vol. 57, 1951, pp. 111-126.

(12) Stenning, A. H. "Instabilities in the Flow of a Boiling Liquid." ASME Paper No. 62-WA-155, 1962.

(13) Stenning, A. H., and T. N. Veziroglu. "Flow Oscillation Modes in Forced-Convection Boiling." Proceedings of the Heat Transfer and Fluid Mechanics Institute, Stanford University Press, 1955, pp. 301-316.

(14) Stenning, A. H., and T. N. Veziroglu. "Density-Wave Oscillations in Boiling Freon-11 Flow." ASME Paper No. 66-WA-HT-49, 1966.

(15) Veziroglu, T. N., and S. S. Lee. "Instabilities in Boiling Upward Flows." International Symposium on Research on Cocurrent Gas-Liquid Flow, Vol. 2, 1968, pp. 1-47.

(16) Maulbetsch, J. S. "A Study of System-Induced Instabilities in Forced-Convection Flows with Subcooled Boiling." Ph.D. Dissertation in the Department of Mechanical Engineering, Massachusetts Institute of Technology, 1965.

(17) Gouse, S. W., and C. C. Andrysiak. "Flow Oscillations in a Closed Loop with Transparent, Parallel, Vertical, Heated Channels." Report No. 8973-2, Department of Mechanical Engineering, MIT, 1963.

(18) Berenson, P. J. "An Experimental Investigation of Flow Stability in Multitube Forced-Convection Vaporizers." ASME Paper No. 65-HT-61, 1965.

(19) Schuster, J. R., and P. J. Berenson. "Flow Stability of a Five-Tube Forced-Convection Boiler." ASME Paper No. 67-WA-HT-20, 1967.

(20) Veziroglu, T. N., and S. S. Lee. "Boiling Flow Instabilities in Parallel Channels." Proceedings of the Institution of Mechanical Engineers, Vol. 184, Part 3C, 1964, pp. 7-17.

(21) Dormer, T. Jr., and A. E. Bergles. "Subcooled Boiling Pressure Drop with Water at Low Pressure." International Journal of Heat and Mass Transfer, Vol. 12, 1964, pp. 459-470.

(22) Bergles, A. E., and W. M. Rohsenow "The Determination of Forced-Convection Surface Boiling Heat Transfer." ASME Paper No. 63-HT-22, 1963.

(23) Bowring, R. W. "Physical Model Based on Bubble Detachment and Calculation of Steam Voidage in the Subcooled Region of a Heated Channel." OECD Report No. HPR-10, 1962.

(24) Whittle, R. H., and R. Forgan. "A Correlation for the Minima in the Pressure Drop Versus Flow Rate Curves for Subcooled Water Flowing in Narrow Heated Channels." Nuclear Engineering and Design, Vol. 6, 1967, pp. 89-99.

(25) Levy, S. "Forced-Convection Subcooled Boiling Prediction of Vapor Volumetric Fraction." International Journal of Heat and Mass Transfer, Vol. 10, 1967, pp. 951-965.

(26) Staub, F. W. "The Void Fraction in Subcooled Boiling - Prediction of the Initial Point of Net Vapor Generation." ASME Paper No. 67-HT-36, 1967.

(27) Parker, J. D., J. H. Boggs, and E. F. Blick. Introduction to Fluid Mechanics and Heat Transfer. Addison-Wesley Publishing Company, Inc., New York, N. Y., 1969.

(28) Wallis, G. B. One-Dimensional Two-Phase Flow. McGraw-Hill Book Company, Inc., New York, N. Y. , 1969.

(29) Collier, J. G. Convective Boiling and Condensation. McGraw-Hill Book Company, Inc. New York, N. Y., 1972.

(30) Lottes, P. A. "Nuclear Reactor Heat Transfer." Argonne National Laboratory Report No. 6469, 1961.

(31) Benedict, R. P. Fundamentals of Temperature, Pressure, and Flow Measurements. John Wiley and Sons, Inc., New York, N. Y., 1969.

(32) Tong, L. S. Boiling Heat Transfer and Two-Phase Flow. John Wiley and Sons, Inc., New York, N. Y., 1965.

(33) Dowing, R. C. "Transport Properties of Freon Fluorocarbons." E. I. DuPont de Nemours and Company, Technical Bulletin No. C-30, 1967.

(34) Benning, A. F., and R. C. McHarness. "Thermodynamic Properties of Freon-113 (Trichlorotrifluoroethan)." E. I. DuPont de Nemours and Company, Technical Bulletin No. T-113A, 1938.

(35) Hodson, A. S. "Hysteresis Effects in Surface Boiling of Water." Journal of Heat Transfer, Trans. ASME, Series C, Vol. 91, pp. 160-162, 1969.

(36) Murphy, R. W., and A. E. Bergles. "Subcooled Flow Boiling of Fluorocarbons-Hysteresis and Dissolved Gas Effects on Heat Transfer." Proceedings of the Heat Transfer and Fluid Mechanics Institute, Stanford University Press, 1972, pp. 400-416.

(37) Crowley, J. B. and A. E. Bergles. "Fluid to Fluid Modeling of the Hydrodynamic Stability of Flow in Boiling Channels." ASME Paper No. 70-HT-28, 1970.

(38) Jordan, D. P., and G. Leppert, "Pressure Drop and Vapor Volume with Subcooled Nucleate Boiling," International Journal of Heat and Mass Transfer, Vol. 5, 1962, pp. 751-761.

(39) Danilova, G. N. "Correlation of Boiling Heat Transfer Data for Freons." Heat Transfer-Soviet Research, Vol. 2, 1970, pp. 73-78.

(40) Aladiev, I. T., Z. L. Miropolsky, V. E. Doroschuk, and M. A. Styrikovich. "Boiling Crisis in Tubes." International Heat Transfer Conference, Published by ASME, 1961, pp. 237-243.

(41) Crowley, J. D., C. Deane, and S. W. Gouse, Jr. "Two-Phase Flow Oscillations in Vertical, Parallel Heated Channels." European Atomic Energy Community Report, Proceedings of Symposium on Two-Phase Flow Dynamics, 1967, pp. 1131-1170

APPENDIX A

DERIVATION OF CRITERIA FOR EXCURSIVE INSTABILITY

The criterion for excursive instability was given by other investigators such as Ledinegg (2), Chilton (3) and Maulbetsch (16). However, the details of a more general and more complete and at the same time more clear derivation are given here.

Consider a horizontal channel of length L and cross section A_c which is subject to some kind of heat flux (not necessarily constant heat flux), and a pressure difference of $(P_1 - P_2)$ which exists at both ends of the channel. A fluid with density ρ_1 and velocity V_1 enters at one end and exits at the other end with density ρ_2 and velocity V_2. The exit fluid might be a fluid with higher temperature, a two-phase fluid or a vapor. If the exit fluid is two-phase, it is assumed to be homogeneous.

Consider Figure 47. If Newton's second law is applied to the control volume through which the fluid is flowing, the resultant equation is:

$$\Sigma F_x = \frac{D(mV)}{Dt}$$

$$P_1A_c - P_2A_c - \tau A = \frac{\partial}{\partial t} \iiint_{c.v.} (V\rho)d(vol.) + \iint_{c.s.} V(\rho V_r \cdot dA_c) \quad (A.1)$$

Since control volume is stationary, $V_r = V$. ρ and V are assumed to be average density and velocity along the channel. We can write:

$$\frac{\partial}{\partial t} \iiint_{c.v.} (V\rho)d(vol.) = \frac{\partial}{\partial t} (V\rho LA_c) = L \frac{\partial}{\partial t} (\dot{m})$$

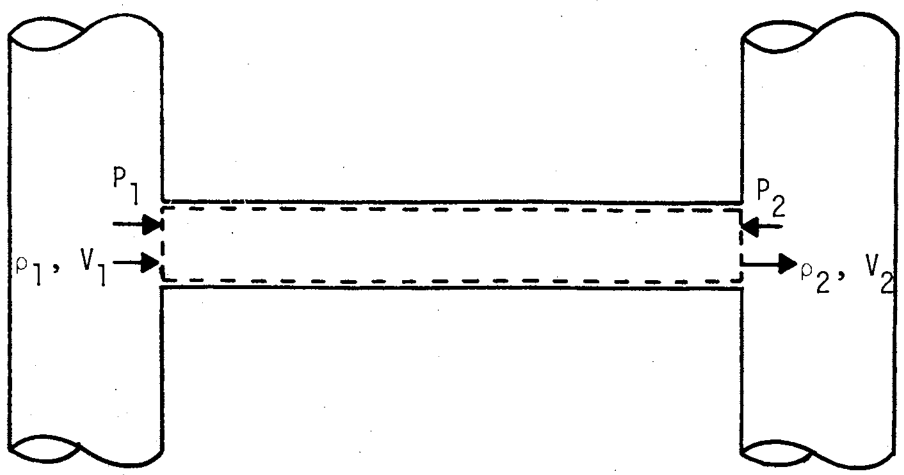

Figure 47. Schematic Diagram of Heated Section

Equation (A.1) becomes:

$$P_1 - P_2 = \tau \frac{A}{A_c} + \frac{L}{A_c} \frac{\partial}{\partial t} (\dot{m}) + \rho_2 V_2^2 - \rho_1 V_1^2 \tag{A.2}$$

$(P_1 - P_2)$ is the external system pressure drop which is imposed on the system, usually by a pump, and will be designated as ΔP_{ext}. $(\tau \frac{A}{A_c})$ accounts for the frictional pressure drop in the channel, which in general is composed of two terms: single phase pressure drop and two-phase pressure drop.

$[\frac{L}{A_c} \frac{\partial}{\partial t} (\dot{m})]$ is the inertia term, which accounts for the local acceleration of the flow.

$(\rho_2 V_2^2 - \rho_1 V_1^2)$ is momentum pressure drop.

$(\tau \frac{A}{A_c} + {}_2 V_2^2 - \rho_1 V_1^2)$, which is the channel total pressure drop, will be designated as ΔP_{int}.

It is obvious that ΔP_{ext} and ΔP_{int} are functions of flow rate ($\dot{m}$); therefore, Equation (A.2) can be written in the following form:

$$\frac{L}{A_c}\frac{d}{dt}(\dot{m}) + \Delta P_{int}(\dot{m}) - \Delta P_{ext}(\dot{m}) = 0.$$

If flow rate is changed by $\Delta\dot{m}$ such that $\dot{m} = \dot{m}_o + \Delta\dot{m}$, we obtain:

$$\frac{L}{A_c}\frac{d}{dt}(\dot{m}_o + \Delta\dot{m}) + \Delta P_{int}(\dot{m}_o + \Delta\dot{m}) - \Delta P_{ext}(\dot{m}_o + \Delta\dot{m}) = 0 \tag{A.3}$$

Applying a Taylor's series expansion to Equation (A.3) and neglecting the second order derivatives, we obtain:

$$\frac{L}{A_c}\frac{d}{dt}(\dot{m}_o) + \frac{L}{A_c}\frac{d(\Delta\dot{m})}{dt} + \Delta P_{int}(\dot{m}_o) + (\Delta\dot{m})\frac{\partial}{\partial\dot{m}}(\Delta P_{int})$$

$$- \Delta P_{ext}(\dot{m}_o) - (\Delta\dot{m})\frac{\partial}{\partial\dot{m}}(\Delta P_{ext}) = 0$$

The steady state condition will cancel out and the resultant equation is:

$$\frac{d}{dt}(\Delta\dot{m}) - \frac{A_c}{L}\left[\frac{\partial}{\partial\dot{m}}(\Delta P_{ext}) - \frac{\partial}{\partial\dot{m}}(\Delta P_{int})\right](\Delta\dot{m}) = 0 \tag{A.4}$$

Solution of differential Equation (A.4) for all values of t (from t = 0 to t = ∞) is:

$$\Delta\dot{m} = \frac{C}{\mathrm{EXP}\ \{-\frac{A_c}{L}\int_0^\infty \left[\frac{\partial}{\partial m}(\Delta P_{ext}) - \frac{\partial}{\partial\dot{m}}(\Delta P_{int})\right] dt}$$

Requirement for stable flow is that ($\dot{m}$) be zero; this happens if and only if

$$\left[\frac{\partial}{\partial\dot{m}}(\Delta P_{ext}) - \frac{\partial}{\partial\dot{m}}(\Delta P_{int})\right]$$

is negative. Thus the criteria for flow stability is:

$$\left[\frac{\partial}{\partial\dot{m}}(\Delta P_{ext}) - \frac{\partial}{\partial\dot{m}}(\Delta P_{int})\right] < 0,$$

and the condition for the onset of flow instability is:

$$\frac{\partial}{\partial\dot{m}}(\Delta P_{ext}) = \frac{\partial}{\partial\dot{m}}(\Delta P_{int}).$$

APPENDIX B

EXPERIMENTAL DATA

This appendix contains the experimental data obtained during the course of this study. All the raw data are presented in the same order as the Figures 10 through 38.

All important calculated data at the point of the minimum pressure drop are also presented in tabular form.

INLET TEMPERATURE = 85.0 DEG.F

EXIT PRESSURE = 25.0 PSIA

HEAT FLUX = 0.0 BTU/HR-SQ.FT

L/D = 204.0

MASS FLOW RATE(LBM/MIN)	PRESSURE DROP(PSI)
9.776	5.098
6.484	2.489
5.122	1.681
4.310	1.241
3.497	0.870
2.685	0.528
1.873	0.283
1.466	0.186
1.060	0.101
0.654	0.050

INLET TEMPERATURE = 95.0 DEG.F

EXIT PRESSURE = 25.0 PSIA

HEAT FLUX = 0.0 BTU/HR-SQ.FT

L/D = 204.0

MASS FLOW RATE(LBM/MIN)	PRESSURE DROP(PSI)
8.949	4.278
6.562	2.526
5.105	1.634
4.296	1.198
3.486	0.850
3.081	0.680
2.676	0.524
2.271	0.407
1.866	0.283
1.462	0.179
1.057	0.077
0.652	0.042

INLET TEMPERATURE = 110.0 DEG.F

EXIT PRESSURE = 25.0 PSIA

HEAT FLUX = 0.0 BTU/HR-SQ.FT

L/D = 204.0

MASS FLOW RATE(LBM/MIN)	PRESSURE DROP(PSI)
10.783	5.829
7.420	3.094
5.080	1.599
4.274	1.202
3.871	0.977
3.468	0.866
3.066	0.700
2.663	0.528
2.260	0.401
1.857	0.283
1.454	0.180
1.051	0.104
0.649	0.047

INLET TEMPERATURE = 120.0 DEG.F

EXIT PRESSURE = 25.0 PSIA

HEAT FLUX = 0.0 BTU/HR-SQ.FT

L/D = 204.0

MASS FLOW RATE(LBM/MIN)	PRESSURE DROP(PSI)
10.154	5.457
8.281	3.767
6.507	2.475
5.062	1.566
4.661	1.358
4.259	1.146
3.858	0.977
3.456	0.798
3.055	0.671
2.653	0.498
2.252	0.378
1.851	0.306
1.449	0.179
1.048	0.104

INLET TEMPERATURE = 85.0 DEG.F

EXIT PRESSURE = 25.0 PSIA

HEAT FLUX = 14250.00 BTU/HR-SQ.FT

L/D = 204.0

MASS FLOW RATE(LBM/MIN)	PRESSURE DROP(PSI)
5.122	1.768
4.310	1.312
3.903	1.104
3.497	0.970
2.685	0.912
2.604	1.065
2.482	1.088
2.279	1.179
2.076	1.296
1.669	1.625
1.466	1.840
1.060	2.198
0.816	2.243
0.654	2.178

INLET TEMPERATURE = 85.0 DEG.F

EXIT PRESSURE = 35.0 PSIA

HEAT FLUX = 14250.00 BTU/HR-SQ.FT

L/D = 204.0

MASS FLOW RATE(LBM/MIN)	PRESSURE DROP(PSI)
11.357	6.411
7.571	3.106
5.122	1.775
4.310	1.276
3.497	0.882
2.685	0.694
2.197	0.681
2.116	0.707
1.873	0.752
1.466	1.006
1.060	1.410
0.654	1.605

INLET TEMPERATURE = 85.0 DEG.F

EXIT PRESSURE = 45.0 PSIA

HEAT FLUX = 14250.00 BTU/HR-SQ.FT

L/D = 204.0

MASS FLOW RATE(LBM/MIN)	PRESSURE DROP(PSI)
11.357	6.416
7.571	3.100
5.122	1.752
4.310	1.280
4.310	0.876
2.685	0.609
1.873	0.544
1.466	0.586
1.060	0.860
0.654	1.156

INLET TEMPERATURE = 85.0 DEG.F

EXIT PRESSURE = 55.0 PSIA

HEAT FLUX = 14250.00 BTU/HR-SQ.FT

L/D = 204.0

MASS FLOW RATE(LBM/MIN)	PRESSURE DROP(PSI)
11.306	6.416
7.571	3.172
9.975	4.283
6.983	2.521
5.122	1.755
4.310	1.286
3.497	0.879
2.685	0.567
2.279	0.440
1.669	0.420
1.466	0.430
1.060	0.576
0.654	0.870

INLET TEMPERATURE = 85.0 DEG.F

EXIT PRESSURE = 70.0 PSIA

HEAT FLUX = 14250.00 BTU/HR-SQ.FT

L/D = 204.0

MASS FLOW RATE(LBM/MIN)	PRESSURE DROP(PSI)
9.576	3.947
6.983	2.475
5.122	1.752
4.310	1.277
3.497	0.873
2.685	0.524
2.279	0.420
1.466	0.404
1.060	0.408
0.654	0.573

INLET TEMPERATURE = 95.0 DEG.F

EXIT PRESSURE = 25.0 PSIA

HEAT FLUX = 14250.00 BTU/HR-SQ.FT

L/D = 204.0

MASS FLOW RATE(LBM/MIN)	PRESSURE DROP(PSI)
11.068	6.145
7.547	3.151
5.105	1.745
4.296	1.286
3.081	1.048
2.879	1.058
2.676	1.090
2.271	1.341
1.866	1.647
1.462	1.995
1.057	2.262
0.854	1.347
0.652	2.187

INLET TEMPERATURE = 95.0 DEG.F

EXIT PRESSURE = 35.0 PSIA

HEAT FLUX = 14250.00 BTU/HR-SQ.FT

L/D = 204.0

MASS FLOW RATE(LBM/MIN)	PRESSURE DROP(PSI)
11.270	6.301
7.547	3.144
5.105	1.738
4.296	1.266
3.486	0.856
3.081	0.736
2.879	0.699
2.474	0.680
2.271	0.690
1.866	0.804
1.462	1.064
1.057	1.403
0.652	1.559

INLET TEMPERATURE = 95.0 DEG.F

EXIT PRESSURE = 45.0 PSIA

HEAT FLUX = 14250.00 BTU/HR-SQ.FT

L/D = 204.0

MASS FLOW RATE(LBM/MIN)	PRESSURE DROP(PSI)
11.068	6.140
7.547	3.106
5.105	1.748
4.296	1.263
3.486	0.892
3.081	0.876
2.676	0.755
2.474	0.700
2.271	0.667
1.866	0.609
1.462	0.667
1.057	0.947
0.652	1.172

INLET TEMPERATURE = 95.0 DEG.F

EXIT PRESSURE = 55.0 PSIA

HEAT FLUX = 14250.00 BTU/HR-SQ.FT

L/D = 204.0

MASS FLOW RATE(LBM/MIN)	PRESSURE DROP(PSI)
11.068	6.148
7.547	3.106
5.105	1.758
4.296	1.309
3.486	0.921
2.676	0.619
2.271	0.521
2.069	0.462
1.866	0.436
1.664	0.394
1.462	0.475
1.057	0.622
0.652	0.869

INLET TEMPERATURE = 95.0 DEG.F

EXIT PRESSURE = 70.0 PSIA

HEAT FLUX = 14250.00 BTU/HR-SQ.FT

L/D = 204.0

MASS FLOW RATE(LBM/MIN)	PRESSURE DROP(PSI)
11.068	6.154
7.547	3.139
5.105	1.749
4.296	1.257
3.486	0.853
2.676	0.524
1.462	0.352
1.057	0.423
0.652	0.557

INLET TEMPERATURE = 110.0 DEG.F

EXIT PRESSURE = 35.0 PSIA

HEAT FLUX = 14250.00 BTU/HR-SQ.FT

L/D = 204.0

MASS FLOW RATE(LBM/MIN)	PRESSURE DROP(PSI)
11.871	5.250
8.805	3.254
5.080	1.755
4.677	1.518
4.274	1.293
3.871	1.117
3.468	0.990
3.066	0.941
2.864	0.905
2.663	0.951
2.260	1.026
1.857	1.205
1.454	1.400
1.051	1.710
0.850	1.733
0.649	1.687

INLET TEMPERATURE = 110.0 DEG.F

EXIT PRESSURE = 45.0 PSIA

HEAT FLUX = 14250.00 BTU/HR-SQ.FT

L/D = 204.0

MASS FLOW RATE(LBM/MIN)	PRESSURE DROP(PSI)
10.882	4.651
8.904	3.367
5.080	1.749
4.274	1.273
3.468	0.883
3.066	0.756
2.663	0.687
2.260	0.671
2.058	0.684
1.857	0.681
1.454	0.824
1.051	1.081
0.649	1.208

INLET TEMPERATURE = 110.0 DEG.F

EXIT PRESSURE = 55.0 PSIA

HEAT FLUX = 14250.00 BTU/HR-SQ.FT

L/D = 204.0

MASS FLOW RATE(LBM/MIN)	PRESSURE DROP(PSI)
11.772	4.813
7.914	2.775
5.080	1.772
4.274	1.277
3.468	0.899
2.663	0.596
2.260	0.524
2.058	0.508
1.978	0.505
1.454	0.547
1.051	0.687
0.649	0.997

INLET TEMPERATURE = 110.0 DEG.F

EXIT PRESSURE = 70.0 PSIA

HEAT FLUX = 14250.00 BTU/HR-SQ.FT

L/D = 204.0

MASS FLOW RATE(LBM/MIN)	PRESSURE DROP(PSI)
10.387	4.132
5.080	1.732
4.274	1.270
3.468	0.856
2.663	0.544
2.260	0.430
1.857	0.388
1.736	0.378
1.535	0.381
1.051	0.440
0.649	0.615

INLET TEMPERATURE = 120.0 DEG.F

EXIT PRESSURE = 45.0 PSIA

HEAT FLUX = 14250.00 BTU/HR-SQ.FT

L/D = 204.0

MASS FLOW RATE(LBM/MIN)	PRESSURE DROP(PSI)
5.062	1.761
4.661	1.556
4.259	1.380
3.858	1.234
3.456	1.100
3.055	1.009
2.453	0.960
2.252	0.967
1.851	1.048
1.449	1.250
1.048	1.501
0.646	1.507

INLET TEMPERATURE = 120.0 DEG.F

EXIT PRESSURE = 55.0 PSIA

HEAT FLUX = 14250.00 BTU/HR-SQ.FT

L/D = 204.0

MASS FLOW RATE(LBM/MIN)	PRESSURE DROP(PSI)
5.062	1.686
4.661	1.475
4.259	1.253
3.858	1.061
3.456	0.882
3.055	0.759
2.653	0.674
2.252	0.638
2.051	0.626
1.851	0.710
1.449	0.798
1.048	1.025
0.646	1.152

INLET TEMPERATURE = 120.0 DEG.F

EXIT PRESSURE = 70.0 PSIA

HEAT FLUX = 14250.00 BTU/HR-SQ.FT

L/D = 204.0

MASS FLOW RATE(LBM/MIN)	PRESSURE DROP(PSI)
8.873	2.607
5.062	1.683
4.661	1.458
4.259	1.243
3.858	1.035
3.456	0.853
3.055	0.693
2.653	0.579
2.252	0.498
1.650	0.492
1.449	0.501
1.048	0.645
0.646	0.781

INLET TEMPERATURE = 85.0 DEG.F

EXIT PRESSURE = 25.0 PSIA

HEAT FLUX = 22500.00 BTU/HR-SQ.FT

L/D = 204.0

MASS FLOW RATE(LBM/MIN)	PRESSURE DROP(PSI)
8.828	4.130
5.122	1.873
4.716	1.713
4.310	1.638
4.107	1.707
3.903	1.733
3.497	1.925
2.685	2.667
1.873	3.846
1.466	4.175
1.263	4.208
1.060	4.068

INLET TEMPERATURE = 85.0 DEG.F

EXIT PRESSURE = 35.0 PSIA

HEAT FLUX = 22500.00 BTU/HR-SQ.FT

L/D = 204.0

MASS FLOW RATE(LBM/MIN)	PRESSURE DROP(PSI)
8.379	3.309
5.122	1.801
4.310	1.384
3.497	1.257
3.091	0.954
2.888	0.990
2.685	1.045
2.279	1.694
1.466	2.035
1.060	2.980

INLET TEMPERATURE = 85.0 DEG.F

EXIT PRESSURE = 45.0 PSIA

HEAT FLUX = 22500.00 BTU/HR-SQ.FT

L/D = 204.0

MASS FLOW RATE(LBM/MIN)	PRESSURE DROP(PSI)
8.878	3.579
5.122	1.755
4.310	1.296
3.497	0.954
2.685	0.941
2.279	1.058
1.873	1.355
1.466	1.775
1.060	1.863
0.654	2.016

INLET TEMPERATURE = 85.0 DEG.F

EXIT PRESSURE = 55.0 PSIA

HEAT FLUX = 22500.00 BTU/HR-SQ.FT

L/D = 204.0

MASS FLOW RATE(LBM/MIN)	PRESSURE DROP(PSI)
7.980	2.918
5.122	1.873
4.310	1.413
3.497	1.094
3.091	0.971
2.685	0.860
2.482	0.830
2.279	0.795
2.076	0.830
1.873	0.889
1.466	1.198
1.060	1.586
0.654	1.628

INLET TEMPERATURE = 85.0 DEG.F

EXIT PRESSURE = 70.0 PSIA

HEAT FLUX = 22500.00 BTU/HR-SQ.FT

L/D = 204.0

MASS FLOW RATE(LBM/MIN)	PRESSURE DROP(PSI)
8.080	3.071
5.122	1.808
4.310	1.361
3.497	1.306
2.685	0.716
2.279	0.622
1.873	0.599
1.669	0.642
1.466	0.749
1.060	1.088
0.654	1.238

INLET TEMPERATURE = 95.0 DEG.F

EXIT PRESSURE = 25.0 PSIA

HEAT FLUX = 22500.00 BTU/HR-SQ.FT

L/D = 204.0

MASS FLOW RATE(LBM/MIN)	PRESSURE DROP(PSI)
7.358	3.328
5.105	2.387
4.903	2.341
4.700	2.325
4.498	2.302
4.296	2.315
4.093	2.413
3.891	2.475
3.486	2.774
3.081	2.970
2.717	3.344
2.271	3.803
1.866	4.178
1.462	4.373
1.259	4.350
1.057	4.194

INLET TEMPERATURE = 95.0 DEG.F

EXIT PRESSURE = 35.0 PSIA

HEAT FLUX = 22500.00 BTU/HR-SQ.FT

L/D = 204.0

MASS FLOW RATE(LBM/MIN)	PRESSURE DROP(PSI)
10.838	4.741
7.954	3.100
5.105	1.817
4.700	1.609
4.296	1.482
3.891	1.416
3.486	1.400
3.283	1.426
3.081	1.429
2.676	1.631
2.271	2.283
1.866	2.686
1.462	2.794
1.057	2.989
0.854	2.895
0.652	2.520

INLET TEMPERATURE = 95.0 DEG.F

EXIT PRESSURE = 45.0 PSIA

HEAT FLUX = 22500.00 BTU/HR-SQ.FT

L/D = 204.0

MASS FLOW RATE(LBM/MIN)	PRESSURE DROP(PSI)
5.105	1.895
4.296	1.563
3.891	1.355
3.486	1.244
3.081	1.172
2.879	1.136
2.676	1.169
2.271	1.244
1.866	1.599
1.462	1.911
1.057	2.243
0.652	2.019

INLET TEMPERATURE = 95.0 DEG.F

EXIT PRESSURE = 55.0 PSIA

HEAT FLUX = 22500.00 BTU/HR-SQ.FT

L/D = 204.0

MASS FLOW RATE(LBM/MIN)	PRESSURE DROP(PSI)
5.105	1.725
4.296	1.289
3.486	1.149
3.081	1.029
2.676	0.938
2.271	0.947
2.190	0.960
1.866	1.078
1.462	1.416
1.057	1.729
0.854	1.787
0.652	1.657

INLET TEMPERATURE = 95.0 DEG.F

EXIT PRESSURE = 70.0 PSIA

HEAT FLUX = 22500.00 BTU/HR-SQ.FT

L/D = 204.0

MASS FLOW RATE(LBM/MIN)	PRESSURE DROP(PSI)
8.451	3.210
5.105	1.830
4.296	1.413
3.486	1.058
2.676	0.811
2.271	0.736
2.069	0.723
1.947	0.726
1.664	0.794
1.462	0.876
1.057	1.299
0.854	1.299
0.652	1.270

INLET TEMPERATURE = 110.0 DEG.F

EXIT PRESSURE = 35.0 PSIA

HEAT FLUX = 22500.00 BTU/HR-SQ.FT

L/D = 204.0

MASS FLOW RATE(LBM/MIN)	PRESSURE DROP(PSI)
8.211	3.145
5.080	2.178
4.677	2.081
4.274	1.999
4.073	2.003
3.871	2.042
3.468	2.087
3.066	2.328
2.663	2.647
2.260	2.940
1.857	3.289
1.454	3.481
1.051	3.386
0.850	3.201

INLET TEMPERATURE = 110.0 DEG.F

EXIT PRESSURE = 45.0 PSIA

HEAT FLUX = 22500.00 BTU/HR-SQ.FT

L/D = 204.0

MASS FLOW RATE(LBM/MIN)	PRESSURE DROP(PSI)
10.783	4.344
7.914	2.953
5.080	1.947
4.677	1.771
4.274	1.638
3.871	1.501
3.468	1.423
3.267	1.403
3.066	1.410
2.864	1.426
2.663	1.475
2.260	1.703
1.857	2.071
1.454	2.380
1.051	2.507
0.850	2.348
0.649	1.973

INLET TEMPERATURE = 110.0 DEG.F

EXIT PRESSURE = 55.0 PSIA

HEAT FLUX = 22500.00 BTU/HR-SQ.FT

L/D = 204.0

MASS FLOW RATE(LBM/MIN)	PRESSURE DROP(PSI)
8.904	3.725
5.080	1.927
4.677	1.742
4.274	1.550
3.871	1.406
3.468	1.286
3.066	1.231
2.864	1.188
2.663	1.192
2.461	1.211
2.260	1.289
1.857	1.537
1.454	1.843
1.051	2.090
0.649	1.641

INLET TEMPERATURE = 110.0 DEG.F

EXIT PRESSURE = 70.0 PSIA

HEAT FLUX = 22500.00 BTU/HR-SQ.FT

L/D = 204.0

MASS FLOW RATE(LBM/MIN)	PRESSURE DROP(PSI)
8.963	3.533
5.080	1.830
4.677	1.605
4.274	1.452
3.871	1.273
3.468	1.126
3.066	1.019
2.663	0.912
2.461	0.886
2.260	0.866
2.099	0.879
1.857	0.899
1.454	1.133
1.051	1.270
0.649	1.341

INLET TEMPERATURE = 120.0 DEG.F

EXIT PRESSURE = 45.0 PSIA

HEAT FLUX = 22500.00 BTU/HR-SQ.FT

L/D = 204.0

MASS FLOW RATE(LBM/MIN)	PRESSURE DROP(PSI)
7.690	3.178
5.062	2.136
4.661	2.006
4.259	1.947
3.858	1.885
3.456	1.901
3.657	1.882
3.256	1.957
3.055	2.002
2.653	2.243
2.252	2.533
1.851	2.793
1.449	2.992
1.248	2.999
1.048	2.875

INLET TEMPERATURE = 120.0 DEG.F

EXIT PRESSURE = 55.0 PSIA

HEAT FLUX = 22500.00 BTU/HR-SQ.FT

L/D = 204.0

MASS FLOW RATE(LBM/MIN)	PRESSURE DROP(PSI)
5.062	2.077
4.661	1.901
4.259	1.745
3.858	1.605
3.456	1.498
3.256	1.452
3.055	1.426
2.653	1.442
2.252	1.599
1.851	1.908
1.449	2.139
1.048	2.237
0.847	2.155

INLET TEMPERATURE = 120.0 DEG.F

EXIT PRESSURE = 70.0 PSIA

HEAT FLUX = 22500.00 BTU/HR-SQ.FT

L/D = 204.0

MASS FLOW RATE(LBM/MIN)	PRESSURE DROP(PSI)
5.062	1.696
4.661	1.488
4.259	1.302
3.858	1.149
3.456	1.035
3.055	0.977
2.653	0.964
2.453	0.964
2.252	0.970
1.851	1.084
1.449	1.302
1.048	1.520
0.847	1.543
0.646	1.332

INLET TEMPERATURE = 85.0 DEG.F

EXIT PRESSURE = 25.0 PSIA

HEAT FLUX = 30600.00 BTU/HR-SQ.FT

L/D = 204.0

MASS FLOW RATE(LBM/MIN)	PRESSURE DROP(PSI)
8.076	4.388
7.193	4.053
6.032	3.828
5.122	3.913
4.919	4.043
4.716	4.160
4.310	4.434
3.903	4.851
3.497	5.398
3.091	6.062
2.685	6.657
2.279	7.110
1.873	7.308
1.669	7.234
1.466	6.856
1.060	5.391

INLET TEMPERATURE = 85.0 DEG.F

EXIT PRESSURE = 35.0 PSIA

HEAT FLUX = 30600.00 BTU/HR-SQ.FT

L/D = 204.0

MASS FLOW RATE(LBM/MIN)	PRESSURE DROP(PSI)
11.105	6.196
7.193	3.379
5.122	2.523
4.716	2.426
4.310	2.380
4.107	2.439
3.903	2.553
3.497	2.836
3.091	3.256
2.685	3.891
2.279	4.473
1.873	4.962
1.669	5.073
1.466	5.007
1.345	4.867
1.263	4.630
1.060	3.933

INLET TEMPERATURE = 85.0 DEG.F

EXIT PRESSURE = 45.0 PSIA

HEAT FLUX = 30600.00 BTU/HR-SQ.FT

L/D = 204.0

MASS FLOW RATE(LBM/MIN)	PRESSURE DROP(PSI)
9.969	5.112
6.562	2.829
5.122	2.129
4.716	1.976
4.310	1.862
3.903	1.797
3.700	1.791
3.497	1.797
3.091	1.947
2.685	2.393
2.279	2.966
1.873	3.510
1.466	3.770
1.385	3.728
1.263	3.653
1.060	3.142

INLET TEMPERATURE = 85.0 DEG.F

EXIT PRESSURE = 55.0 PSIA

HEAT FLUX = 30600.00 BTU/HR-SQ.FT

L/D = 204.0

MASS FLOW RATE(LBM/MIN)	PRESSURE DROP(PSI)
9.590	4.854
6.562	2.842
5.122	1.866
4.716	1.696
4.310	1.556
3.903	1.491
3.497	1.439
3.091	1.426
2.929	1.442
2.685	1.579
2.279	2.012
1.873	2.439
1.466	2.885
1.304	2.898
1.060	2.611

INLET TEMPERATURE = 85.0 DEG.F

EXIT PRESSURE = 70.0 PSIA

HEAT FLUX = 30600.00 BTU/HR-SQ.FT

L/D = 204.0

MASS FLOW RATE(LBM/MIN)	PRESSURE DROP(PSI)
9.565	4.705
6.562	2.719
5.122	1.794
4.716	1.576
4.310	1.413
3.903	1.286
3.497	1.195
3.091	1.133
2.685	1.110
2.482	1.133
2.279	1.244
1.873	1.615
1.466	1.999
1.263	2.103
1.060	1.970
0.857	1.644

INLET TEMPERATURE = 95.0 DEG.F

EXIT PRESSURE = 25.0 PSIA

HEAT FLUX = 30600.00 BTU/HR-SQ.FT

L/D = 204.0

MASS FLOW RATE(LBM/MIN)	PRESSURE DROP(PSI)
9.559	5.124
7.547	4.261
6.792	4.140
6.289	4.163
6.037	4.192
5.105	4.466
4.700	4.717
4.296	5.075
3.891	5.466
3.486	6.134
3.081	6.593
2.676	7.160
2.271	7.525
2.069	7.600
1.866	7.564
1.785	7.538
1.097	5.733

INLET TEMPERATURE = 95.0 DEG.F

EXIT PRESSURE = 35.0 PSIA

HEAT FLUX = 30600.00 BTU/HR-SQ.FT

L/D = 204.0

MASS FLOW RATE(LBM/MIN)	PRESSURE DROP(PSI)
11.068	6.082
9.056	4.270
7.547	3.316
5.105	2.707
4.700	2.668
4.498	2.642
4.296	2.671
3.891	2.831
3.486	3.153
3.081	3.694
2.676	4.199
2.271	4.687
1.866	4.987
1.664	5.088
1.462	4.990
1.057	3.779

INLET TEMPERATURE = 95.0 DEG.F

EXIT PRESSURE = 45.0 PSIA

HEAT FLUX = 30600.00 BTU/HR-SQ.FT

L/D = 204.0

MASS FLOW RATE(LBM/MIN)	PRESSURE DROP(PSI)
9.056	4.394
6.037	2.557
5.105	2.078
4.700	1.948
4.296	1.883
3.891	1.857
3.688	1.883
3.486	1.899
3.081	2.153
2.676	2.593
2.271	3.042
1.866	3.576
1.664	3.641
1.462	3.713
1.259	3.576
1.057	3.225

INLET TEMPERATURE = 95.0 DEG.F

EXIT PRESSURE = 55.0 PSIA

HEAT FLUX = 30600.00 BTU/HR-SQ.FT

L/D = 204.0

MASS FLOW RATE(LBM/MIN)	PRESSURE DROP(PSI)
11.068	6.094
6.792	2.821
5.105	2.029
4.700	1.857
4.296	1.642
3.891	1.534
3.486	1.469
3.283	1.462
3.081	1.475
2.676	1.612
2.271	1.954
1.866	2.560
1.624	2.840
1.462	2.941
1.057	2.664

INLET TEMPERATURE = 95.0 DEG.F

EXIT PRESSURE = 70.0 PSIA

HEAT FLUX = 30600.00 BTU/HR-SQ.FT

L/D = 204.0

MASS FLOW RATE(LBM/MIN)	PRESSURE DROP(PSI)
9.811	4.954
6.289	2.909
5.105	2.006
4.700	1.850
4.296	1.622
3.891	1.475
3.486	1.332
3.081	1.228
2.676	1.169
2.474	1.199
2.271	1.267
1.866	1.629
1.462	1.948
1.057	2.052
0.854	1.687

INLET TEMPERATURE = 110.0 DEG.F

EXIT PRESSURE = 35.0 PSIA

HEAT FLUX = 30600.00 BTU/HR-SQ.FT

L/D = 204.0

MASS FLOW RATE(LBM/MIN)	PRESSURE DROP(PSI)
10.988	5.936
10.011	5.141
8.510	4.206
7.008	3.708
6.007	3.607
5.080	3.744
4.274	4.177
3.468	5.083
2.663	5.757
1.857	6.080
2.058	6.125
1.454	5.663
1.051	4.620

INLET TEMPERATURE = 110.0 DEG.F

EXIT PRESSURE = 45.0 PSIA

HEAT FLUX = 30600.00 BTU/HR-SQ.FT

L/D = 204.0

MASS FLOW RATE(LBM/MIN)	PRESSURE DROP(PSI)
9.511	4.802
7.509	3.460
6.257	2.919
5.080	2.704
4.677	2.668
4.475	2.652
4.274	2.710
3.871	2.880
3.468	3.202
2.663	4.049
1.857	4.619
1.696	4.597
1.454	4.333
1.051	3.316

INLET TEMPERATURE = 110.0 DEG.F

EXIT PRESSURE = 55.0 PSIA

HEAT FLUX = 30600.00 BTU/HR-SQ.FT

L/D = 204.0

MASS FLOW RATE(LBM/MIN)	PRESSURE DROP(PSI)
11.038	6.043
8.760	3.668
7.008	3.186
5.080	2.241
4.677	2.137
4.274	2.078
3.871	2.052
3.468	2.111
3.066	2.310
2.663	2.723
1.857	3.548
1.454	3.421
1.051	2.730

INLET TEMPERATURE = 110.0 DEG.F

EXIT PRESSURE = 70.0 PSIA

HEAT FLUX = 30600.00 BTU/HR-SQ.FT

L/D = 204.0

MASS FLOW RATE(LBM/MIN)	PRESSURE DROP(PSI)
11.063	6.105
8.259	3.694
6.758	2.665
5.080	1.909
4.274	1.661
3.871	1.583
3.468	1.525
3.066	1.492
2.864	1.531
2.663	1.616
2.260	1.932
1.857	2.300
1.454	2.469
1.253	2.274
1.051	2.020

INLET TEMPERATURE = 120.0 DEG.F

EXIT PRESSURE = 45.0 PSIA

HEAT FLUX = 30600.00 BTU/HR-SQ.FT

L/D = 204.0

MASS FLOW RATE(LBM/MIN)	PRESSURE DROP(PSI)
10.750	5.922
8.979	4.463
7.482	3.551
5.986	3.117
5.487	3.062
5.062	3.042
4.661	3.072
4.259	3.130
3.456	3.632
2.653	4.430
2.252	4.756
1.851	4.785
1.449	4.489
1.048	3.251

INLET TEMPERATURE = 120.0 DEG.F

EXIT PRESSURE = 55.0 PSIA

HEAT FLUX = 30600.00 BTU/HR-SQ.FT

L/D = 204.0

MASS FLOW RATE(LBM/MIN)	PRESSURE DROP(PSI)
8.979	4.163
6.485	2.710
5.062	2.397
4.661	2.339
4.259	2.257
4.018	2.215
3.858	2.300
3.456	2.450
2.653	3.095
2.252	3.427
2.051	3.691
1.851	3.668
1.449	3.531
1.048	3.531

INLET TEMPERATURE = 120.0 DEG.F

EXIT PRESSURE = 70.0 PSIA

HEAT FLUX = 30600.00 BTU/HR-SQ.FT

L/D = 204.0

MASS FLOW RATE(LBM/MIN)	PRESSURE DROP(PSI)
10.999	5.994
7.981	3.580
5.062	2.182
4.661	2.039
4.259	1.915
3.858	1.801
3.456	1.694
3.296	1.739
3.055	1.766
2.653	1.961
2.252	2.290
1.851	2.681
1.610	2.661
1.449	2.599
1.048	2.013

INLET TEMPERATURE = 85.0 DEG.F

EXIT PRESSURE = 25.0 PSIA

HEAT FLUX = 35700.00 BTU/HR-SQ.FT

L/D = 204.0

MASS FLOW RATE(LBM/MIN)	PRESSURE DROP(PSI)
10.877	6.053
9.590	5.076
8.076	4.352
7.067	4.095
6.814	4.105
6.562	4.121
6.057	4.147
5.122	4.444
4.310	5.242
3.497	6.424
2.685	7.558
2.279	8.102
1.873	8.066
1.466	7.134

INLET TEMPERATURE = 85.0 DEG.F

EXIT PRESSURE = 35.0 PSIA

HEAT FLUX = 35700.00 BTU/HR-SQ.FT

L/D = 204.0

MASS FLOW RATE(LBM/MIN)	PRESSURE DROP(PSI)
9.086	4.476
7.571	3.584
6.057	2.991
5.122	2.844
4.716	2.851
4.310	3.079
3.903	3.515
3.497	4.137
3.091	4.786
2.685	5.398
2.279	5.923
1.873	6.046
1.669	5.857
1.466	5.427
1.263	4.300

INLET TEMPERATURE = 85.0 DEG.F

EXIT PRESSURE = 45.0 PSIA

HEAT FLUX = 35700.00 BTU/HR-SQ.FT

L/D = 204.0

MASS FLOW RATE(LBM/MIN)	PRESSURE DROP(PSI)
8.581	4.039
7.571	3.342
6.057	2.498
5.122	2.248
4.716	2.160
4.310	2.137
4.107	2.209
3.903	2.248
3.497	2.508
3.091	3.023
2.685	3.616
2.279	4.283
1.873	4.596
1.669	4.508
1.466	4.173
1.060	3.127

INLET TEMPERATURE = 85.0 DEG.F

EXIT PRESSURE = 55.0 PSIA

HEAT FLUX = 35700.00 BTU/HR-SQ.FT

L/D = 204.0

MASS FLOW RATE(LBM/MIN)	PRESSURE DROP(PSI)
11.105	6.169
9.086	4.387
6.057	2.417
5.122	2.078
4.310	1.883
3.903	1.844
3.700	1.830
3.497	1.847
3.091	2.091
2.685	2.573
2.279	2.830
1.873	3.612
1.629	3.576
1.466	3.348
1.060	2.606

INLET TEMPERATURE = 85.0 DEG.F

EXIT PRESSURE = 70.0 PSIA

HEAT FLUX = 35700.00 BTU/HR-SQ.FT

L/D = 204.0

MASS FLOW RATE(LBM/MIN)	PRESSURE DROP(PSI)
11.130	6.153
9.086	4.306
6.057	2.606
5.122	1.863
4.310	1.596
3.903	1.488
3.497	1.420
3.294	1.401
3.091	1.401
2.685	1.544
2.279	1.896
1.873	2.417
1.669	2.554
1.466	2.469
1.060	1.909

INLET TEMPERATURE = 95.0 DEG.F

EXIT PRESSURE = 25.0 PSIA

HEAT FLUX = 35700.00 BTU/HR-SQ.FT

L/D = 204.0

MASS FLOW RATE(LBM/MIN)	PRESSURE DROP(PSI)
10.817	6.226
9.559	5.408
8.553	5.023
8.050	4.994
7.547	4.939
7.044	4.958
6.037	5.154
5.105	5.532
4.296	6.232
3.486	7.353
2.676	8.506
2.474	8.701
2.271	8.832
2.069	8.780
1.866	8.565
1.462	7.265

INLET TEMPERATURE = 95.0 DEG.F

EXIT PRESSURE = 35.0 PSIA

HEAT FLUX = 35700.00 BTU/HR-SQ.FT

L/D = 204.0

MASS FLOW RATE(LBM/MIN)	PRESSURE DROP(PSI)
11.194	6.151
8.553	4.023
6.540	3.307
5.786	3.294
5.283	3.352
5.105	3.355
4.700	3.460
4.296	3.759
3.891	4.229
3.486	4.870
2.676	5.880
2.271	6.336
2.069	6.385
1.866	6.369
1.462	5.603
1.057	4.326

INLET TEMPERATURE = 95.0 DEG.F

EXIT PRESSURE = 45.0 PSIA

HEAT FLUX = 35700.00 BTU/HR-SQ.FT

L/D = 204.0

MASS FLOW RATE(LBM/MIN)	PRESSURE DROP(PSI)
11.320	6.290
8.050	3.626
6.540	2.792
5.105	2.476
4.700	2.424
4.498	2.407
4.296	2.430
3.891	2.606
3.486	2.974
2.676	4.042
2.271	4.580
2.028	4.769
1.866	4.860
1.664	4.743
1.462	4.326
1.057	3.323

INLET TEMPERATURE = 95.0 DEG.F

EXIT PRESSURE = 55.0 PSIA

HEAT FLUX = 35700.00 BTU/HR-SQ.FT

L/D = 204.0

MASS FLOW RATE(LBM/MIN)	PRESSURE DROP(PSI)
11.320	6.241
8.553	3.977
7.044	2.886
5.105	2.052
4.700	1.928
4.296	1.902
3.891	1.870
3.688	1.876
3.486	1.922
3.081	2.176
2.676	2.612
2.271	3.277
1.866	3.687
1.664	3.707
1.462	3.492
1.057	2.704

INLET TEMPERATURE = 95.0 DEG.F

EXIT PRESSURE = 70.0 PSIA

HEAT FLUX = 35700.00 BTU/HR-SQ.FT

L/D = 204.0

MASS FLOW RATE(LBM/MIN)	PRESSURE DROP(PSI)
11.320	6.209
8.553	3.831
7.044	2.736
5.105	1.811
4.700	1.648
4.296	1.537
3.891	1.453
3.486	1.401
3.283	1.397
2.676	1.606
2.271	2.007
1.866	2.450
1.664	2.599
1.462	2.528
1.057	1.987

INLET TEMPERATURE = 110.0 DEG.F

EXIT PRESSURE = 35.0 PSIA

HEAT FLUX = 35700.00 BTU/HR-SQ.FT

L/D = 204.0

MASS FLOW RATE(LBM/MIN)	PRESSURE DROP(PSI)
10.762	6.011
10.011	5.516
8.510	4.747
7.509	4.546
7.008	4.422
6.758	4.487
6.507	4.500
6.007	4.519
5.080	4.780
4.274	5.457
3.468	6.252
2.663	7.007
2.461	7.085
2.260	7.118
1.857	6.870
1.454	5.959

INLET TEMPERATURE = 110.0 DEG.F

EXIT PRESSURE = 45.0 PSIA

HEAT FLUX = 35700.00 BTU/HR-SQ.FT

L/D = 204.0

MASS FLOW RATE(LBM/MIN)	PRESSURE DROP(PSI)
11.013	6.161
9.010	4.630
6.507	3.360
5.757	3.178
5.080	3.145
4.878	3.191
4.677	3.256
4.274	3.425
3.871	3.745
3.468	4.226
2.663	5.053
2.461	5.294
2.260	5.418
2.058	5.431
1.857	5.353
1.454	4.624
1.253	4.233

INLET TEMPERATURE = 110.0 DEG.F

EXIT PRESSURE = 55.0 PSIA

HEAT FLUX = 35700.00 BTU/HR-SQ.FT

L/D = 204.0

MASS FLOW RATE(LBM/MIN)	PRESSURE DROP(PSI)
11.013	6.071
7.509	3.452
6.007	2.801
5.080	2.527
4.677	2.430
4.274	2.377
4.073	2.384
3.871	2.430
3.468	2.586
3.066	2.899
2.663	3.335
2.260	3.758
1.857	3.986
1.454	3.602
1.051	3.029

INLET TEMPERATURE = 110.0 DEG.F

EXIT PRESSURE = 70.0 PSIA

HEAT FLUX = 35700.00 BTU/HR-SQ.FT

L/D = 204.0

MASS FLOW RATE(LBM/MIN)	PRESSURE DROP(PSI)
11.088	6.142
9.010	4.364
6.007	2.410
5.080	2.104
4.274	1.869
3.871	1.772
3.468	1.720
3.267	1.733
3.066	1.778
2.663	2.045
2.260	2.417
1.857	2.820
1.454	2.638
1.051	2.019

INLET TEMPERATURE = 120.0 DEG.F

EXIT PRESSURE = 45.0 PSIA

HEAT FLUX = 35700.00 BTU/HR-SQ.FT

L/D = 204.0

MASS FLOW RATE(LBM/MIN)	PRESSURE DROP(PSI)
10.875	5.874
8.480	4.285
7.482	3.933
6.984	3.855
6.734	3.797
6.485	3.751
6.235	3.725
5.986	3.758
5.487	3.790
5.062	3.849
4.259	4.285
3.456	5.099
3.055	5.438
2.653	5.744
2.252	5.815
1.851	5.587
1.449	4.624
1.048	3.451

INLET TEMPERATURE = 120.0 DEG.F

EXIT PRESSURE = 55.0 PSIA

HEAT FLUX = 35700.00 BTU/HR-SQ.FT

L/D = 204.0

MASS FLOW RATE(LBM/MIN)	PRESSURE DROP(PSI)
8.480	4.246
6.984	3.347
5.986	2.983
5.487	2.878
5.062	2.747
4.661	2.768
4.259	2.774
3.858	2.944
3.456	3.211
3.055	3.601
2.653	3.985
2.252	4.344
1.851	4.331
1.449	3.745
1.048	2.800

INLET TEMPERATURE = 120.0 DEG.F

EXIT PRESSURE = 70.0 PSIA

HEAT FLUX = 35700.00 BTU/HR-SQ.FT

L/D = 204.0

MASS FLOW RATE(LBM/MIN)	PRESSURE DROP(PSI)
8.480	3.927
6.984	2.957
5.986	2.403
5.062	2.234
4.661	2.129
4.259	2.058
4.058	2.032
3.858	2.006
3.657	2.064
3.456	2.136
3.055	2.354
2.653	2.709
2.252	3.061
1.851	3.256
1.449	2.690
1.048	2.090

INLET TEMPERATURE = 95.0 DEG.F

EXIT PRESSURE = 25.0 PSIA

HEAT FLUX = 40800.00 BTU/HR-SQ.FT

L/D = 204.0

MASS FLOW RATE(LBM/MIN)	PRESSURE DROP(PSI)
10.465	6.397
9.559	6.026
9.056	5.947
8.553	5.892
8.050	5.908
7.798	5.915
7.547	5.928
7.044	5.941
6.540	6.032
6.037	6.228
5.105	6.755
4.700	7.140
4.296	7.700
3.486	9.107
3.081	9.726
2.676	10.227
2.271	10.286
1.866	9.250
1.462	7.719

INLET TEMPERATURE = 95.0 DEG.F

EXIT PRESSURE = 35.0 PSIA

HEAT FLUX = 40800.00 BTU/HR-SQ.FT

L/D = 204.0

MASS FLOW RATE(LBM/MIN)	PRESSURE DROP(PSI)
11.018	6.146
9.559	5.052
8.553	4.518
7.547	4.192
7.044	4.094
6.792	4.042
6.540	4.075
6.037	4.094
5.786	4.127
5.105	4.381
4.296	5.159
3.486	6.348
2.676	7.361
2.474	7.534
2.271	7.586
2.069	7.469
1.866	7.100
1.462	5.798

INLET TEMPERATURE = 95.0 DEG.F

EXIT PRESSURE = 45.0 PSIA

HEAT FLUX = 40800.00 BTU/HR-SQ.FT

L/D = 204.0

MASS FLOW RATE(LBM/MIN)	PRESSURE DROP(PSI)
11.169	6.133
8.553	3.889
7.044	3.198
6.037	2.957
5.534	2.951
5.105	2.977
4.700	3.016
4.296	3.172
3.891	3.426
3.486	4.039
2.676	5.224
2.474	5.459
2.271	5.622
2.069	5.693
1.866	5.504
1.462	4.443
1.259	3.987

INLET TEMPERATURE = 95.0 DEG.F

EXIT PRESSURE = 55.0 PSIA

HEAT FLUX = 40800.00 BTU/HR-SQ.FT

L/D = 204.0

MASS FLOW RATE(LBM/MIN)	PRESSURE DROP(PSI)
11.320	6.259
7.547	3.328
6.037	2.905
5.105	2.397
4.700	2.299
4.498	2.254
4.296	2.260
4.093	2.267
3.891	2.306
3.486	2.905
3.081	3.042
2.676	3.648
2.271	4.188
2.069	4.312
1.866	4.279
1.462	3.498
1.259	3.172

INLET TEMPERATURE = 95.0 DEG.F

EXIT PRESSURE = 70.0 PSIA

HEAT FLUX = 40800.00 BTU/HR-SQ.FT

L/D = 204.0

MASS FLOW RATE(LBM/MIN)	PRESSURE DROP(PSI)
11.320	6.175
7.547	3.094
6.037	2.221
5.105	1.935
4.700	1.824
4.296	1.759
3.891	1.687
3.688	1.674
3.486	1.680
3.283	1.739
3.081	1.817
2.676	2.202
2.271	2.723
2.069	2.996
1.866	3.074
1.664	2.899
1.462	2.566

INLET TEMPERATURE = 110.0 DEG.F

EXIT PRESSURE = 35.0 PSIA

HEAT FLUX = 40800.00 BTU/HR-SQ.FT

L/D = 204.0

MASS FLOW RATE(LBM/MIN)	PRESSURE DROP(PSI)
10.512	6.299
9.511	5.811
8.510	5.426
8.009	5.374
7.759	5.355
7.509	5.361
7.008	5.426
6.507	5.465
6.007	5.687
4.505	6.547
4.274	7.270
3.468	8.201
3.066	8.475
2.663	8.566
2.260	8.306
1.857	7.068
1.454	5.928

INLET TEMPERATURE = 110.0 DEG.F

EXIT PRESSURE = 45.0 PSIA

HEAT FLUX = 40800.00 BTU/HR-SQ.FT

L/D = 204.0

MASS FLOW RATE(LBM/MIN)	PRESSURE DROP(PSI)
10.888	6.058
9.010	4.781
8.009	4.299
7.008	4.045
6.507	3.980
6.007	3.960
5.757	3.999
5.256	4.084
5.080	4.195
4.274	5.041
3.468	5.895
3.066	6.409
2.663	6.579
2.260	6.403
1.857	5.419
1.454	4.527

INLET TEMPERATURE = 110.0 DEG.F

EXIT PRESSURE = 55.0 PSIA

HEAT FLUX = 40800.00 BTU/HR-SQ.FT

L/D = 204.0

MASS FLOW RATE(LBM/MIN)	PRESSURE DROP(PSI)
11.013	5.985
9.010	4.312
7.509	3.530
6.507	3.204
5.757	3.081
5.256	3.028
5.006	3.035
4.505	3.055
4.274	3.269
3.468	4.103
3.066	4.507
2.663	4.898
2.260	5.047
1.857	4.390
1.454	3.660
1.253	3.289

INLET TEMPERATURE = 110.0 DEG.F

EXIT PRESSURE = 70.0 PSIA

HEAT FLUX = 40800.00 BTU/HR-SQ.FT

L/D = 204.0

MASS FLOW RATE(LBM/MIN)	PRESSURE DROP(PSI)
11.088	6.161
8.510	4.090
6.507	2.924
5.757	2.625
5.006	2.468
4.505	2.377
4.005	2.332
3.754	2.351
3.504	2.416
3.003	2.742
3.066	3.081
2.663	3.504
2.260	3.738
1.857	3.178
1.454	2.677
1.051	2.175

INLET TEMPERATURE = 120.0 DEG.F

EXIT PRESSURE = 45.0 PSIA

HEAT FLUX = 40800.00 BTU/HR-SQ.FT

L/D = 204.0

MASS FLOW RATE(LBM/MIN)	PRESSURE DROP(PSI)
10.525	6.084
9.478	5.452
8.480	5.022
7.482	4.768
6.984	4.658
6.734	4.632
6.235	4.651
5.986	4.677
5.487	4.827
5.062	5.062
4.259	5.680
3.456	6.540
3.055	6.814
2.653	6.918
2.252	6.592
1.851	5.504
1.449	4.592

INLET TEMPERATURE = 120.0 DEG.F

EXIT PRESSURE = 55.0 PSIA

HEAT FLUX = 40800.00 BTU/HR-SQ.FT

L/D = 204.0

MASS FLOW RATE(LBM/MIN)	PRESSURE DROP(PSI)
10.750	5.968
7.482	3.994
5.986	3.538
5.487	3.518
5.238	3.538
5.062	3.635
4.661	3.844
4.259	4.163
3.456	4.971
3.055	5.290
2.653	5.492
2.252	5.323
1.851	4.463
1.449	3.720

INLET TEMPERATURE = 120.0 DEG.F

EXIT PRESSURE = 70.0 PSIA

HEAT FLUX = 40800.00 BTU/HR-SQ.FT

L/D = 204.0

MASS FLOW RATE(LBM/MIN)	PRESSURE DROP(PSI)
10.974	5.902
7.482	3.381
5.986	2.880
5.487	2.749
5.062	2.717
4.861	2.704
4.661	2.658
4.460	2.665
4.259	2.678
3.858	2.756
3.456	3.036
3.055	3.388
2.653	3.733
2.252	3.935
1.851	3.355
1.449	2.847
1.248	2.541

INLET TEMPERATURE = 95.0 DEG.F

EXIT PRESSURE = 35.0 PSIA

HEAT FLUX = 0.0 BTU/HR-SQ.FT

L/D = 153.0

MASS FLOW RATE(LBM/MIN)	PRESSURE DROP(PSI)
12.452	5.932
10.062	4.053
7.547	2.430
5.966	1.651
5.369	1.384
4.773	1.117
4.176	0.873
3.579	0.664
2.983	0.476
2.386	0.318
1.790	0.197
1.193	0.090
0.597	0.031

INLET TEMPERATURE = 110.0 DEG.F

EXIT PRESSURE = 35.0 PSIA

HEAT FLUX = 0.0 BTU/HR-SQ.FT

L/D = 153.0

MASS FLOW RATE(LBM/MIN)	PRESSURE DROP(PSI)
12.264	5.708
10.012	3.904
7.509	2.351
5.936	1.596
5.342	1.317
4.749	1.065
4.155	0.841
3.561	0.637
2.968	0.468
2.374	0.315
1.781	0.177
1.187	0.090
0.594	0.031

INLET TEMPERATURE = 95.0 DEG.F

EXIT PRESSURE = 35.0 PSIA

HEAT FLUX = 22500.00 BTU/HR-SQ.FT

L/D = 153.0

MASS FLOW RATE(LBM/MIN)	PRESSURE DROP(PSI)
12.326	5.769
10.062	3.932
7.547	2.379
5.966	1.596
5.369	1.321
4.773	1.097
4.176	0.983
3.878	0.944
3.579	0.928
3.281	0.904
2.983	0.897
2.685	0.924
2.386	0.995
1.790	1.329
1.193	1.691
0.895	1.781
0.597	1.514

INLET TEMPERATURE = 95.0 DEG.F

EXIT PRESSURE = 45.0 PSIA

HEAT FLUX = 22500.00 BTU/HR-SQ.FT

L/D = 153.0

MASS FLOW RATE(LBM/MIN)	PRESSURE DROP(PSI)
12.402	5.769
10.062	3.916
7.547	2.340
5.966	1.589
5.369	1.321
4.773	1.066
4.176	0.861
3.579	0.739
2.983	0.704
2.685	0.653
2.386	0.637
2.088	0.668
1.790	0.724
1.193	1.022
0.597	1.140

INLET TEMPERATURE = 110.0 DEG.F

EXIT PRESSURE = 35.0 PSIA

HEAT FLUX = 22500.00 BTU/HR-SQ.FT

L/D = 153.0

MASS FLOW RATE(LBM/MIN)	PRESSURE DROP(PSI)
12.264	5.595
10.012	3.857
7.509	2.292
5.936	1.573
5.342	1.317
4.749	1.207
4.452	1.180
4.155	1.180
3.858	1.180
3.561	1.164
3.265	1.180
2.968	1.207
2.671	1.294
2.374	1.415
1.781	1.702
1.484	1.797
1.187	1.903
0.890	1.860
0.594	1.494

INLET TEMPERATURE = 110.0 DEG.F

EXIT PRESSURE = 45.0 PSIA

HEAT FLUX = 22500.00 BTU/HR-SQ.FT

L/D = 153.0

MASS FLOW RATE(LBM/MIN)	PRESSURE DROP(PSI)
12.264	5.621
10.012	3.848
7.509	2.304
5.936	1.576
5.342	1.313
4.749	1.081
4.155	0.967
3.561	0.916
2.968	0.873
2.671	0.865
2.374	0.896
2.077	0.955
1.781	1.097
1.187	1.329
0.594	1.160

INLET TEMPERATURE = 95.0 DEG.F

EXIT PRESSURE = 35.0 PSIA

HEAT FLUX = 30600.00 BTU/HR-SQ.FT

L/D = 153.0

MASS FLOW RATE(LBM/MIN)	PRESSURE DROP(PSI)
12.452	5.713
10.062	3.912
7.547	2.312
5.966	1.702
5.369	1.612
4.773	1.553
4.176	1.510
3.878	1.502
3.579	1.518
3.281	1.620
2.983	1.820
2.386	2.253
1.790	2.733
1.491	2.878
1.193	2.878
0.895	2.646
0.597	1.573

INLET TEMPERATURE = 95.0 DEG.F

EXIT PRESSURE = 45.0 PSIA

HEAT FLUX = 30600.00 BTU/HR-SQ.FT

L/D = 153.0

MASS FLOW RATE(LBM/MIN)	PRESSURE DROP(PSI)
12.452	5.693
10.062	3.873
7.547	2.316
5.966	1.588
5.369	1.372
4.773	1.262
4.176	1.195
3.878	1.148
3.579	1.109
3.281	1.101
2.983	1.109
2.685	1.168
2.386	1.337
1.790	1.809
1.491	1.982
1.193	2.198
0.895	2.045
0.597	1.258

INLET TEMPERATURE = 110.0 DEG.F

EXIT PRESSURE = 35.0 PSIA

HEAT FLUX = 30600.00 BTU/HR-SQ.FT

L/D = 153.0

MASS FLOW RATE(LBM/MIN)	PRESSURE DROP(PSI)
12.264	5.508
10.012	3.810
7.509	2.323
5.936	1.887
5.342	1.860
5.045	1.828
4.749	1.848
4.452	1.895
4.155	1.977
3.561	2.202
2.968	2.544
2.374	2.831
2.077	2.929
1.781	3.110
1.484	3.161
1.187	3.043
0.890	2.673

INLET TEMPERATURE = 110.0 DEG.F

EXIT PRESSURE = 45.0 PSIA

HEAT FLUX = 30600.00 BTU/HR-SQ.FT

L/D = 153.0

MASS FLOW RATE(LBM/MIN)	PRESSURE DROP(PSI)
12.264	5.508
10.012	3.794
7.509	2.280
5.936	1.671
5.342	1.565
4.749	1.490
4.155	1.435
3.858	1.415
3.561	1.392
3.265	1.419
2.968	1.470
2.374	1.848
1.781	2.237
1.484	2.504
1.187	2.441
0.890	1.730

INLET TEMPERATURE = 95.0 DEG.F

EXIT PRESSURE = 35.0 PSIA

HEAT FLUX = 0.0 BTU/HR-SQ.FT

L/D = 102.0

MASS FLOW RATE(LBM/MIN)	PRESSURE DROP(PSI)
12.452	4.074
10.062	2.824
7.547	1.719
5.966	1.184
5.369	0.971
4.773	0.787
4.176	0.629
3.579	0.472
2.983	0.342
2.386	0.236
1.790	0.142
1.193	0.079
0.597	0.020

INLET TEMPERATURE = 110.0 DEG.F

EXIT PRESSURE = 35.0 PSIA

HEAT FLUX = 0.0 BTU/HR-SQ.FT

L/D = 102.0

MASS FLOW RATE(LBM/MIN)	PRESSURE DROP(PSI)
12.389	4.015
10.012	2.796
7.509	1.695
5.936	1.156
5.342	0.948
4.749	0.783
4.155	0.621
3.561	0.472
2.968	0.338
2.374	0.232
1.781	0.138
1.187	0.079
0.594	0.020

INLET TEMPERATURE = 95.0 DEG.F

EXIT PRESSURE = 35.0 PSIA

HEAT FLUX = 22500.00 BTU/HR-SQ.FT

L/D = 102.0

MASS FLOW RATE(LBM/MIN)	PRESSURE DROP(PSI)
12.452	4.023
10.062	2.753
7.547	1.652
5.966	1.117
5.369	0.936
4.773	0.755
4.176	0.633
3.579	0.594
3.281	0.551
2.983	0.519
2.685	0.484
2.386	0.464
2.088	0.456
1.790	0.472
1.491	0.543
1.193	0.649
0.895	0.771
0.597	0.790

INLET TEMPERATURE = 95.0 DEG.F

EXIT PRESSURE = 45.0 PSIA

HEAT FLUX = 22500.00 BTU/HR-SQ.FT

L/D = 102.0

MASS FLOW RATE(LBM/MIN)	PRESSURE DROP(PSI)
12.452	4.023
10.062	2.753
7.547	1.652
5.966	1.117
5.369	0.928
4.773	0.747
3.579	0.515
2.983	0.448
2.386	0.381
2.088	0.346
1.790	0.322
1.491	0.330
1.193	0.381
0.895	0.480
0.597	0.566

INLET TEMPERATURE = 110.0 DEG.F

EXIT PRESSURE = 35.0 PSIA

HEAT FLUX = 22500.00 BTU/HR-SQ.FT

L/D = 102.0

MASS FLOW RATE(LBM/MIN)	PRESSURE DROP(PSI)
12.264	3.881
10.012	2.690
7.509	1.636
5.936	1.101
5.342	0.908
4.749	0.798
4.155	0.763
3.561	0.704
2.968	0.637
2.671	0.629
2.374	0.629
2.077	0.669
1.781	0.716
1.484	0.806
1.187	0.873
0.890	0.924
0.594	0.865

INLET TEMPERATURE = 110.0 DEG.F

EXIT PRESSURE = 45.0 PSIA

HEAT FLUX = 22500.00 BTU/HR-SQ.FT

L/D = 102.0

MASS FLOW RATE(LBM/MIN)	PRESSURE DROP(PSI)
12.314	3.893
10.012	2.686
7.509	1.632
5.936	1.101
5.342	0.912
4.749	0.747
4.155	0.645
3.561	0.598
2.968	0.523
2.374	0.452
2.077	0.440
1.781	0.456
1.484	0.480
1.187	0.570
0.890	0.661
0.594	0.661

INLET TEMPERATURE = 95.0 DEG.F

EXIT PRESSURE = 35.0 PSIA

HEAT FLUX = 30600.00 BTU/HR-SQ.FT

L/D = 102.0

MASS FLOW RATE(LBM/MIN)	PRESSURE DROP(PSI)
12.326	3.976
10.062	2.713
7.547	1.648
5.966	1.117
5.369	1.022
4.773	0.963
4.176	0.865
3.579	0.787
2.983	0.720
2.685	0.708
2.386	0.747
1.790	0.979
1.193	1.251
0.895	1.310
0.597	1.101

INLET TEMPERATURE = 95.0 DEG.F

EXIT PRESSURE = 45.0 PSIA

HEAT FLUX = 30600.00 BTU/HR-SQ.FT

L/D = 102.0

MASS FLOW RATE(LBM/MIN)	PRESSURE DROP(PSI)
12.452	3.968
10.062	2.713
7.547	1.652
5.966	1.121
5.369	0.944
4.773	0.822
4.176	0.743
3.579	0.637
2.983	0.574
2.685	0.551
2.386	0.527
2.088	0.535
1.790	0.558
1.491	0.629
1.193	0.826
0.895	0.944
0.597	0.865

INLET TEMPERATURE = 110.0 DEG.F

EXIT PRESSURE = 35.0 PSIA

HEAT FLUX = 30600.00 BTU/HR-SQ.FT

L/D = 102.0

MASS FLOW RATE(LBM/MIN)	PRESSURE DROP(PSI)
12.264	3.861
10.012	2.642
7.509	1.585
5.936	1.258
5.342	1.140
4.749	1.066
4.155	1.007
3.858	0.963
3.561	0.944
3.265	0.951
2.968	1.014
2.374	1.191
1.781	1.400
1.484	1.494
1.187	1.510
0.890	1.455
0.594	1.180

INLET TEMPERATURE = 110.0 DEG.F

EXIT PRESSURE = 45.0 PSIA

HEAT FLUX = 30600.00 BTU/HR-SQ.FT

L/D = 102.0

MASS FLOW RATE(LBM/MIN)	PRESSURE DROP(PSI)
12.389	3.920
10.012	2.678
7.509	1.612
5.936	1.121
5.342	1.010
4.749	0.908
4.155	0.826
3.561	0.716
2.968	0.668
2.671	0.649
2.374	0.657
2.077	0.672
1.781	0.751
1.484	0.893
1.187	0.983
0.890	1.022
0.594	0.747

INLET TEMPERATURE = 95.0 DEG.F

EXIT PRESSURE = 35.0 PSIA

HEAT FLUX = 0.0 BTU/HR-SQ.FT

L/D = 51.0

MASS FLOW RATE(LBM/MIN)	PRESSURE DROP(PSI)
12.452	2.451
10.062	1.676
7.547	1.023
5.966	0.700
5.369	0.582
4.773	0.472
4.176	0.378
3.579	0.287
2.983	0.205
2.386	0.142
1.790	0.083
1.193	0.047
0.597	0.012

INLET TEMPERATURE = 110.0 DEG.F

EXIT PRESSURE = 35.0 PSIA

HEAT FLUX = 0.0 BTU/HR-SQ.FT

L/D = 51.0

MASS FLOW RATE(LBM/MIN)	PRESSURE DROP(PSI)
12.389	2.438
10.012	1.660
7.509	1.015
5.936	0.696
5.342	0.570
4.749	0.464
4.155	0.370
3.561	0.275
2.968	0.205
2.374	0.138
1.781	0.079
1.187	0.043
0.594	0.012

INLET TEMPERATURE = 95.0 DEG.F

EXIT PRESSURE = 35.0 PSIA

HEAT FLUX = 37700.00 BTU/HR-SQ.FT

L/D = 51.0

MASS FLOW RATE(LBM/MIN)	PRESSURE DROP(PSI)
12.326	2.356
10.062	1.612
7.547	0.991
5.966	0.735
5.369	0.645
4.773	0.558
4.176	0.480
3.579	0.417
2.983	0.378
2.386	0.346
2.088	0.338
1.790	0.346
1.491	0.358
1.193	0.401
0.895	0.484
0.597	0.452

INLET TEMPERATURE = 95.0 DEG.F

EXIT PRESSURE = 45.0 PSIA

HEAT FLUX = 37700.00 BTU/HR-SQ.FT

L/D = 51.0

MASS FLOW RATE(LBM/MIN)	PRESSURE DROP(PSI)
12.452	2.391
10.062	1.632
7.547	1.003
5.966	0.696
5.369	0.606
4.773	0.527
4.176	0.444
3.579	0.377
2.983	0.319
2.386	0.263
1.790	0.236
1.491	0.236
1.193	0.252
0.895	0.307
0.597	0.334

INLET TEMPERATURE = 110.0 DEG.F

EXIT PRESSURE = 35.0 PSIA

HEAT FLUX = 37700.00 BTU/HR-SQ.FT

L/D = 51.0

MASS FLOW RATE(LBM/MIN)	PRESSURE DROP(PSI)
12.389	2.335
10.012	1.608
7.509	1.026
5.936	0.790
5.342	0.704
4.749	0.625
4.155	0.550
3.561	0.480
2.968	0.448
2.671	0.436
2.374	0.436
2.077	0.448
1.781	0.464
1.484	0.503
1.187	0.566
0.890	0.621
0.594	0.523

INLET TEMPERATURE = 110.0 DEG.F

EXIT PRESSURE = 45.0 PSIA

HEAT FLUX = 37700.00 BTU/HR-SQ.FT

L/D = 51.0

MASS FLOW RATE(LBM/MIN)	PRESSURE DROP(PSI)
12.389	2.339
10.012	1.612
7.509	0.991
5.936	0.727
5.342	0.633
4.749	0.550
4.155	0.476
3.561	0.401
2.968	0.354
2.374	0.318
2.077	0.307
1.781	0.307
1.484	0.318
1.187	0.334
0.890	0.397
0.594	0.373

INLET TEMPERATURE = 95.0 DEG.F

EXIT PRESSURE = 35.0 PSIA

HEAT FLUX = 47000.00 BTU/HR-SQ.FT

L/D = 51.0

MASS FLOW RATE(LBM/MIN)	PRESSURE DROP(PSI)
12.452	2.367
10.062	1.604
7.547	1.097
5.966	0.837
5.369	0.731
4.773	0.641
4.176	0.566
3.579	0.531
2.983	0.480
2.685	0.472
2.386	0.472
2.088	0.495
1.790	0.519
1.491	0.570
1.193	0.692
0.895	0.747

INLET TEMPERATURE = 95.0 DEG.F

EXIT PRESSURE = 45.0 PSIA

HEAT FLUX = 47000.00 BTU/HR-SQ.FT

L/D = 51.0

MASS FLOW RATE(LBM/MIN)	PRESSURE DROP(PSI)
12.452	2.371
10.062	1.612
5.966	0.790
4.176	0.531
3.579	0.460
2.983	0.405
2.386	0.370
2.088	0.358
1.790	0.385
1.491	0.417
1.193	0.472
0.835	0.550
0.597	0.511

INLET TEMPERATURE = 110.0 DEG.F

EXIT PRESSURE = 35.0 PSIA

HEAT FLUX = 47000.00 BTU/HR-SQ.FT

L/D = 51.0

MASS FLOW RATE(LBM/MIN)	PRESSURE DROP(PSI)
12.389	2.351
10.012	1.612
7.509	1.132
5.936	0.884
5.342	0.786
4.749	0.715
4.155	0.668
3.561	0.645
3.265	0.629
2.968	0.637
2.374	0.660
1.781	0.778
1.484	0.857
1.187	0.900
0.890	0.916
0.594	0.747

INLET TEMPERATURE = 110.0 DEG.F

EXIT PRESSURE = 45.0 PSIA

HEAT FLUX = 47000.00 BTU/HR-SQ.FT

L/D = 51.0

MASS FLOW RATE(LBM/MIN)	PRESSURE DROP(PSI)
12.389	2.354
10.012	1.608
7.509	1.085
5.936	0.825
5.342	0.727
4.749	0.668
4.155	0.590
3.561	0.511
2.968	0.464
2.671	0.440
2.374	0.444
2.077	0.456
1.781	0.472
1.484	0.523
1.187	0.594
0.890	0.649
0.594	0.511

CALCULATED DATA FOR TEST SECTION WITH L/D = 204
AND ZERO ORIFICE PRESSURE DROP

$\frac{\dot{q}/A}{Gh_{fg}} \times 10^4$	$\frac{C_p(T_s-T_i)}{h_{fg}}$	$\frac{\dot{q}}{\dot{q}_{se}}$	$\frac{\dot{q}/A}{Gh_{fg}} \times 10^4$	$\frac{C_p(T_s-T_i)}{h_{fg}}$	$\frac{\dot{q}}{\dot{q}_{se}}$
2.46	0.226	0.89	2.19	0.190	0.94
2.42	0.226	0.88	2.15	0.190	0.92
2.55	0.226	0.92	2.88	0.276	0.85
2.39	0.226	0.86	3.09	0.276	0.91
3.11	0.312	0.82	3.14	0.276	0.93
3.49	0.312	0.91	2.96	0.276	0.88
3.40	0.312	0.89	2.93	0.276	0.87
3.48	0.312	0.91	3.77	0.349	0.88
4.21	0.385	0.89	3.85	0.349	0.90
4.13	0.385	0.87	3.88	0.349	0.91
4.08	0.385	0.86	3.91	0.349	0.92
4.18	0.385	0.88	3.78	0.349	0.88
4.81	0.453	0.87	4.34	0.415	0.85
5.00	0.453	0.90	4.61	0.415	0.90
5.00	0.453	0.90	4.58	0.415	0.90
4.89	0.453	0.88	4.65	0.415	0.91
5.93	0.544	0.89	4.59	0.415	0.90
5.99	0.544	0.89	5.50	0.506	0.89
5.99	0.544	0.89	5.71	0.506	0.92
5.88	0.544	0.88	5.58	0.506	0.90
2.15	0.190	0.92	5.54	0.506	0.89
2.27	0.190	0.97	5.81	0.506	0.94
2.09	0.190	0.89	2.38	0.224	0.87
2.52	0.224	0.92	3.73	0.327	0.93
2.44	0.224	0.89	3.74	0.327	0.93
2.44	0.224	0.89	3.57	0.327	0.89
2.52	0.224	0.92	3.60	0.327	0.90
3.25	0.296	0.89	4.54	0.416	0.89
3.39	0.296	0.93	4.63	0.416	0.91

$\frac{\dot{q}/A}{Gh_{fg}} \times 10^4$	$\frac{C_p(T_s-T_i)}{h_{fg}}$	$\frac{\dot{q}}{\dot{q}_{se}}$	$\frac{\dot{q}/A}{Gh_{fg}} \times 10^4$	$\frac{C_p(T_s-T_i)}{h_{fg}}$	$\frac{\dot{q}}{\dot{q}_{se}}$
3.3	0.296	0.90	4.65	0.416	0.91
3.25	0.296	0.89	4.74	0.416	0.93
3.20	0.296	0.88	4.60	0.416	0.90
3.80	0.363	0.85			
3.98	0.363	0.89			
4.00	0.363	0.90			
4.04	0.363	0.91			
3.93	0.363	0.88			
4.86	0.453	0.88			
5.01	0.453	0.90			
5.02	0.453	0.90			
5.11	0.453	0.92			
5.36	0.453	0.96			
2.86	0.261	0.89			
2.87	0.261	0.90			
2.92	0.261	0.91			
2.82	0.261	0.88			
2.93	0.261	0.92			
3.52	0.327	0.88			

CALCULATED DATA FOR TEST SECTION WITH
$L/D = 204$ AND $\Delta P_o/\Delta P_{adb} = 0.5$

$\frac{\dot{q}/A}{Gh_{fg}} \times 10^4$	$\frac{C_p(T_s-T_i)}{h_{fg}}$	$\frac{\dot{q}}{\dot{q}_{se}}$	$\frac{\dot{q}/A}{Gh_{fg}} \times 10^4$	$\frac{C_p(T_s-T_i)}{h_{fg}}$	$\frac{\dot{q}}{\dot{q}_{se}}$
2.61	0.226	0.95	6.07	0.506	0.98
2.74	0.226	0.99	2.62	0.224	0.96
3.73	0.312	0.98	2.76	0.224	1.00
3.63	0.312	0.95	3.45	0.296	0.95
4.45	0.385	0.95	3.54	0.296	0.97
4.47	0.385	0.95	3.55	0.296	0.97
5.28	0.453	0.95	4.38	0.363	0.98
5.23	0.453	0.94	4.22	0.363	0.95
5.29	0.453	0.95	5.35	0.453	0.96
6.42	0.544	0.96	5.38	0.453	0.97
6.57	0.544	0.98	3.12	0.261	0.97
2.29	0.190	0.98	3.24	0.261	1.00
2.35	0.190	1.00	3.93	0.327	0.98
3.33	0.276	0.98	3.85	0.327	0.96
3.35	0.276	0.99	3.83	0.327	0.96
3.30	0.276	0.97	5.02	0.416	0.98
4.06	0.349	0.95	4.86	0.416	0.95
4.10	0.349	0.96			
4.10	0.349	0.96			
5.02	0.415	0.98			
4.87	0.415	0.96			
4.90	0.415	0.96			
5.94	0.506	0.96			

CALCULATED DATA FOR TEST SECTION WITH
$L/D = 204$ AND $\Delta P_o/\Delta P_{adb} = 1.0$

$\frac{\dot{q}/A}{Gh_{fg}} \times 10^4$	$\frac{C_p(T_s-T_i)}{h_{fg}}$	$\frac{\dot{q}}{\dot{q}_{se}}$	$\frac{\dot{q}/A}{Gh_{fg}} \times 10^4$	$\frac{C_p(T_s-T_i)}{h_{fg}}$	$\frac{\dot{q}}{\dot{q}_{se}}$
2.83	0.226	1.02	2.89	0.224	1.05
2.96	0.226	1.07	3.02	0.224	1.10
3.87	0.312	1.02	3.00	0.224	1.09
3.78	0.312	1.00	3.83	0.296	1.05
4.79	0.385	1.02	3.90	0.296	1.07
4.87	0.385	1.03	3.83	0.296	1.05
5.70	0.453	1.03	4.81	0.363	1.08
5.77	0.453	1.04	4.63	0.363	1.04
7.06	0.544	1.06	4.71	0.363	1.06
6.99	0.544	1.05	5.89	0.453	1.06
2.47	0.19	1.06	5.98	0.453	1.08
2.61	0.19	1.10	5.91	0.453	1.06
3.58	0.276	1.06	3.43	0.261	1.07
3.64	0.276	1.07	3.48	0.261	1.08
4.49	0.349	1.05	4.29	0.327	1.07
4.53	0.349	1.06	4.34	0.327	1.08
4.58	0.349	1.07	5.35	0.416	1.05
5.38	0.415	1.06	5.44	0.416	1.06
5.34	0.415	1.05			
5.31	0.415	1.04			
6.50	0.506	1.05			
6.52	0.506	1.05			

CALCULATED DATA FOR TEST SECTION WITH
$L/D = 204$ AND $\Delta P_o/\Delta P_{adb} = 2.0$

$\frac{\dot{q}/A}{Gh_{fg}} \times 10^4$	$\frac{C_p(T_s-T_i)}{h_{fg}}$	$\frac{\dot{q}}{\dot{q}_{se}}$	$\frac{\dot{q}/A}{Gh_{fg}} \times 10^4$	$\frac{C_p(T_s-T_i)}{h_{fg}}$	$\frac{\dot{q}}{\dot{q}_{se}}$
3.17	0.226	1.15	3.28	0.224	1.19
3.29	0.226	1.19	4.27	0.296	1.17
4.36	0.312	1.14	4.11	0.296	1.13
4.31	0.312	1.13	4.22	0.296	1.16
5.39	0.385	1.14	5.05	0.363	1.14
5.20	0.385	1.11	5.22	0.363	1.17
6.33	0.453	1.14	5.04	0.363	1.13
6.24	0.453	1.12	6.36	0.453	1.15
7.88	0.544	1.18	6.40	0.453	1.15
7.55	0.544	1.13	3.79	0.261	1.18
2.67	0.19	1.14	3.81	0.261	1.19
3.85	0.276	1.14	4.66	0.327	1.16
3.86	0.276	1.14	4.62	0.327	1.15
3.89	0.276	1.15	4.63	0.327	1.15
4.82	0.349	1.13	6.00	0.416	1.17
4.90	0.349	1.15	6.06	0.416	1.18
4.91	0.349	1.15	6.05	0.416	1.18
5.79	0.415	1.14			
5.87	0.415	1.15			
5.82	0.415	1.14			
7.39	0.506	1.19			
7.01	0.506	1.13			
3.28	0.224	1.19			

CALCULATED DATA FOR TEST SECTION WITH L/D = 153
AND ZERO ORIFICE PRESSURE DROP

$\frac{\dot{q}/A}{Gh_{fg}} \times 10^4$	$\frac{C_p(T_s-T_i)}{h_{fg}}$	$\frac{\dot{q}}{\dot{q}_{se}}$	$\frac{\dot{q}/A}{Gh_{fg}} \times 10^4$	$\frac{C_p(T_s-T_i)}{h_{fg}}$	$\frac{\dot{q}}{\dot{q}_{se}}$
3.81	0.276	0.84	4.15	0.296	0.86
3.78	0.276	0.84	4.24	0.296	0.87
4.82	0.349	0.85	6.79	0.506	0.82
4.60	0.349	0.81	2.63	0.19	0.84
3.03	0.224	0.83	5.76	0.415	0.85
2.99	0.224	0.82			

CALCULATED DATA FOR TEST SECTION WITH
L/D = 153 AND $\Delta P_o/\Delta P_{adb}$ = 0.5

$\frac{\dot{q}/A}{Gh_{fg}} \times 10^4$	$\frac{C_p(T_s-T_i)}{h_{fg}}$	$\frac{\dot{q}}{\dot{q}_{se}}$	$\frac{\dot{q}/A}{Gh_{fg}} \times 10^4$	$\frac{C_p(T_s-T_i)}{h_{fg}}$	$\frac{\dot{q}}{\dot{q}_{se}}$
4.01	0.276	0.89	3.46	0.224	0.89
4.10	0.276	0.90	3.29	0.224	0.9
4.96	0.349	0.87	4.40	0.296	0.9
5.06	0.349	0.89	4.42	0.296	0.91

CALCULATED DATA FOR TEST SECTION WITH
$L/D = 153$ AND $\Delta P_o/\Delta P_{adb} = 1.0$

$\frac{\dot{q}/A}{Gh_{fg}} \times 10^4$	$\frac{C_p(T_s-T_i)}{h_{fg}}$	$\frac{\dot{q}}{\dot{q}_{se}}$	$\frac{\dot{q}/A}{Gh_{fg}} \times 10^4$	$\frac{C_p(T_s-T_i)}{h_{fg}}$	$\frac{\dot{q}}{\dot{q}_{se}}$
4.52	0.276	1.00	3.64	0.224	0.99
4.28	0.276	0.95	3.62	0.224	0.99
5.72	0.349	1.00	4.99	0.296	1.03
5.62	0.349	0.99	4.85	0.296	1.00

CALCULATED DATA FOR TEST SECTION WITH
$L/D = 153$ AND $\Delta P_o/\Delta P_{adb} = 2.0$

$\frac{\dot{q}/A}{Gh_{fg}} \times 10^4$	$\frac{C_p(T_s-T_i)}{h_{fg}}$	$\frac{\dot{q}}{\dot{q}_{se}}$	$\frac{\dot{q}/A}{Gh_{fg}} \times 10^4$	$\frac{C_p(T_s-T_i)}{h_{fg}}$	$\frac{\dot{q}}{\dot{q}_{se}}$
5.16	0.276	1.14	4.27	0.224	1.16
4.92	0.276	1.09	5.34	0.296	1.10
6.20	0.349	1.09	5.65	0.296	1.16
6.29	0.349	1.10			

CALCULATED DATA FOR TEST SECTION WITH L/D = 102
AND ZERO ORIFICE PRESSURE DROP

$\frac{\dot{q}/A}{Gh_{fg}} \times 10^4$	$\frac{C_p(T_s-T_i)}{h_{fg}}$	$\frac{\dot{q}}{\dot{q}_{se}}$	$\frac{\dot{q}/A}{Gh_{fg}} \times 10^4$	$\frac{C_p(T_s-T_i)}{h_{fg}}$	$\frac{\dot{q}}{\dot{q}_{se}}$
5.16	0.276	0.76	5.34	0.296	0.74
5.178	0.276	0.77	5.65	0.296	0.77
6.20	0.349	0.73	9.54	0.506	0.77
6.33	0.349	0.74	3.52	0.19	0.75
4.28	0.224	0.78	7.67	0.415	0.76
4.12	0.224	0.75			

CALCULATED DATA FOR TEST SECTION WITH
L/D = 102 AND $\Delta P_o/\Delta P_{adb}$ = 0.5

$\frac{\dot{q}/A}{Gh_{fg}} \times 10^4$	$\frac{C_p(T_s-T_i)}{h_{fg}}$	$\frac{\dot{q}}{\dot{q}_{se}}$	$\frac{\dot{q}/A}{Gh_{fg}} \times 10^4$	$\frac{C_p(T_s-T_i)}{h_{fg}}$	$\frac{\dot{q}}{\dot{q}_{se}}$
5.56	0.276	0.82	4.54	0.224	0.83
5.78	0.276	0.85	4.49	0.224	0.82
6.77	0.349	0.79	6.23	0.296	0.86
7.23	0.349	0.84	6.36	0.296	0.87

CALCULATED DATA FOR TEST SECTION WITH
$L/D = 102$ AND $\Delta P_o/\Delta P_{adb} = 1.0$

$\frac{\dot{q}/A}{Gh_{fg}} \times 10^4$	$\frac{C_p(T_s-T_i)}{h_{fg}}$	$\frac{\dot{q}}{\dot{q}_{se}}$	$\frac{\dot{q}/A}{Gh_{fg}} \times 10^4$	$\frac{C_p(T_s-T_i)}{h_{fg}}$	$\frac{\dot{q}}{\dot{q}_{se}}$
6.03	0.276	0.89	5.19	0.224	0.94
6.15	0.276	0.91	4.94	0.224	0.9
7.44	0.349	0.87	6.80	0.296	0.93
7.78	0.349	0.91	6.78	0.296	0.93

CALCULATED DATA FOR TEST SECTION WITH
$L/D = 102$ AND $\Delta P_o/\Delta P_{adb} = 2.0$

$\frac{\dot{q}/A}{Gh_{fg}} \times 10^4$	$\frac{C_p(T_s-T_i)}{h_{fg}}$	$\frac{\dot{q}}{\dot{q}_{se}}$	$\frac{\dot{q}/A}{Gh_{fg}} \times 10^4$	$\frac{C_p(T_s-T_i)}{h_{fg}}$	$\frac{\dot{q}}{\dot{q}_{se}}$
6.58	0.276	0.97	5.59	0.224	1.02
6.82	0.276	1.00	5.49	0.224	1.00
8.27	0.349	0.97	7.48	0.296	1.03
8.43	0.349	0.99	7.27	0.296	1.00

CALCULATED DATA FOR TEST SECTION WITH L/D = 51
AND ZERO ORIFICE PRESSURE DROP

$\frac{\dot{q}/A}{Gh_{fg}} \times 10^4$	$\frac{C_p(T_s-T_i)}{h_{fg}}$	$\frac{\dot{q}}{\dot{q}_{se}}$	$\frac{\dot{q}/A}{Gh} \times 10^4$	$\frac{C_p(T_s-T_i)}{h_{fg}}$	$\frac{\dot{q}}{\dot{q}_{se}}$
8.66	0.276	0.64	9.64	0.296	0.66
8.89	0.276	0.66	8.68	0.296	0.60
11.34	0.349	0.66	16.29	0.506	0.66
11.10	0.349	0.65	5.93	0.19	0.63
7.17	0.224	0.65	13.64	0.405	0.67
6.90	0.224	0.63			

CALCULATED DATA FOR TEST SECTION WITH
L/D = 51 AND $\Delta P_o/\Delta P_{adb}$ = 0.5

$\frac{\dot{q}/A}{Gh_{fg}} \times 10^4$	$\frac{C_p(T_s-T_i)}{h_{fg}}$	$\frac{\dot{q}}{\dot{q}_{se}}$	$\frac{\dot{q}/A}{Gh_{fg}} \times 10^4$	$\frac{C_p(T_s-T_i)}{h_{fg}}$	$\frac{\dot{q}}{\dot{q}_{se}}$
10.10	0.276	0.75	8.72	0.224	0.79
9.44	0.276	0.70	8.44	0.224	0.77
12.47	0.349	0.73	10.44	0.296	0.72
11.96	0.349	0.70	10.42	0.296	0.72

CALCULATED DATA FOR TEST SECTION WITH
$L/D = 51$ AND $\Delta P_o/\Delta P_{adb} = 1.0$

$\frac{\dot{q}/A}{Gh_{fg}} \times 10^4$	$\frac{C_p(T_s-T_i)}{h_{fg}}$	$\frac{\dot{q}}{\dot{q}_{se}}$	$\frac{\dot{q}/A}{Gh_{fg}} \times 10^4$	$\frac{C_p(T_s-T_i)}{h_{fg}}$	$\frac{\dot{q}}{\dot{q}_{se}}$
11.02	0.275	0.81	9.37	0.226	0.85
10.79	0.276	0.80	9.49	0.226	0.86
13.86	0.349	0.81	12.53	0.296	0.86
12.95	0.349	0.76	12.02	0.296	0.83

CALCULATED DATA FOR TEST SECTION WITH
$L/D = 51$ AND $\Delta P_o/\Delta P_{adb} = 2.0$

$\frac{\dot{q}/A}{Gh_{fg}} \times 10^4$	$\frac{C_p(T_s-T_i)}{h_{fg}}$	$\frac{\dot{q}}{\dot{q}_{se}}$	$\frac{\dot{q}/A}{Gh_{fg}} \times 10^4$	$\frac{C_p(T_s-T_i)}{h_{fg}}$	$\frac{\dot{q}}{\dot{q}_{se}}$
12.12	0.276	0.90	11.07	0.224	1.00
12.59	0.276	0.93	10.24	0.224	0.93
15.59	0.349	0.91	13.93	0.296	0.96
15.55	0.349	0.91	13.63	0.296	0.94

APPENDIX C

CALIBRATION CURVES FOR MEASURING DEVICES

The calibration curves for measuring devices are presented in this appendix. The curves were obtained by applying the least square criteria to the data obtained from the calibration of each device.

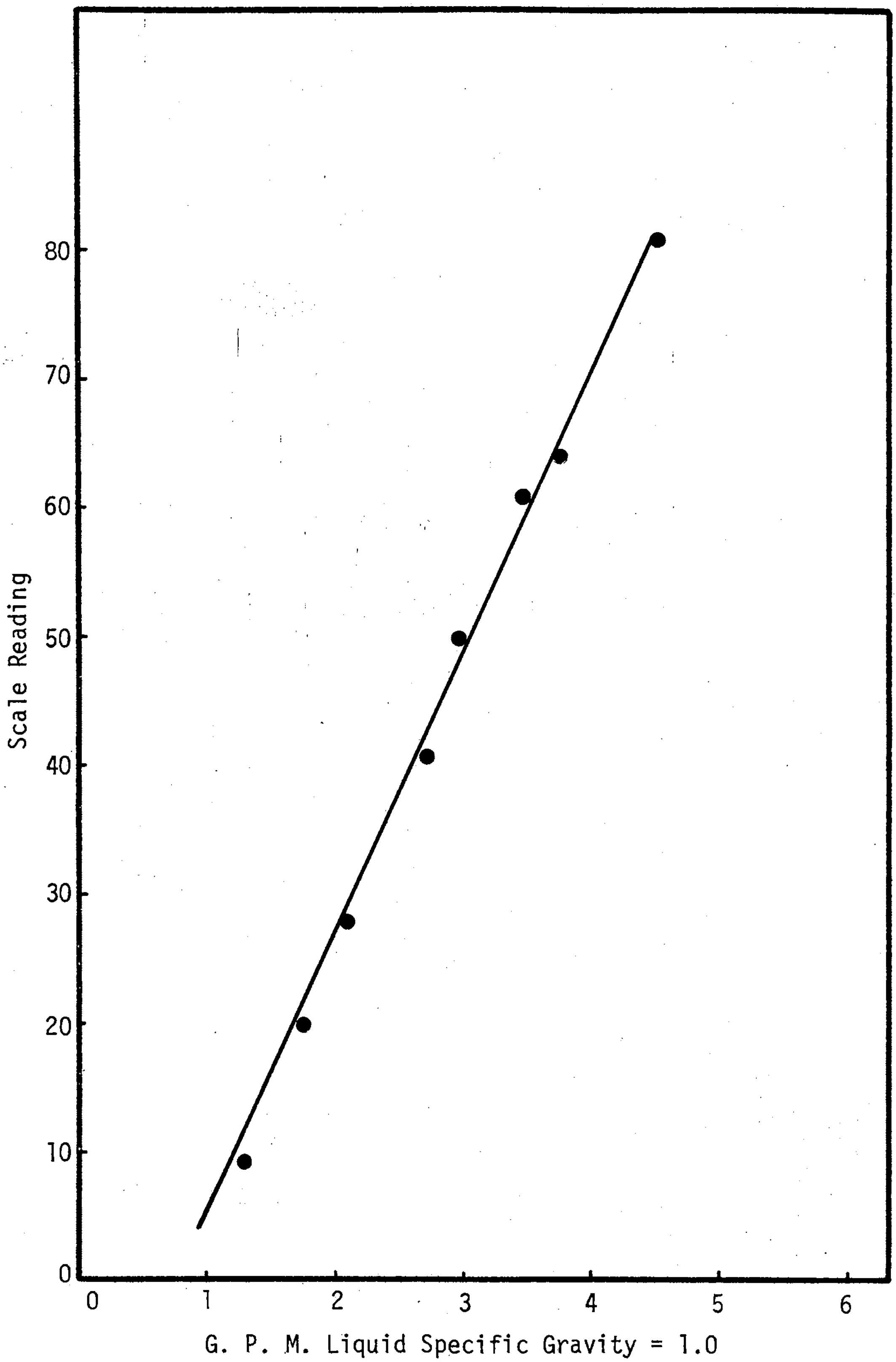

Figure 48. Calibration Curve for Water Flow Meter

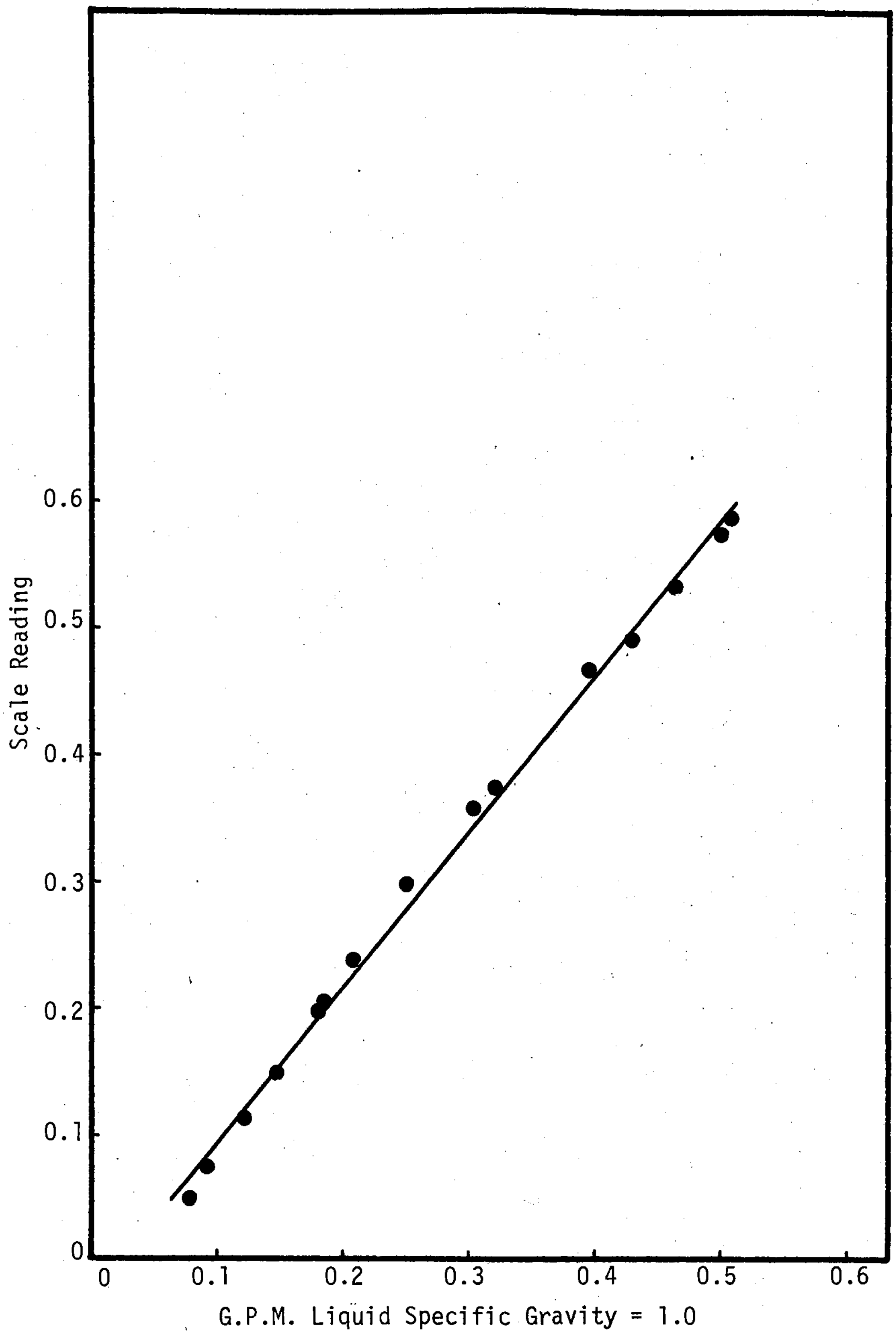

Figure 49. Calibration Curve for Freon Flow Meter (Cox Rotameter)

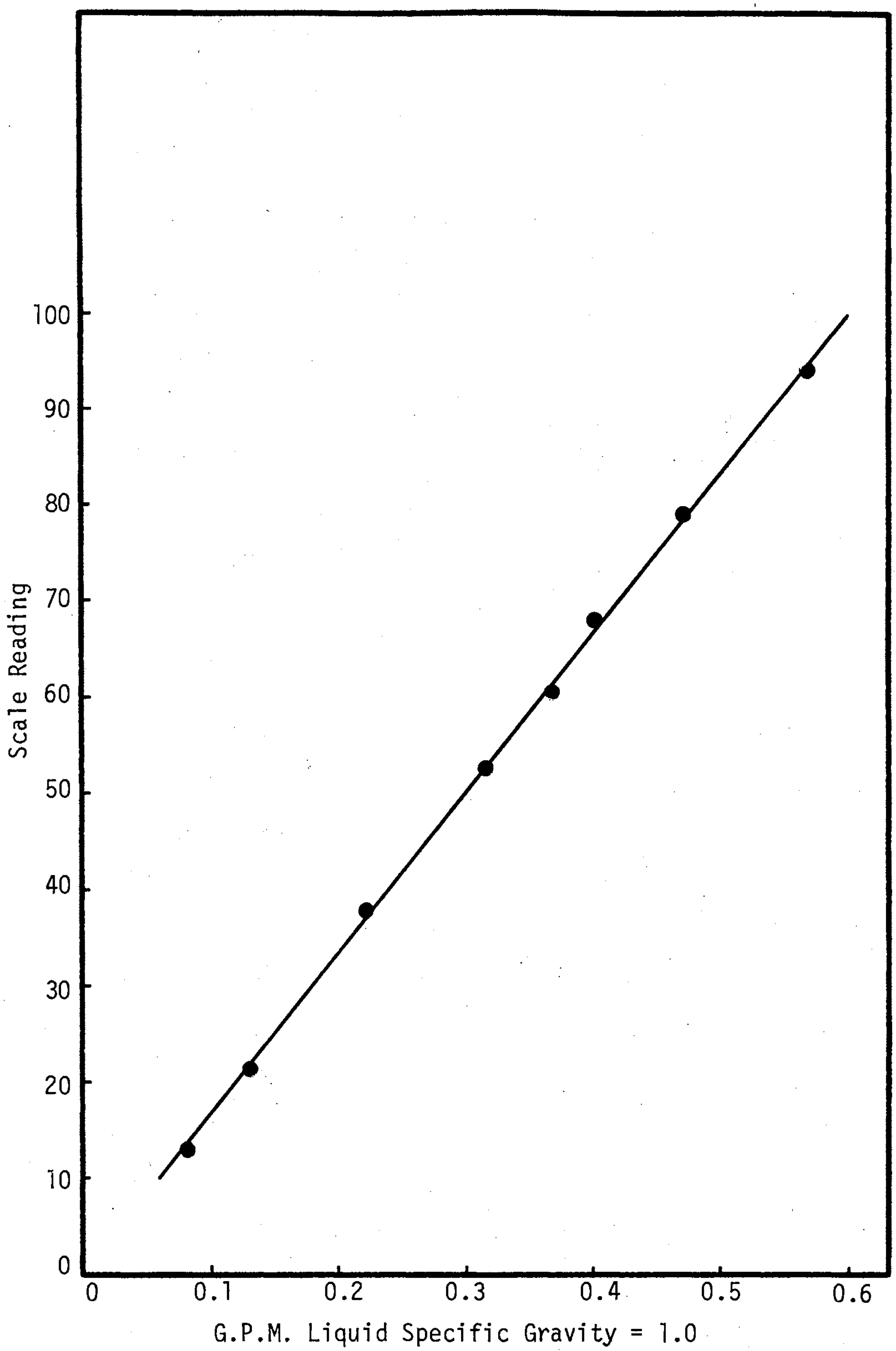

Figure 50. Calibration Curve for Freon Flow Meter
(Fischer & Porter Rotameter)

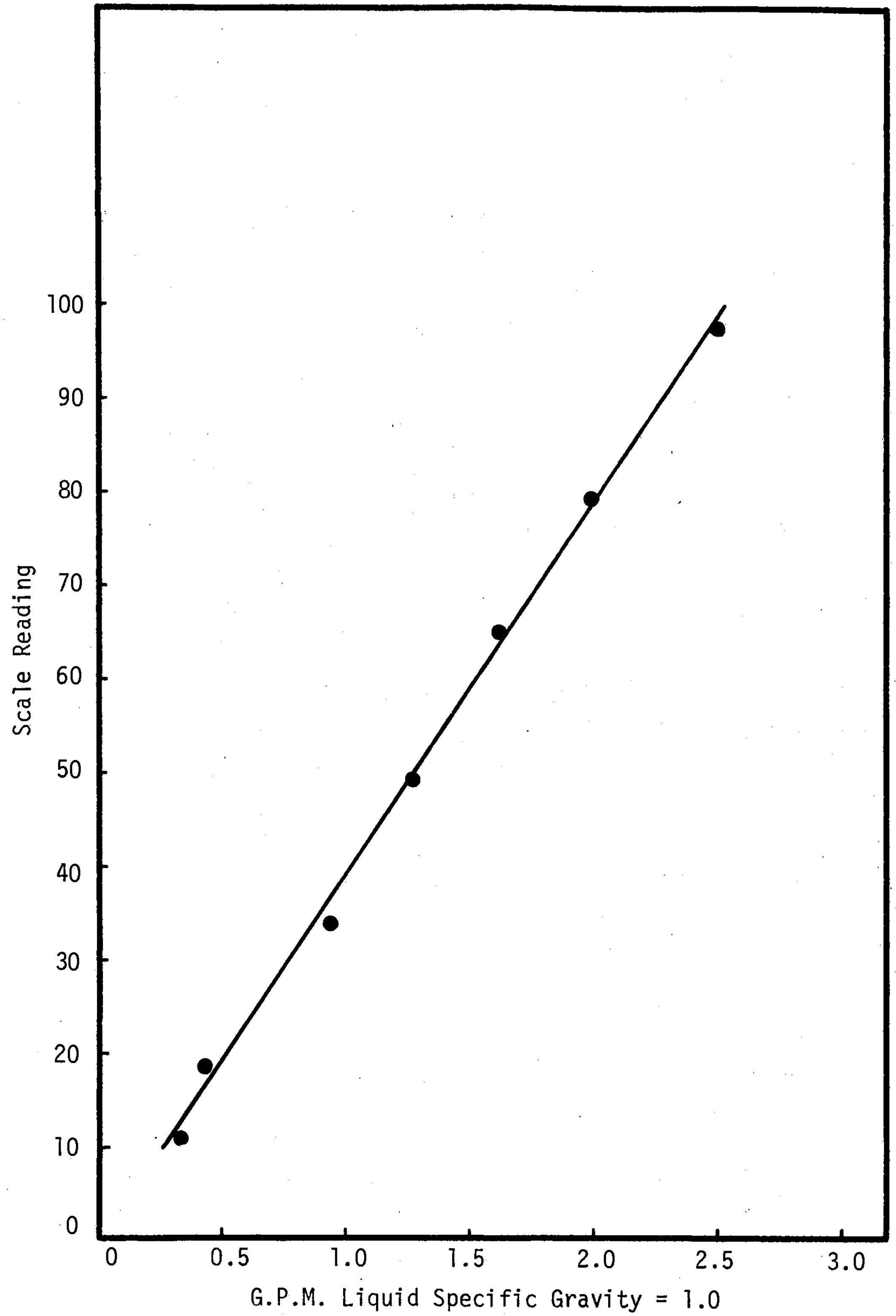

Figure 51. Calibration Curve for Freon Flow Meter
(Brooks Rotameter)

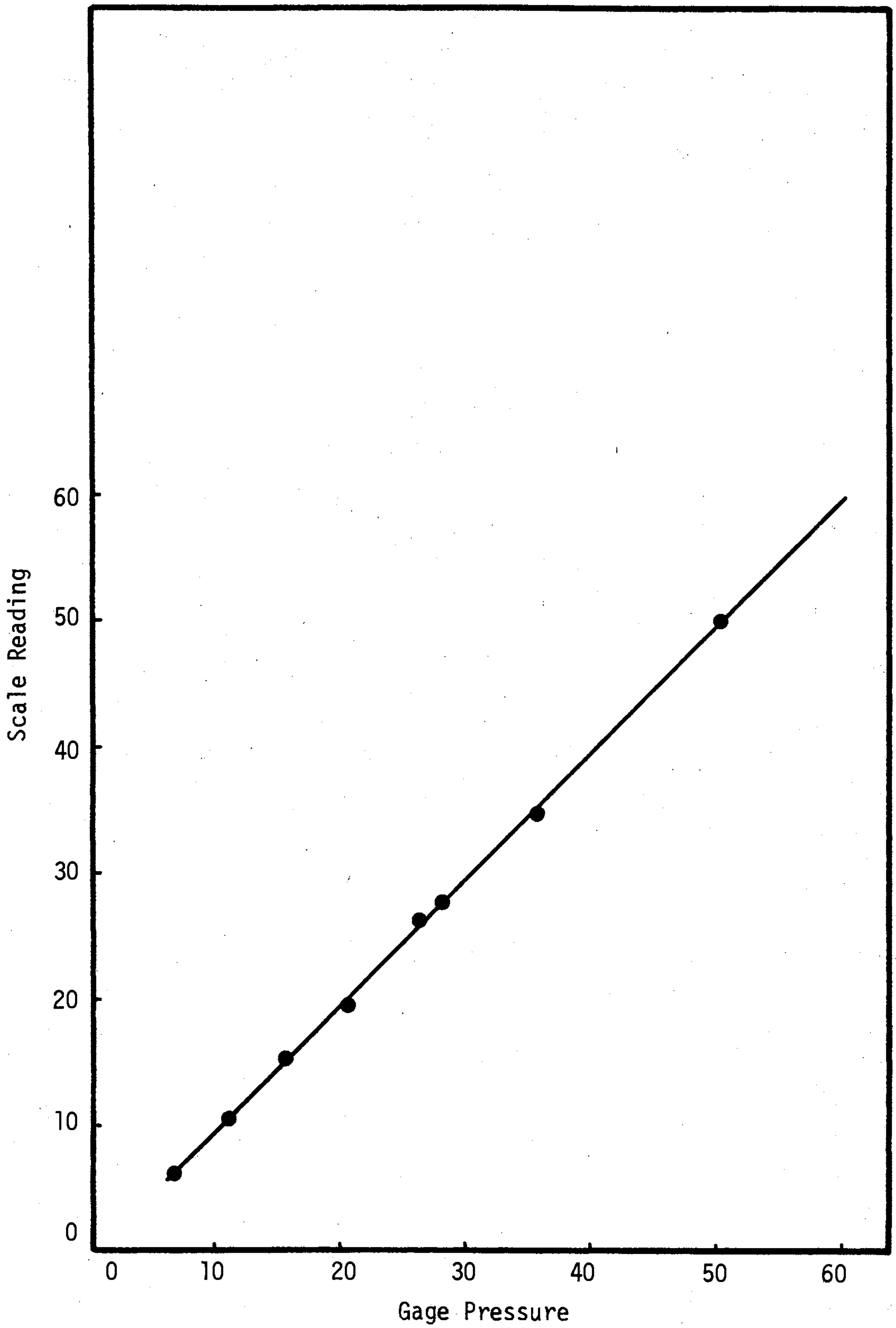

Figure 52. Calibration Curve for Gage Pressure

3

VITA

Hamid Neshan

Candidate for the Degree of

Doctor of Philosophy

Thesis: TWO-PHASE FLOW STABILITY IN HORIZONTAL CHANNELS

Major Field: Mechanical Engineering

Biographical:

Personal Data: Born in Daregaz, Iran, May 9, 1944, the son of Jahangeer and Zahra Neshan.

Education: Graduated from Nader-Shah High School, Mashhad, Iran in 1963; received the Bachelor of Science degree in Mechanical Engineering from Tehran Polytechnic Institute, Tehran, Iran, in May, 1967. Received the Master of Science degree in Mechanical Engineering in January, 1971, from Oklahoma State University, Stillwater, Oklahoma; completed requirements for the degree of Doctor of Philosophy at Oklahoma State University in December, 1973.

Professional Experience: Employed as Design Engineer with Urban Consulting Engineers, Tehran, Iran, summer 1967; served as Design Engineer in Iranian National Steel Corporation, 1967-1969, in Isfahan, Iran. Graduate teaching and research assistant, School of Mechanical and Aerospace Engineering, Oklahoma State University, Stillwater, Oklahoma, 1971-1973.

Professional Affiliations: American Society of Mechanical Engineers, American Institute of Chemical Engineers.